

An Optimised Chemical Kinetic Model for the Combustion of Fuel Mixtures of Syngas and Natural Gas

**Supplementary Materials: Performance of Chemical Kinetic Model on
Experimental Data**

Torsten Methling, Marina Braun-Unkhoff and Uwe Riedel

German Aerospace Center (DLR)
Institute of Combustion Technology

Contents

List of Figures	5
1 Ignition delay times in shock tubes	15
2 Species profiles in flow reactors	37
3 Species profiles in jet stirred reactors	55
4 Laminar burning velocities	67
5 Species profiles in burner stabilised flames	89
Bibliography	93

List of Figures

1.1	Ignition delay times from shock tube by Thi, Zhang, and Huang [1] and corresponding simulation; fuel: $\text{H}_2/\text{CO} = 70/30$, $\varphi = 1.0$	16
1.2	Ignition delay times from shock tube by Herzler, Naumann, and Griebel [2] and corresponding simulation; fuel: $\text{H}_2/\text{CO} = 50/50$, $\varphi = 1.0$	16
1.3	Ignition delay times from shock tube by Thi, Zhang, and Huang [1] and corresponding simulation; fuel: $\text{H}_2/\text{CO} = 33/67$, $\varphi = 1.0$	17
1.4	Ignition delay times from shock tube by Kalitan et al. [3] and corresponding simulation; fuel: $\text{H}_2/\text{CO} = 20/80$, $\varphi = 0.5$	17
1.5	Ignition delay times from shock tube by Kalitan et al. [3] and corresponding simulation; fuel: $\text{H}_2/\text{CO} = 10/90$, $\varphi = 0.5$	18
1.6	Ignition delay times from shock tube by Kalitan et al. [3] and corresponding simulation; fuel: $\text{H}_2/\text{CO} = 5/95$, $\varphi = 0.5$	18
1.7	Ignition delay times from shock tube by Herzler, Naumann, and Griebel [2] and corresponding simulation; fuel: $\text{H}_2/\text{CO} = 5/95$, $\varphi = 1.0$	19
1.8	Ignition delay times from shock tube by Thi, Zhang, and Huang [1] and corresponding simulation; fuel: $\text{H}_2/\text{CO} = 27/73$, $\varphi = 1.0$, with N_2 in diluent	19
1.9	Ignition delay times from shock tube by Thi, Zhang, and Huang [1] and corresponding simulation; fuel: $\text{H}_2/\text{CO} = 50/50$, $\varphi = 1.0$, with CO_2 in diluent	20
1.10	Ignition delay times from shock tube by Herzler and Naumann [4] and corresponding simulation; fuel: CH_3OH , $\varphi = 1.0$	20
1.11	Ignition delay times from shock tube by Petersen et al. [5] and corresponding simulation; fuel: CH_4 , $\varphi = 0.5$	21
1.12	Ignition delay times from shock tube by Herzler et al. [6] and corresponding simulation; fuel: CH_4 , $\varphi = 0.5$, $X_{\text{Ar}} = 0.95$	21
1.13	Ignition delay times from shock tube by Herzler et al. [6] and corresponding simulation; fuel: CH_4 , $\varphi = 1.0$, $X_{\text{Ar}} = 0.94$	22

1.14	Ignition delay times from shock tube by Zeng et al. [7] and corresponding simulation; fuel: CH_4 , $\varphi = 2.0$, $X_{\text{N}_2} = 0.72$	22
1.15	Ignition delay times from shock tube by Zeng et al. [7] and corresponding simulation; fuel: CH_4 , $\varphi = 2.0$, $X_{\text{N}_2} = 0.83$	23
1.16	Ignition delay times from shock tube by Zeng et al. [7] and corresponding simulation; fuel: CH_4 , $\varphi = 2.0$, $X_{\text{CO}_2} = 0.20$, $X_{\text{N}_2} = 0.52$	23
1.17	Ignition delay times from shock tube by Zeng et al. [7] and corresponding simulation; fuel: CH_4 , $\varphi = 2.0$, $X_{\text{CO}_2} = 0.50$, $X_{\text{N}_2} = 0.33$	24
1.18	Ignition delay times from shock tube by Koroglu et al. [8] and corresponding simulation; fuel: CH_4 , $\varphi = 2.0$, $X_{\text{CO}_2} = 0.30$, $X_{\text{Ar}} = 0.56$	24
1.19	Ignition delay times from shock tube by Herzler et al. [6] and corresponding simulation; fuel: $\text{H}_2/\text{CO}/\text{CH}_4/\text{CO}_2 = 5/31/38/2$, $\varphi = 0.5$, $X_{\text{Ar}} = 0.93$. . .	25
1.20	Ignition delay times from shock tube by Herzler et al. [6] and corresponding simulation; fuel: $\text{H}_2/\text{CO}/\text{CH}_4/\text{CO}_2 = 5/31/38/2$, $\varphi = 0.5$, $X_{\text{Ar}} = 0.98$. . .	25
1.21	Ignition delay times from shock tube by Herzler et al. [6] and corresponding simulation; fuel: $\text{H}_2/\text{CO}/\text{CH}_4/\text{CO}_2 = 5/31/38/2$, $\varphi = 1.0$, $X_{\text{Ar}} = 0.91$. . .	26
1.22	Ignition delay times from shock tube by Herzler et al. [6] and corresponding simulation; fuel: $\text{H}_2/\text{CO}/\text{CH}_4/\text{CO}_2 = 5/31/38/2$, $\varphi = 1.0$, $X_{\text{Ar}} = 0.95$. . .	26
1.23	Ignition delay times from shock tube by Lokachari et al. [9] and corresponding simulation; fuel: C_2H_2 , $\varphi = 0.5$	27
1.24	Ignition delay times from shock tube by Lokachari et al. [9] and corresponding simulation; fuel: C_2H_2 , $\varphi = 1.0$	27
1.25	Ignition delay times from shock tube by Lokachari et al. [9] and corresponding simulation; fuel: C_2H_2 , $\varphi = 2.0$	28
1.26	Ignition delay times from shock tube by Lokachari et al. [9] and corresponding simulation; fuel: C_2H_2 , $\varphi = 1.0$, $X_{\text{N}_2} = 0.43$, $X_{\text{Ar}} = 0.43$	28
1.27	Ignition delay times from shock tube by Lokachari et al. [9] and corresponding simulation; fuel: C_2H_2 , $\varphi = 1.0$, $X_{\text{N}_2} = 0.48$, $X_{\text{Ar}} = 0.48$	29
1.28	Ignition delay times from shock tube by Rickard, Hall, and Petersen [10] and corresponding simulation; fuel: C_2H_2 , $\varphi = 0.5$	29
1.29	Ignition delay times from shock tube by Rickard, Hall, and Petersen [10] and corresponding simulation; fuel: C_2H_2 , $\varphi = 1.0$	30
1.30	Ignition delay times from shock tube by Petersen et al. [11] and corresponding simulation; fuel: C_2H_4 , $\varphi = 1.0$	30

1.31	Ignition delay times from shock tube by Vries et al. [12] and corresponding simulation; fuel: C_2H_6 , $\varphi = 0.5$	31
1.32	Ignition delay times from shock tube by Vries et al. [12] and corresponding simulation; fuel: C_2H_6 , $\varphi = 1.0$	31
1.33	Ignition delay times from shock tube by Herzler and Naumann [13] and corresponding simulation; fuel: RG, $\varphi = 1.0$, $\text{RG} = \text{C}_2\text{H}_6/\text{CH}_4 = 8/92$	32
1.34	Ignition delay times from shock tube by Herzler and Naumann [13] and corresponding simulation; fuel: $\text{RG}/\text{H}_2 = 60/40$, $\varphi = 0.5$, $\text{RG} = \text{C}_2\text{H}_6/\text{CH}_4 = 8/92$	32
1.35	Ignition delay times from shock tube by Herzler and Naumann [13] and corresponding simulation; fuel: $\text{RG}/\text{H}_2 = 60/40$, $\varphi = 1.0$, $\text{RG} = \text{C}_2\text{H}_6/\text{CH}_4 = 8/92$	33
1.36	Ignition delay times from shock tube by Herzler and Naumann [13] and corresponding simulation; fuel: $\text{RG}/\text{H}_2 = 20/80$, $\varphi = 0.5$, $\text{RG} = \text{C}_2\text{H}_6/\text{CH}_4 = 8/92$	33
1.37	Ignition delay times from shock tube by Herzler and Naumann [13] and corresponding simulation; fuel: $\text{RG}/\text{H}_2 = 20/80$, $\varphi = 1.0$, $\text{RG} = \text{C}_2\text{H}_6/\text{CH}_4 = 8/92$	34
1.38	Ignition delay times from shock tube by Herzler and Naumann [14] and corresponding simulation; fuel: $\text{RG}/\text{CO} = 31/69$, $\varphi = 1.0$, $\text{RG} = \text{C}_2\text{H}_6/\text{CH}_4 = 8/92$	34
1.39	Ignition delay times from shock tube by Herzler and Naumann [14] and corresponding simulation; fuel: $\text{RG}/\text{CO} = 8/92$, $\varphi = 1.0$, $\text{RG} = \text{C}_2\text{H}_6/\text{CH}_4 = 8/92$	35
2.1	Flow reactor results by Mueller et al. [15] and its simulation; fuel: H_2 , $T = 880$ K, $p = 0.3$ atm, $\varphi = 0.5$,	38
2.2	Flow reactor results by Mueller et al. [15] and its simulation; fuel: H_2 , $T = 896$ K, $p = 0.6$ atm, $\varphi = 0.3$,	38
2.3	Flow reactor results by Mueller et al. [15] and its simulation; fuel: H_2 , $T = 897$ K, $p = 0.6$ atm, $\varphi = 0.8$,	39
2.4	Flow reactor results by Mueller et al. [15] and its simulation; fuel: H_2 , $T = 943$ K, $p = 2.5$ atm, $\varphi = 0.3$,	39
2.5	Flow reactor results by Mueller et al. [15] and its simulation; fuel: H_2 , $T = 933$ K, $p = 3.44$ atm, $\varphi = 1$,	40

2.6	Flow reactor results by Mueller et al. [15] and its simulation; fuel: H_2 , $T = 934$ K, $p = 6.0$ atm, $\varphi = 1$,	40
2.7	Flow reactor results by Mueller et al. [15] and its simulation; fuel: H_2 , $T = 884$ K, $p = 6.5$ atm, $\varphi = 0.3$,	41
2.8	Flow reactor results by Mueller et al. [15] and its simulation; fuel: H_2 , $T = 889$ K, $p = 6.5$ atm, $\varphi = 0.3$,	41
2.9	Flow reactor results by Mueller et al. [15] and its simulation; fuel: H_2 , $T = 906$ K, $p = 6.5$ atm, $\varphi = 0.3$,	42
2.10	Flow reactor results by Mueller et al. [15] and its simulation; fuel: H_2 , $T = 914$ K, $p = 6.5$ atm, $\varphi = 0.3$,	42
2.11	Flow reactor results by Mueller et al. [15] and its simulation; fuel: H_2 , $T = 934$ K, $p = 6.5$ atm, $\varphi = 0.3$,	43
2.12	Flow reactor results by Mueller et al. [15] and its simulation; fuel: H_2 , $T = 914$ K, $p = 15.7$ atm, $\varphi = 0.3$,	43
2.13	Flow reactor results by Mueller et al. [15] and its simulation; fuel: H_2 , $T = 914$ K, $p = 15.7$ atm, $\varphi = 1$,	44
2.14	Flow reactor results by Mueller, Yetter, and Dryer [16] and its simulation; fuel: CO , $T = 1038$ K, $p = 3.5$ atm, $\varphi = 1$,	44
2.15	Flow reactor results by Mueller, Yetter, and Dryer [16] and its simulation; fuel: CO , $T = 1040$ K, $p = 9.6$ atm, $\varphi = 1$,	45
2.16	Flow reactor results by Li et al. [17] and its simulation; fuel: CH_2O , $T = 852$ K, $p = 6.0$ atm, $\lambda = 150$	45
2.17	Flow reactor results by Li et al. [17] and its simulation; fuel: CH_2O , $T = 902$ K, $p = 3.0$ atm, $\lambda = 200$	46
2.18	Flow reactor results by Li et al. [17] and its simulation; fuel: CH_2O , $T = 948$ K, $p = 1.5$ atm, $\lambda = 200$	46
2.19	Flow reactor results by Li et al. [17] and its simulation; fuel: CH_2O , $T = 924$ K, $p = 2.5$ atm, $\lambda = 225$	47
2.20	Flow reactor results by Oßwald and Köhler [18] and its simulation; fuel: CH_4 , $\varphi = 0.5$,	47
2.21	Flow reactor results by Oßwald and Köhler [18] and its simulation; fuel: CH_4 , $\varphi = 1$,	48
2.22	Flow reactor results by Oßwald and Köhler [18] and its simulation; fuel: CH_4 , $\varphi = 2$,	49

2.23	Flow reactor results by Hashemi et al. [19] and its simulation; fuel: CH ₄ , $\varphi = 0.006$,	50
2.24	Flow reactor results by Hashemi et al. [19] and its simulation; fuel: CH ₄ , $\varphi = 1$,	50
2.25	Flow reactor results by Hashemi et al. [19] and its simulation; fuel: CH ₄ , $\varphi = 19.7$,	51
2.26	Flow reactor results by Alzueta et al. [20] and its simulation; fuel: C ₂ H ₂ , $\varphi = 1$,	51
2.27	Flow reactor results by Alzueta et al. [20] and its simulation; fuel: C ₂ H ₂ , $\varphi = 1.4$,	52
2.28	Flow reactor results by Oßwald and Köhler [18] and its simulation; fuel: C ₂ H ₄ , $\varphi = 0.5$,	52
2.29	Flow reactor results by Oßwald and Köhler [18] and its simulation; fuel: C ₂ H ₄ , $\varphi = 1$,	53
2.30	Flow reactor results by Carriere et al. [21] and its simulation; fuel: C ₂ H ₄ , $T = 950$ K, $p = 5.0$ atm, $\varphi = 2.5$,	53
2.31	Flow reactor results by Carriere et al. [21] and its simulation; fuel: C ₂ H ₄ , $T = 850$ K, $p = 10.0$ atm, $\varphi = 2.5$,	54
3.1	JSR results by Le Cong, Dagaut, and Dayma [22] and its simulation; fuel: H ₂ , $p = 1.0$ atm, $\varphi = 0.2$,	56
3.2	JSR results by Dagaut et al. [23] and its simulation; fuel: H ₂ /CO = 50/50, $p = 1.0$ atm, $\varphi = 0.1$,	56
3.3	JSR results by Burke et al. [24] and its simulation; fuel: CH ₃ OH, $p = 1.0$ atm, $\varphi = 0.5$,	57
3.4	JSR results by Burke et al. [24] and its simulation; fuel: CH ₃ OH, $p = 1.0$ atm, $\varphi = 1$,	57
3.5	JSR results by Burke et al. [24] and its simulation; fuel: CH ₃ OH, $p = 10.0$ atm, $\varphi = 0.2$,	58
3.6	JSR results by Burke et al. [24] and its simulation; fuel: CH ₃ OH, $p = 10.0$ atm, $\varphi = 1$,	58
3.7	JSR results by Burke et al. [24] and its simulation; fuel: CH ₃ OH, $p = 10.0$ atm, $\varphi = 2$,	58
3.8	JSR results by Burke et al. [24] and its simulation; fuel: CH ₃ OH, $p = 20.0$ atm, $\varphi = 1$,	59
3.9	JSR results by Le Cong, Dagaut, and Dayma [22] and its simulation; fuel: CH ₄ , $p = 1.0$ atm, $\varphi = 0.1$, $X_{N_2} = 79$	59

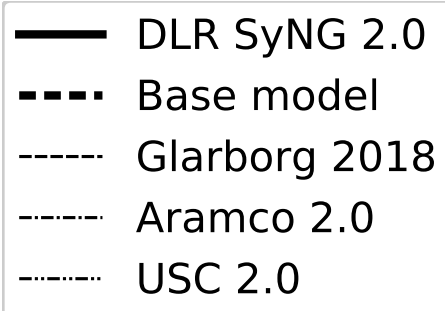
3.10	JSR results by Dagaut, Boettner, and Cathonnet [25] and its simulation; fuel: CH ₄ , $p = 1.0$ atm, $\varphi = 0.1$, $X_{N_2} = 94$	60
3.11	JSR results by Dagaut, Boettner, and Cathonnet [25] and its simulation; fuel: CH ₄ , $p = 10.0$ atm, $\varphi = 0.5$,	60
3.12	JSR results by Dagaut, Boettner, and Cathonnet [25] and its simulation; fuel: CH ₄ , $p = 10.0$ atm, $\varphi = 1$,	61
3.13	JSR results by Le Cong and Dagaut [26] and its simulation; fuel: CH ₄ , $p = 10.0$ atm, $\varphi = 1.5$,	61
3.14	JSR results by Le Cong, Dagaut, and Dayma [22] and its simulation; fuel: CH ₄ /H ₂ = 50/50, $p = 1.0$ atm, $\varphi = 0.3$, $X_{CO_2} = 20$, $X_{N_2} = 72$	61
3.15	JSR results by Le Cong, Dagaut, and Dayma [22] and its simulation; fuel: CH ₄ /H ₂ = 50/50, $p = 1.0$ atm, $\varphi = 0.3$, $X_{N_2} = 92$	62
3.16	JSR results by Le Cong and Dagaut [26] and its simulation; fuel: CH ₄ /H ₂ = 50/50, $p = 1.0$ atm, $\varphi = 1.5$, $X_{CO_2} = 20$, $X_{N_2} = 77$	62
3.17	JSR results by Le Cong and Dagaut [26] and its simulation; fuel: CH ₄ /H ₂ = 50/50, $p = 1.0$ atm, $\varphi = 1.5$, $X_{N_2} = 97$	62
3.18	JSR results by Le Cong, Dagaut, and Dayma [22] and its simulation; fuel: CH ₄ /H ₂ = 50/50, $p = 10.0$ atm, $\varphi = 0.3$,	63
3.19	JSR results by Le Cong and Dagaut [26] and its simulation; fuel: CH ₄ /H ₂ = 50/50, $p = 10.0$ atm, $\varphi = 1$,	63
3.20	JSR results by Le Cong and Dagaut [26] and its simulation; fuel: CH ₄ /H ₂ /CO = 50/25/25, $p = 1.0$ atm, $\varphi = 0.3$,	64
3.21	JSR results by Le Cong and Dagaut [26] and its simulation; fuel: CH ₄ /H ₂ /CO = 50/25/25, $p = 1.0$ atm, $\varphi = 1.5$,	64
3.22	JSR results by Tan et al. [27] and its simulation; fuel: C ₂ H ₂ , $p = 1.0$ atm, $\varphi = 0.4$,	65
3.23	JSR results by Tan et al. [27] and its simulation; fuel: C ₂ H ₂ , $p = 1.0$ atm, $\varphi = 1$,	65
4.1	Burning velocities by Krejci et al. [28] and corresponding simulation; fuel: H ₂ ,	68
4.2	Burning velocities by Park et al. [29] and corresponding simulation; fuel: H ₂ , oxidiser: O ₂ /N ₂ = 9.5/90.5	68
4.3	Burning velocities by Voss, Hartl, and Hasse [30] and corresponding simulation; fuel: H ₂ /N ₂ = 30/70,	69

4.4	Burning velocities by Voss, Hartl, and Hasse [30] and corresponding simulation; fuel: $\text{H}_2/\text{N}_2 = 25/75$,	69
4.5	Burning velocities by Alekseev and Konnov [31] and corresponding simulation; fuel: $\text{H}_2/\text{N}_2 = 25/75$, oxidiser: $\text{O}_2/\text{He} = 12.5/87.5$	70
4.6	Burning velocities by Sun et al. [32] and corresponding simulation; fuel: $\text{H}_2/\text{CO} = 5/95$,	70
4.7	Burning velocities by Sun et al. [32] and corresponding simulation; fuel: $\text{H}_2/\text{CO} = 25/75$,	71
4.8	Burning velocities by Krejci et al. [28] and corresponding simulation; fuel: $\text{H}_2/\text{CO} = 50/50$, $p = 1$ atm,	71
4.9	Burning velocities by Sun et al. [32] and corresponding simulation; fuel: $\text{H}_2/\text{CO} = 50/50$, $p = 2$ atm,	72
4.10	Burning velocities by Voss, Hartl, and Hasse [30] and corresponding simulation; fuel: $\text{H}_2/\text{CO}/\text{N}_2 = 24/6/70$,	72
4.11	Burning velocities by Lohöfener et al. [33] and corresponding simulation; fuel: $\text{H}_2/\text{CO}/\text{N}_2 = 20/10/70$,	73
4.12	Burning velocities by Voss, Hartl, and Hasse [30] and corresponding simulation; fuel: $\text{H}_2/\text{CO}/\text{N}_2 = 15/15/70$,	73
4.13	Burning velocities by Lohöfener et al. [33] and corresponding simulation; fuel: $\text{H}_2/\text{CO}/\text{N}_2 = 20/20/60$,	74
4.14	Burning velocities by Voss, Hartl, and Hasse [30] and corresponding simulation; fuel: $\text{H}_2/\text{CO}/\text{N}_2 = 10/20/70$,	74
4.15	Burning velocities by Konnov, Dyakov, and Ruyck [34] and corresponding simulation; fuel: $\text{H}_2/\text{CO}/\text{CO}_2 = 5/45/50$,	75
4.16	Burning velocities by Kishore, Ravi, and Ray [35] and corresponding simulation; fuel: $\text{H}_2/\text{CO}/\text{CO}_2 = 40/10/50$,	75
4.17	Burning velocities by Kishore, Ravi, and Ray [35] and corresponding simulation; fuel: $\text{H}_2/\text{CO}/\text{CO}_2 = 25/25/50$,	76
4.18	Burning velocities by Kishore, Ravi, and Ray [35] and corresponding simulation; fuel: $\text{H}_2/\text{CO}/\text{CO}_2 = 30/30/40$,	76
4.19	Burning velocities by Kishore, Ravi, and Ray [35] and corresponding simulation; fuel: $\text{H}_2/\text{CO}/\text{CO}_2 = 10/40/50$,	77
4.20	Burning velocities by Kishore, Ravi, and Ray [35] and corresponding simulation; fuel: $\text{H}_2/\text{CO}/\text{CO}_2 = 12/48/40$,	77

4.21	Burning velocities by Sileghem et al. [36] and corresponding simulation; fuel: CH ₃ OH, $T = 298$ K,	78
4.22	Burning velocities by Sileghem et al. [36] and corresponding simulation; fuel: CH ₃ OH, $T = 338$ K,	78
4.23	Burning velocities by Park et al. [37] and corresponding simulation; fuel: CH ₄ , $p = 1$ atm,	79
4.24	Burning velocities by Park et al. [37] and corresponding simulation; fuel: CH ₄ , $p = 2$ atm,	79
4.25	Burning velocities by Park et al. [37] and corresponding simulation; fuel: CH ₄ , $p = 4$ atm,	80
4.26	Burning velocities by Burrell [38] and corresponding simulation; fuel: CH ₄ , $p = 0.1$ atm,	80
4.27	Burning velocities by Burrell [38] and corresponding simulation; fuel: CH ₄ , $p = 0.25$ atm,	81
4.28	Burning velocities by Yan et al. [39] and corresponding simulation; fuel: CH ₄ , $T = 358$ K,	81
4.29	Burning velocities by Konnov and Dyakov [40] and corresponding simulation; fuel: CH ₄ , oxidiser: O ₂ /Ar = 17/83	82
4.30	Burning velocities by Hermanns [41] and corresponding simulation; fuel: H ₂ /CH ₄ = 30/70,	82
4.31	Burning velocities by Nilsson et al. [42] and corresponding simulation; fuel: H ₂ /CH ₄ = 35/65,	83
4.32	Burning velocities by Coppens, De Ruyck, and Konnov [43] and corresponding simulation; fuel: H ₂ /CH ₄ = 35/65, oxidiser: O ₂ /N ₂ = 16/84	83
4.33	Burning velocities by Coppens, De Ruyck, and Konnov [43] and corresponding simulation; fuel: H ₂ /CH ₄ = 35/65, oxidiser: O ₂ /N ₂ = 18/82	84
4.34	Burning velocities by Hermanns [41] and corresponding simulation; fuel: H ₂ /CH ₄ = 40/60,	84
4.35	Burning velocities by Nilsson et al. [42] and corresponding simulation; fuel: H ₂ /CH ₄ = 50/50,	85
4.36	Burning velocities by Yan et al. [39] and corresponding simulation; fuel: Biogenic mix 1,	85
4.37	Burning velocities by Yan et al. [39] and corresponding simulation; fuel: Biogenic mix 2,	86

4.38	Burning velocities by Park, Veloo, and Egolfopoulos [44] and corresponding simulation; fuel: C_2H_2 ,	86
4.39	Burning velocities by Park, Veloo, and Egolfopoulos [44] and corresponding simulation; fuel: C_2H_4 ,	87
4.40	Burning velocities by Park, Veloo, and Egolfopoulos [44] and corresponding simulation; fuel: C_2H_6 ,	87
4.41	Burning velocities by Nilsson et al. [42] and corresponding simulation; fuel: $H_2/CH_4/C_2H_6 = 35/52/13$,	88
5.1	Burner flame species profiles by Fomin et al. [45, 46] and corresponding simulation; fuel CH_4 , $\varphi = 1.0$	90
5.2	Burner flame species profiles by Fomin et al. [45, 46] and corresponding simulation; fuel CH_4 , $\varphi = 1.5$	90
5.3	Burner flame species profiles by Fomin et al. [45, 46] and corresponding simulation; fuel CH_4 , $\varphi = 1.9$	91

1 Ignition delay times in shock tubes



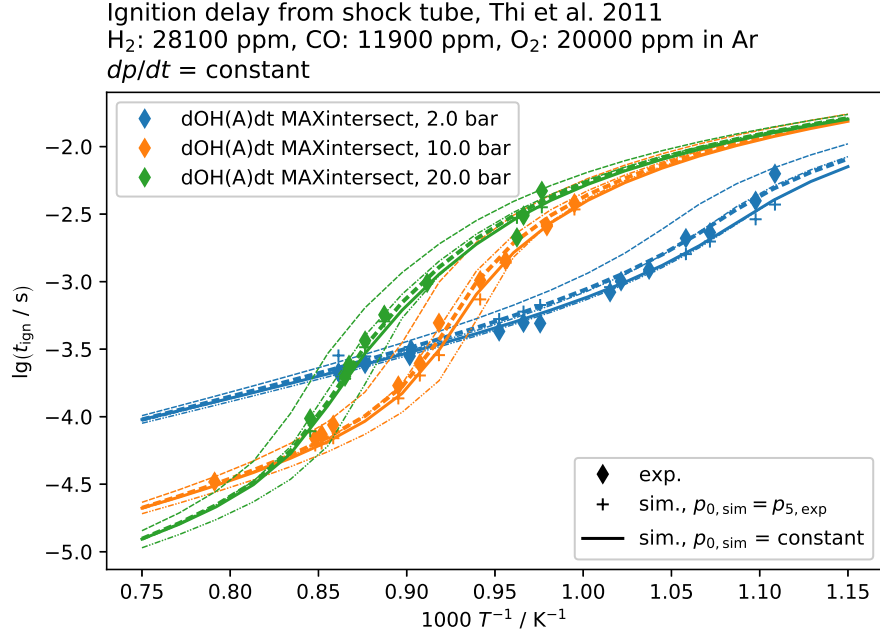


Figure 1.1: Ignition delay times from shock tube by Thi, Zhang, and Huang [1] and corresponding simulation; fuel: $\text{H}_2/\text{CO} = 70/30$, $\varphi = 1.0$

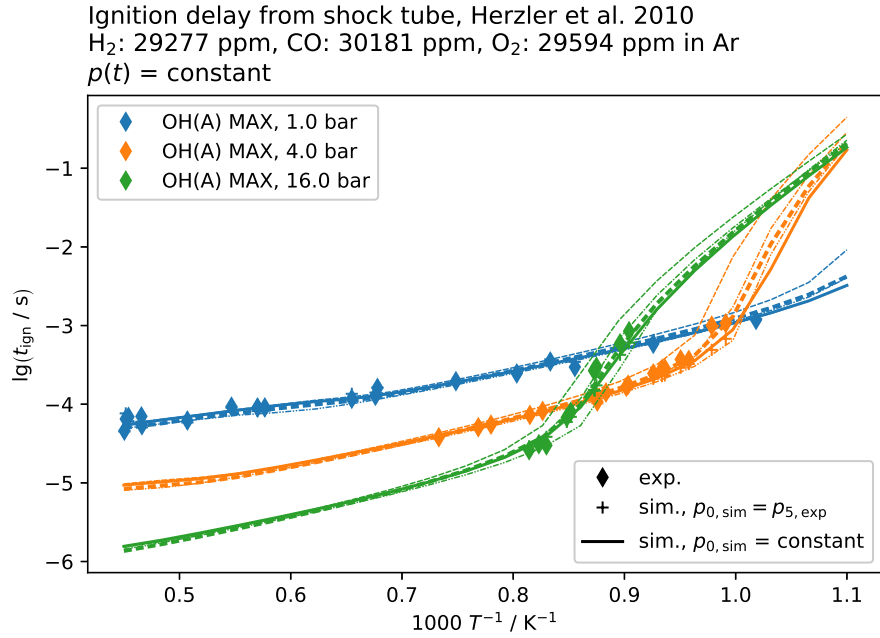


Figure 1.2: Ignition delay times from shock tube by Herzler, Naumann, and Griebel [2] and corresponding simulation; fuel: $\text{H}_2/\text{CO} = 50/50$, $\varphi = 1.0$

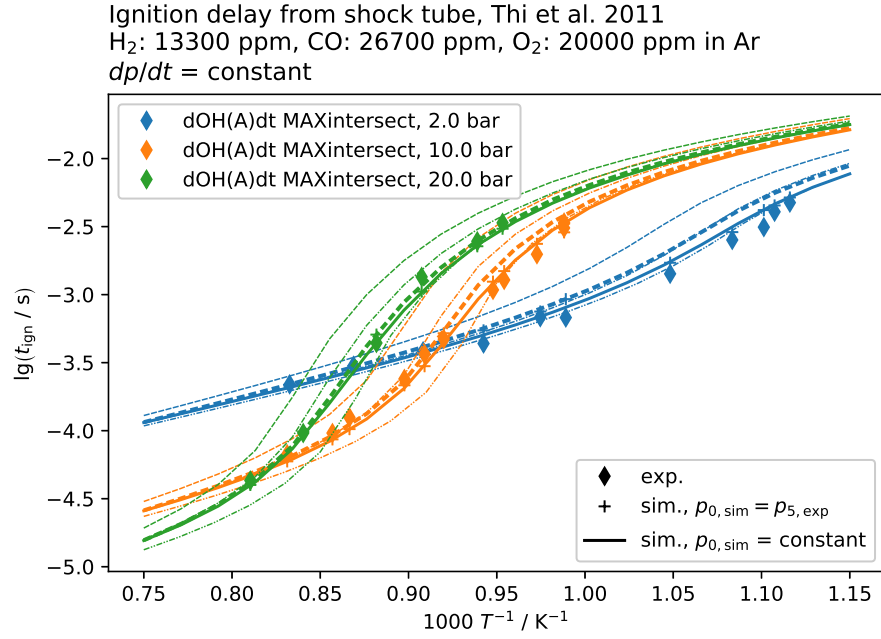


Figure 1.3: Ignition delay times from shock tube by Thi, Zhang, and Huang [1] and corresponding simulation; fuel: $\text{H}_2/\text{CO} = 33/67$, $\varphi = 1.0$

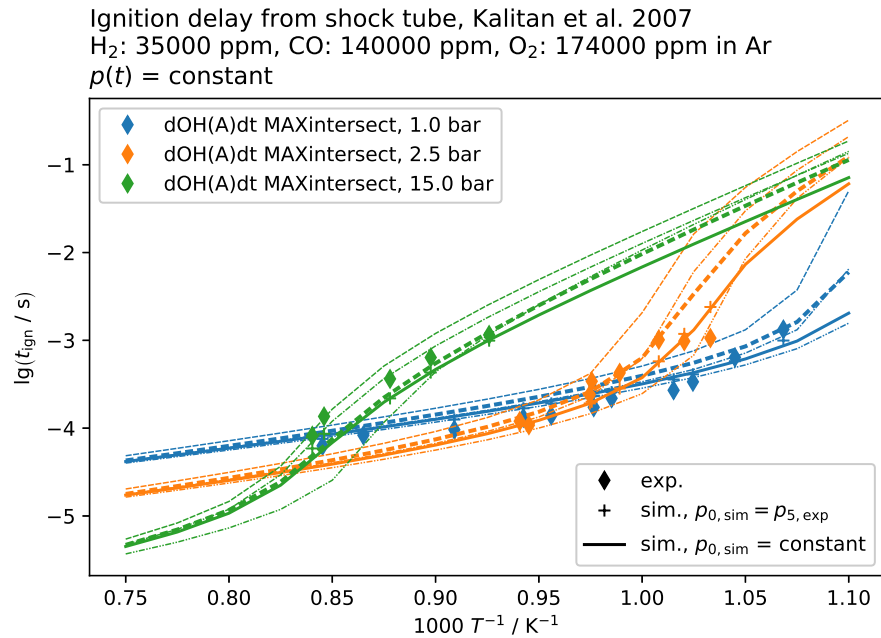


Figure 1.4: Ignition delay times from shock tube by Kalitan et al. [3] and corresponding simulation; fuel: $\text{H}_2/\text{CO} = 20/80$, $\varphi = 0.5$

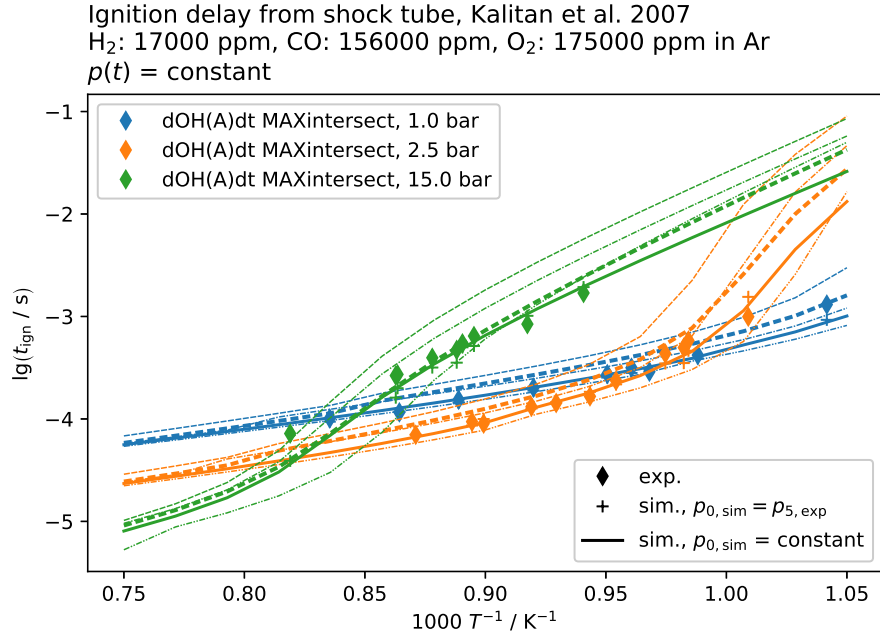


Figure 1.5: Ignition delay times from shock tube by Kalitan et al. [3] and corresponding simulation; fuel: $\text{H}_2/\text{CO} = 10/90$, $\varphi = 0.5$

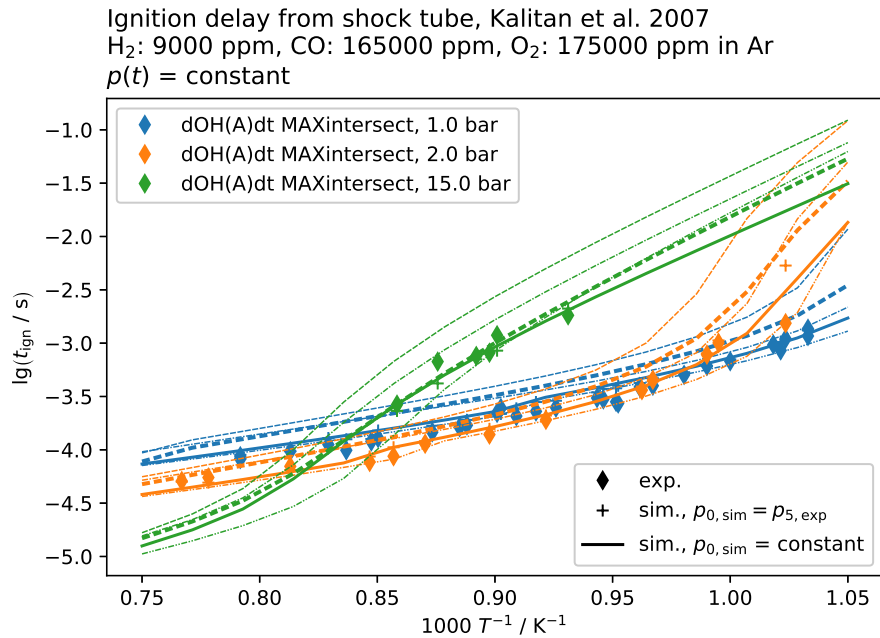


Figure 1.6: Ignition delay times from shock tube by Kalitan et al. [3] and corresponding simulation; fuel: $\text{H}_2/\text{CO} = 5/95$, $\varphi = 0.5$

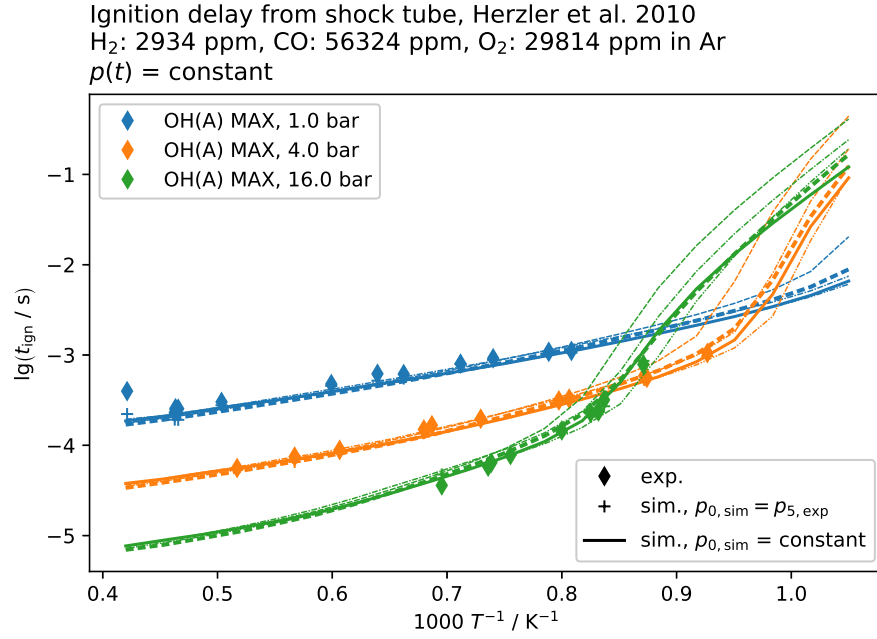


Figure 1.7: Ignition delay times from shock tube by Herzler, Naumann, and Griebel [2] and corresponding simulation; fuel: $\text{H}_2/\text{CO} = 5/95$, $\varphi = 1.0$

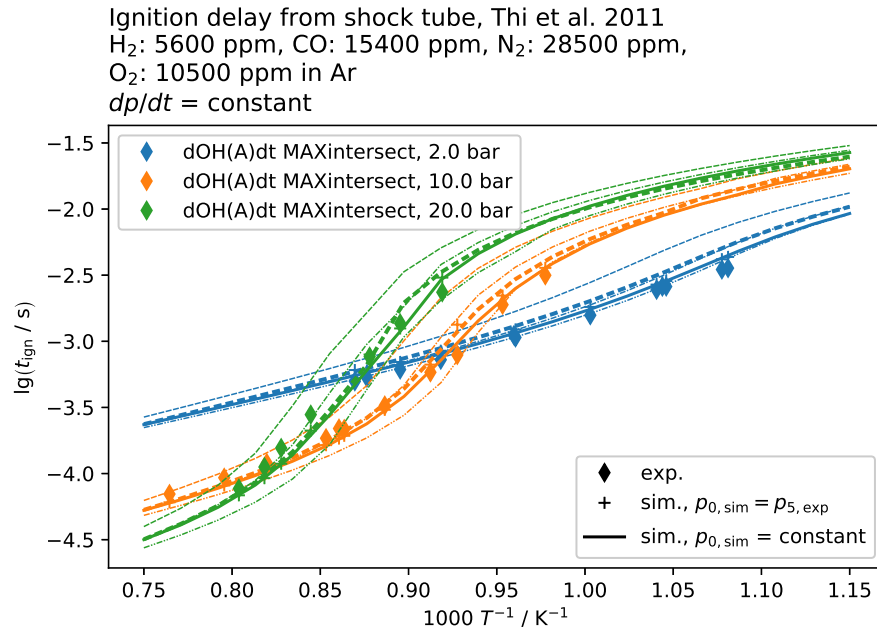


Figure 1.8: Ignition delay times from shock tube by Thi, Zhang, and Huang [1] and corresponding simulation; fuel: $\text{H}_2/\text{CO} = 27/73$, $\varphi = 1.0$, with N_2 in diluent

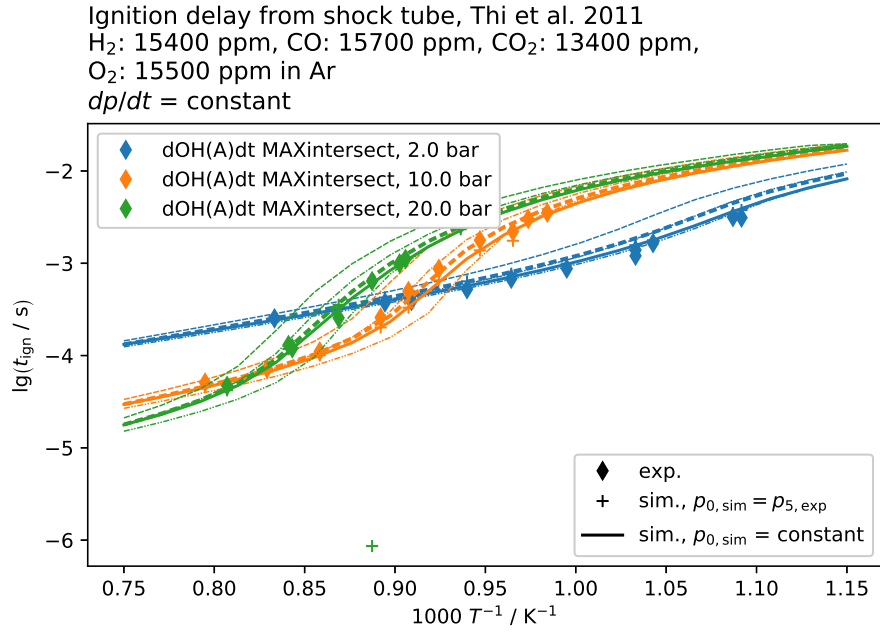


Figure 1.9: Ignition delay times from shock tube by Thi, Zhang, and Huang [1] and corresponding simulation; fuel: $\text{H}_2/\text{CO} = 50/50$, $\varphi = 1.0$, with CO_2 in diluent

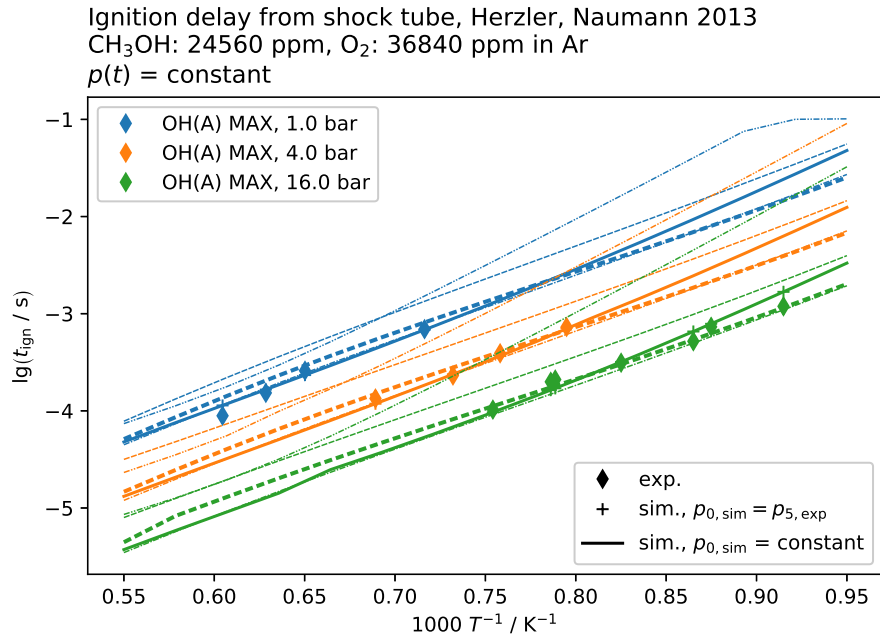


Figure 1.10: Ignition delay times from shock tube by Herzler and Naumann [4] and corresponding simulation; fuel: CH_3OH , $\varphi = 1.0$

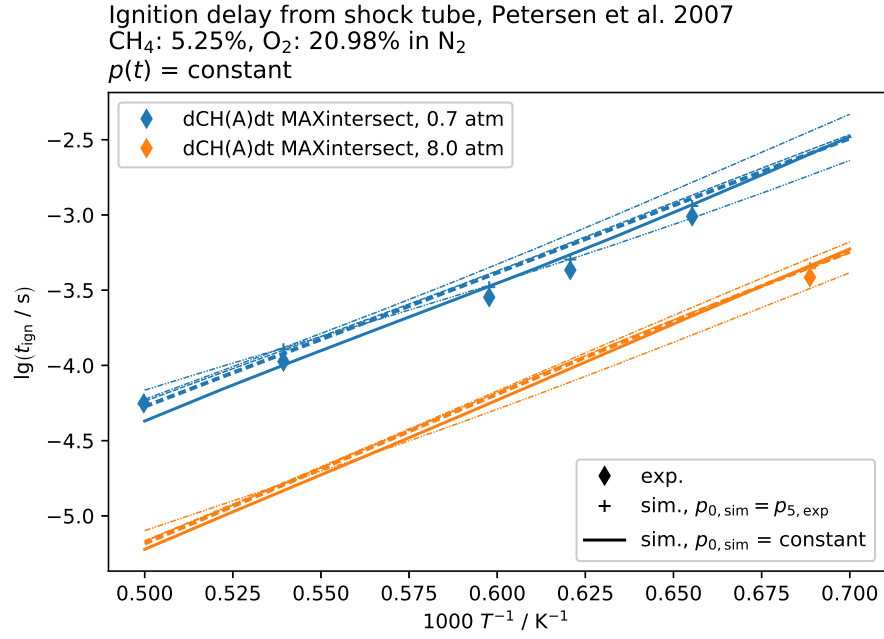


Figure 1.11: Ignition delay times from shock tube by Petersen et al. [5] and corresponding simulation; fuel: CH_4 , $\varphi = 0.5$

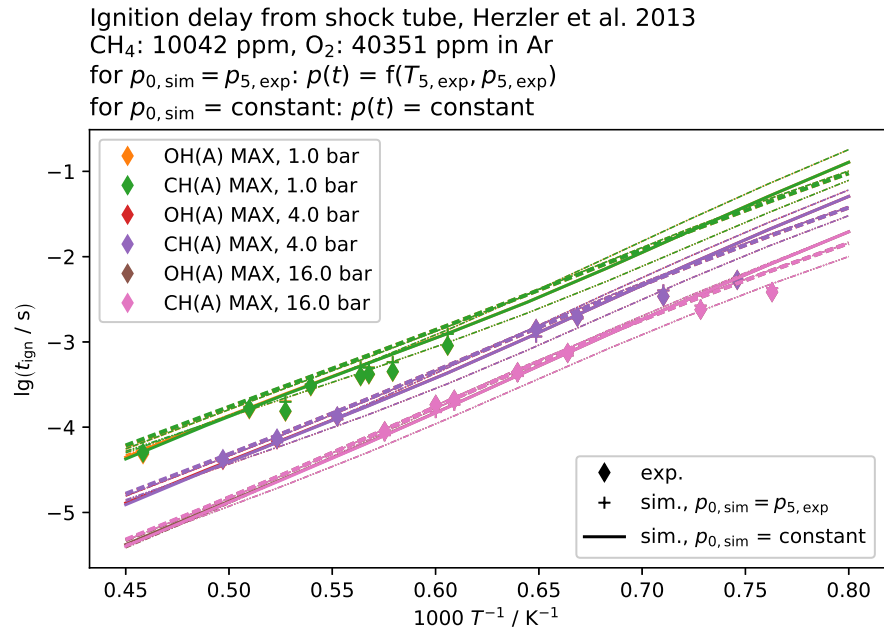


Figure 1.12: Ignition delay times from shock tube by Herzler et al. [6] and corresponding simulation; fuel: CH_4 , $\varphi = 0.5$, $X_{\text{Ar}} = 0.95$

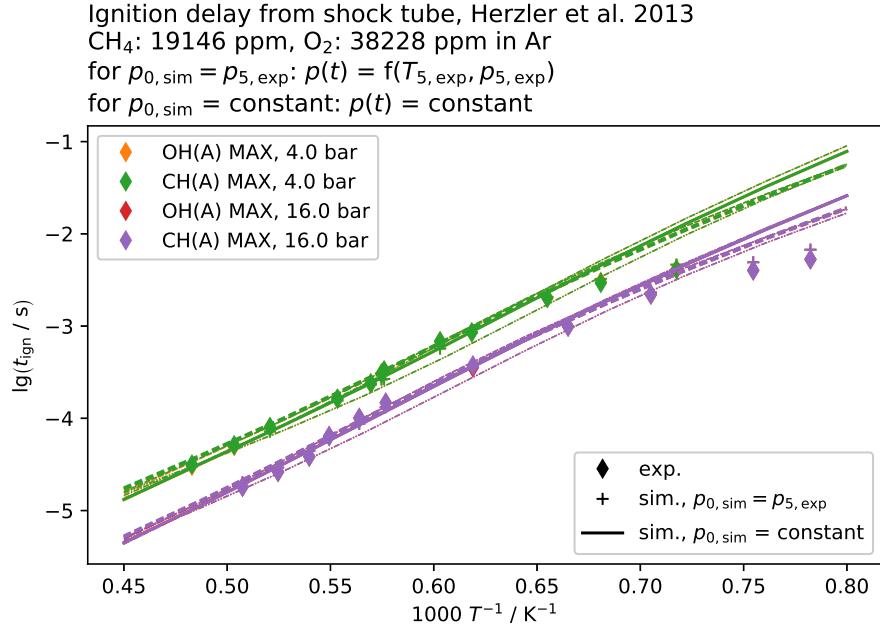


Figure 1.13: Ignition delay times from shock tube by Herzler et al. [6] and corresponding simulation; fuel: CH_4 , $\varphi = 1.0$, $X_{\text{Ar}} = 0.94$

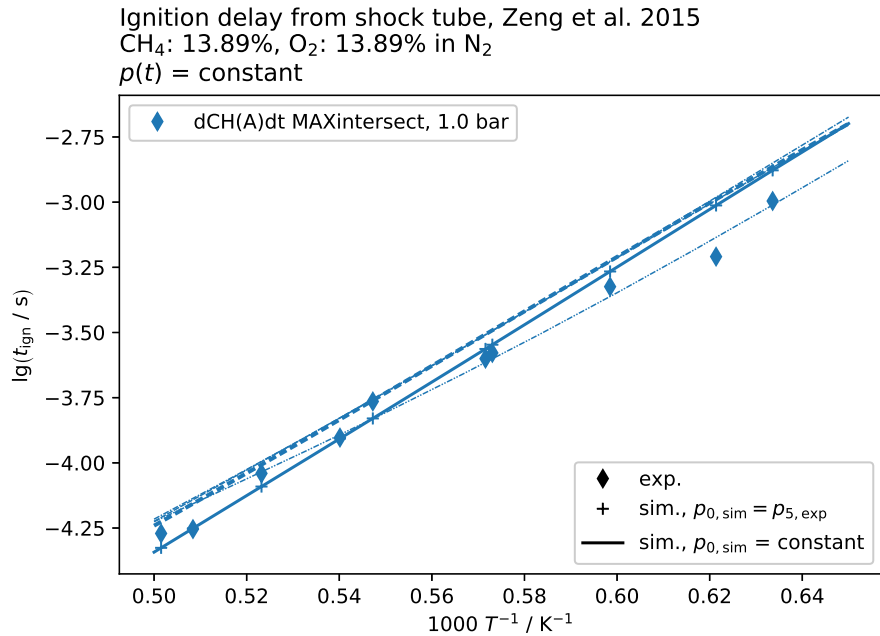


Figure 1.14: Ignition delay times from shock tube by Zeng et al. [7] and corresponding simulation; fuel: CH_4 , $\varphi = 2.0$, $X_{\text{N}_2} = 0.72$

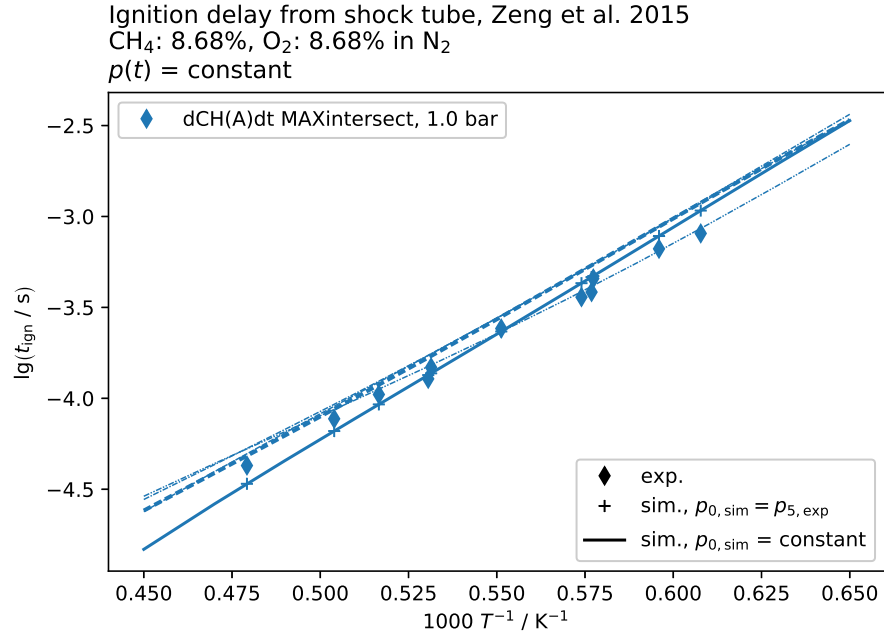


Figure 1.15: Ignition delay times from shock tube by Zeng et al. [7] and corresponding simulation; fuel: CH_4 , $\varphi = 2.0$, $X_{\text{N}_2} = 0.83$

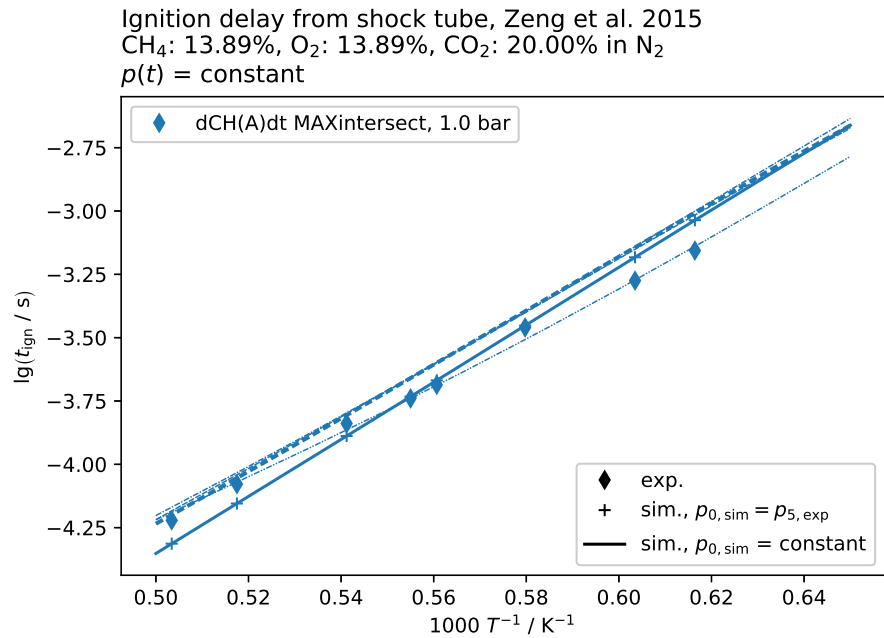


Figure 1.16: Ignition delay times from shock tube by Zeng et al. [7] and corresponding simulation; fuel: CH_4 , $\varphi = 2.0$, $X_{\text{CO}_2} = 0.20$, $X_{\text{N}_2} = 0.52$

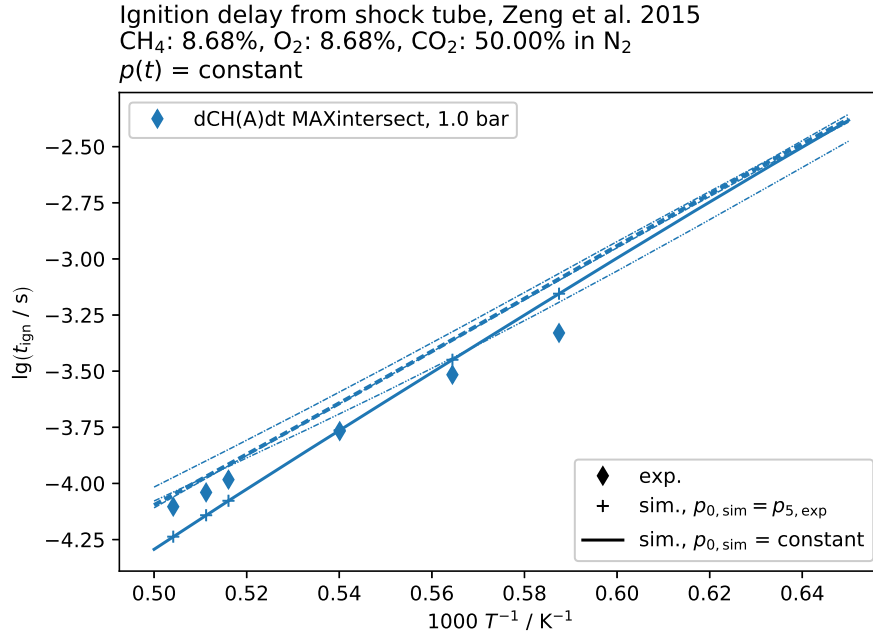


Figure 1.17: Ignition delay times from shock tube by Zeng et al. [7] and corresponding simulation; fuel: CH_4 , $\varphi = 2.0$, $X_{\text{CO}_2} = 0.50$, $X_{\text{N}_2} = 0.33$

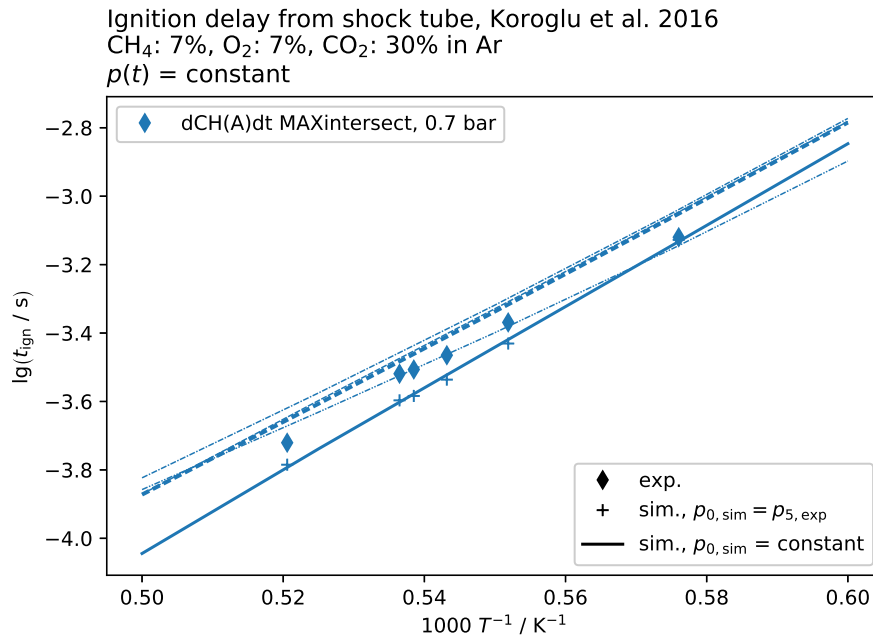


Figure 1.18: Ignition delay times from shock tube by Koroglu et al. [8] and corresponding simulation; fuel: CH_4 , $\varphi = 2.0$, $X_{\text{CO}_2} = 0.30$, $X_{\text{Ar}} = 0.56$

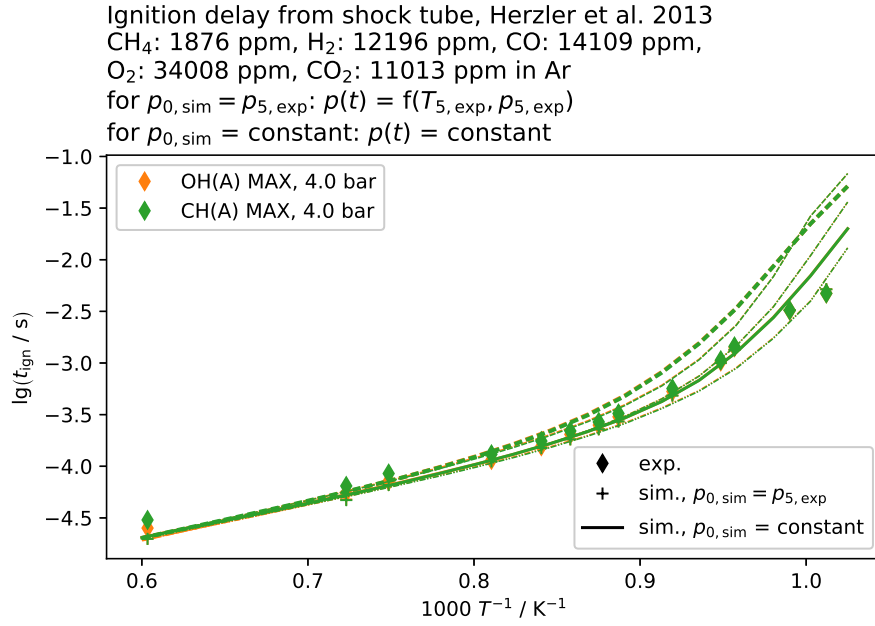


Figure 1.19: Ignition delay times from shock tube by Herzler et al. [6] and corresponding simulation; fuel: $\text{H}_2/\text{CO}/\text{CH}_4/\text{CO}_2 = 5/31/38/2$, $\varphi = 0.5$, $X_{\text{Ar}} = 0.93$

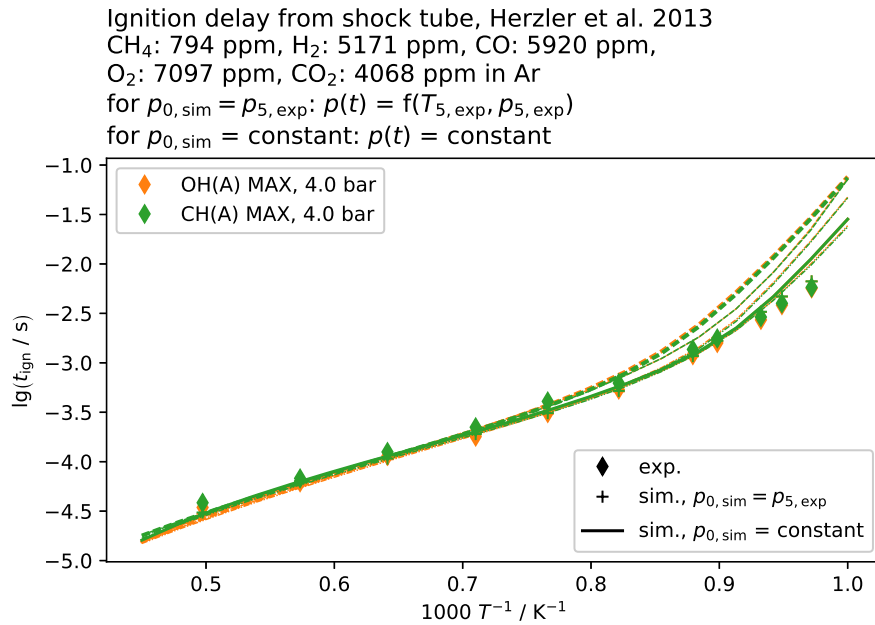


Figure 1.20: Ignition delay times from shock tube by Herzler et al. [6] and corresponding simulation; fuel: $\text{H}_2/\text{CO}/\text{CH}_4/\text{CO}_2 = 5/31/38/2$, $\varphi = 0.5$, $X_{\text{Ar}} = 0.98$

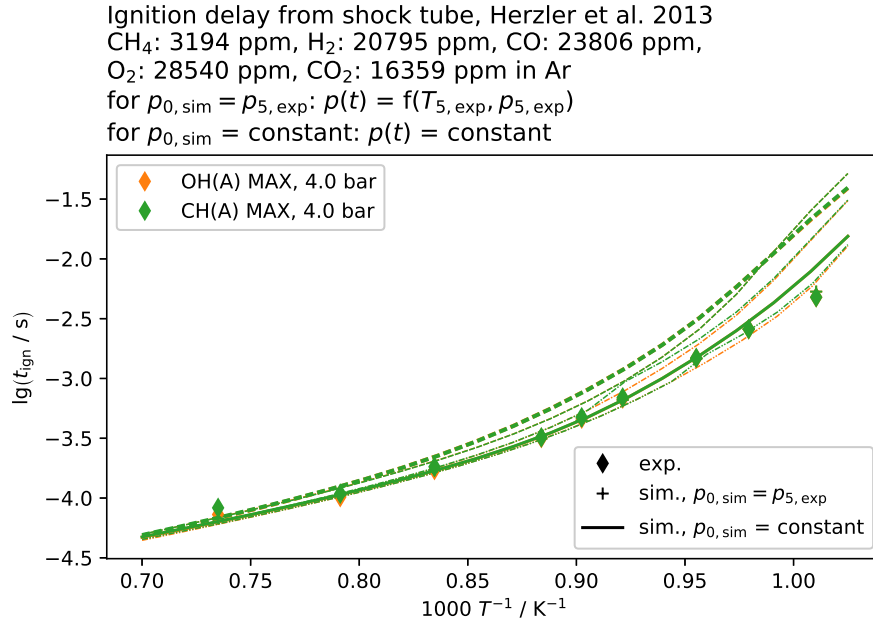


Figure 1.21: Ignition delay times from shock tube by Herzler et al. [6] and corresponding simulation; fuel: $\text{H}_2/\text{CO}/\text{CH}_4/\text{CO}_2 = 5/31/38/2$, $\varphi = 1.0$, $X_{\text{Ar}} = 0.91$

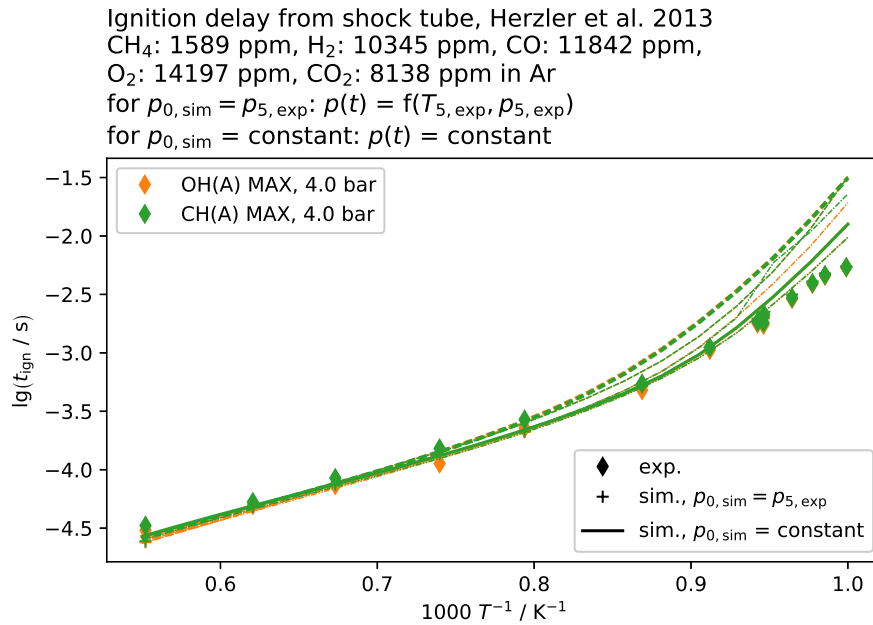


Figure 1.22: Ignition delay times from shock tube by Herzler et al. [6] and corresponding simulation; fuel: $\text{H}_2/\text{CO}/\text{CH}_4/\text{CO}_2 = 5/31/38/2$, $\varphi = 1.0$, $X_{\text{Ar}} = 0.95$

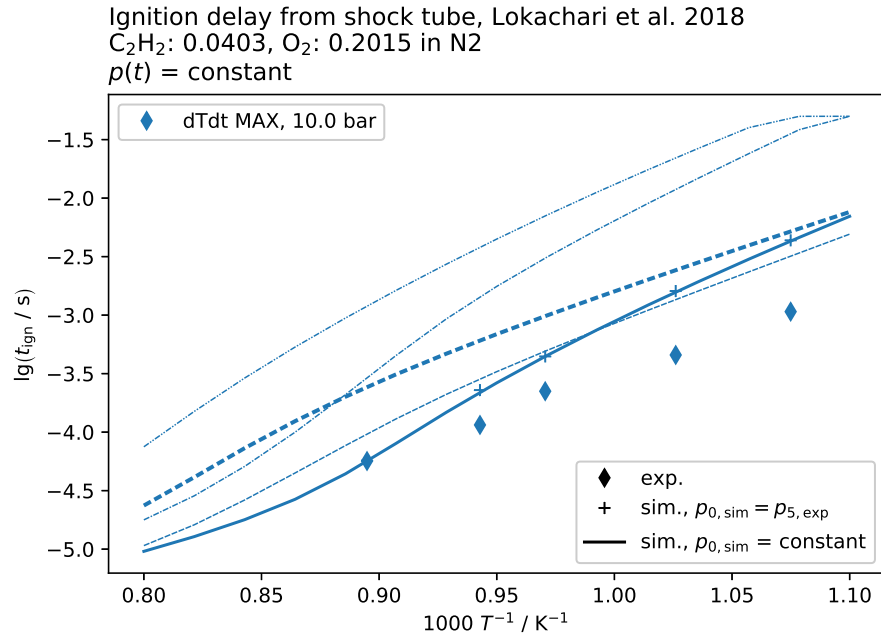


Figure 1.23: Ignition delay times from shock tube by Lokachari et al. [9] and corresponding simulation; fuel: C_2H_2 , $\varphi = 0.5$

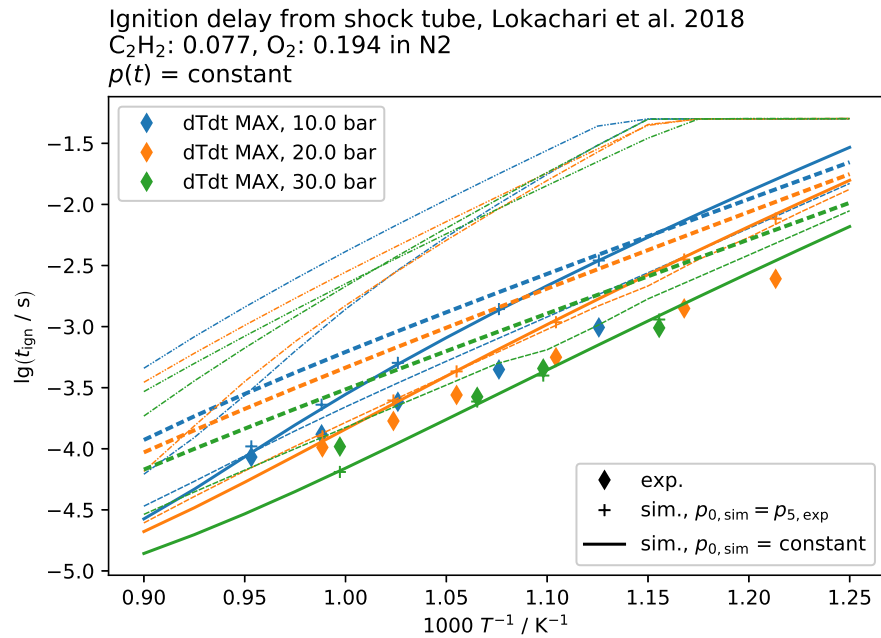


Figure 1.24: Ignition delay times from shock tube by Lokachari et al. [9] and corresponding simulation; fuel: C_2H_2 , $\varphi = 1.0$

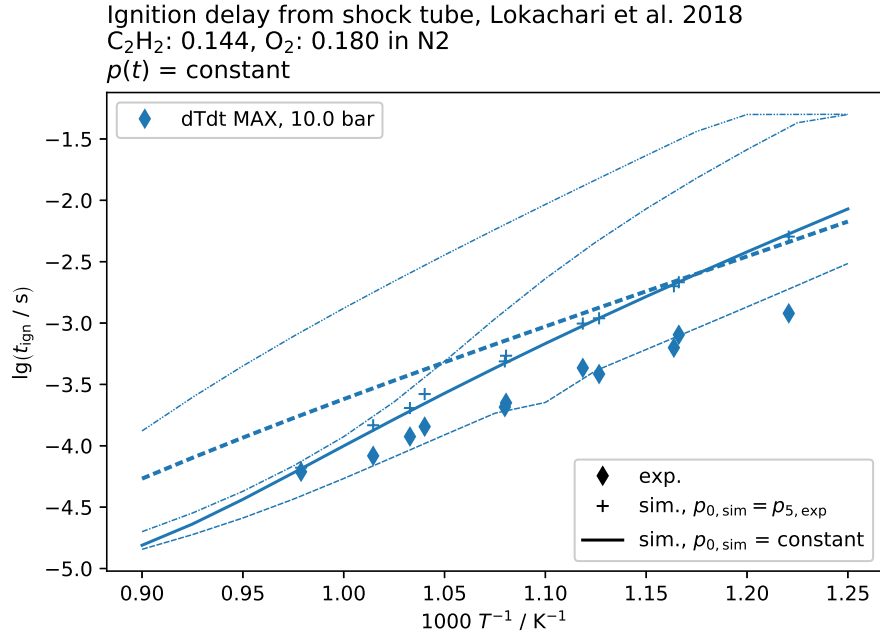


Figure 1.25: Ignition delay times from shock tube by Lokachari et al. [9] and corresponding simulation; fuel: C_2H_2 , $\varphi = 2.0$

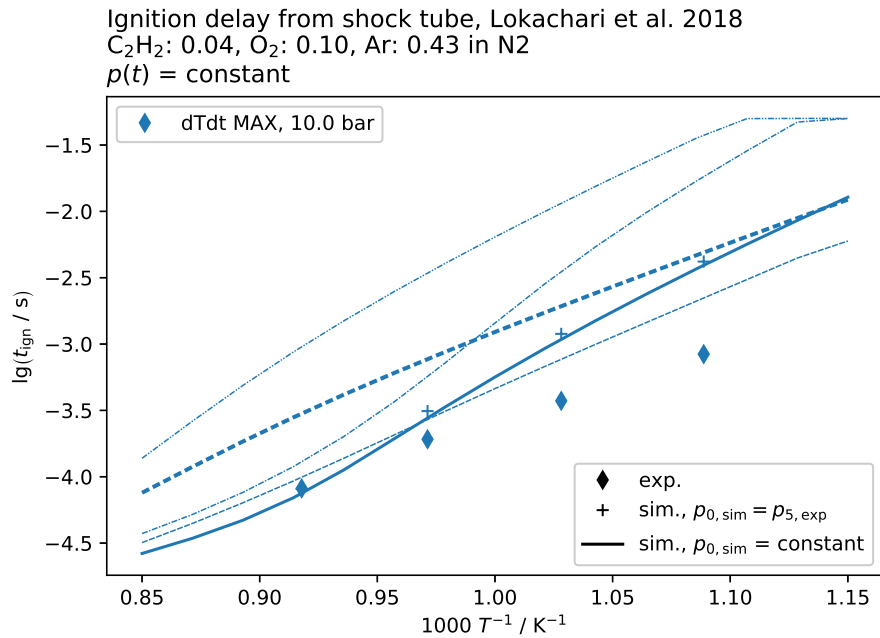


Figure 1.26: Ignition delay times from shock tube by Lokachari et al. [9] and corresponding simulation; fuel: C_2H_2 , $\varphi = 1.0$, $X_{\text{N}_2} = 0.43$, $X_{\text{Ar}} = 0.43$

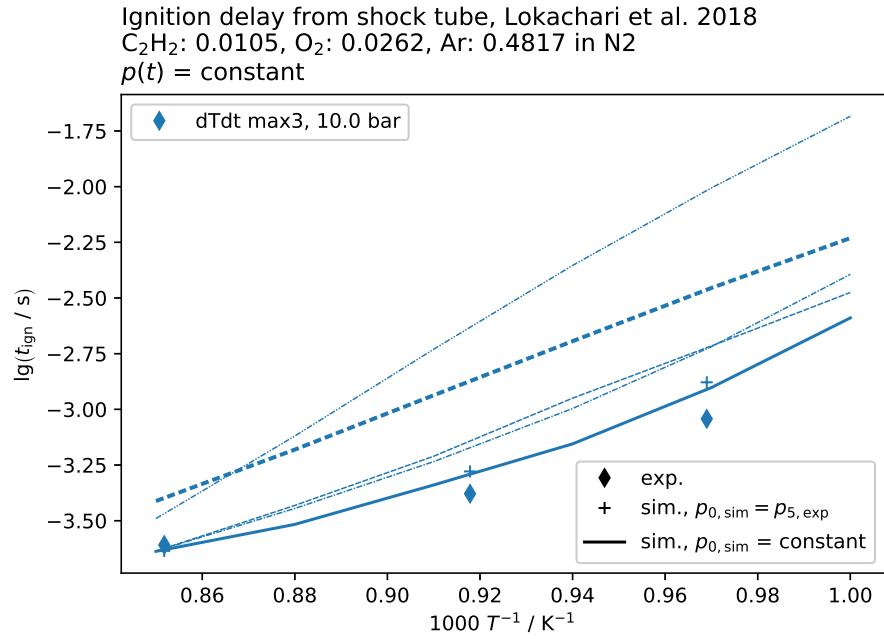


Figure 1.27: Ignition delay times from shock tube by Lokachari et al. [9] and corresponding simulation; fuel: C_2H_2 , $\varphi = 1.0$, $X_{\text{N}_2} = 0.48$, $X_{\text{Ar}} = 0.48$

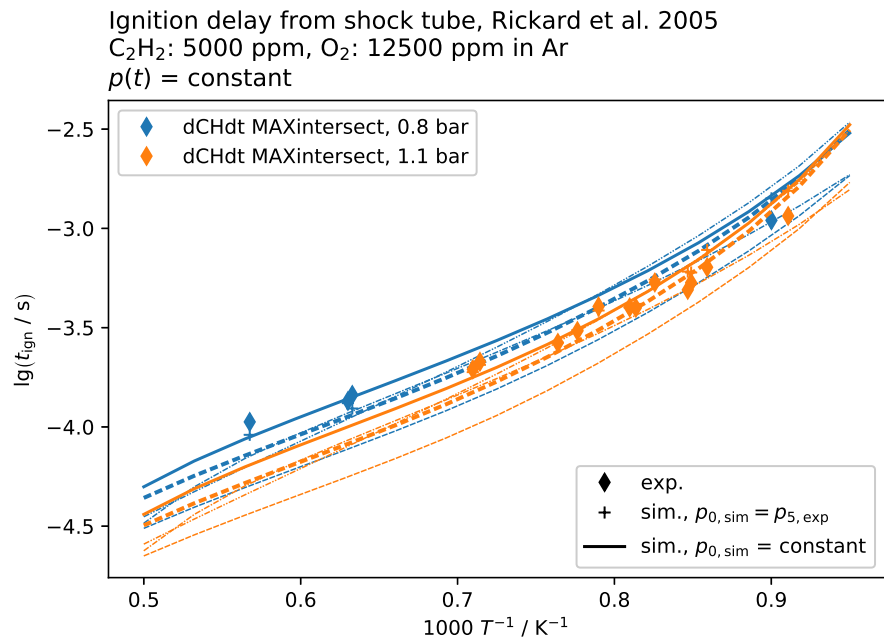


Figure 1.28: Ignition delay times from shock tube by Rickard, Hall, and Petersen [10] and corresponding simulation; fuel: C_2H_2 , $\varphi = 0.5$

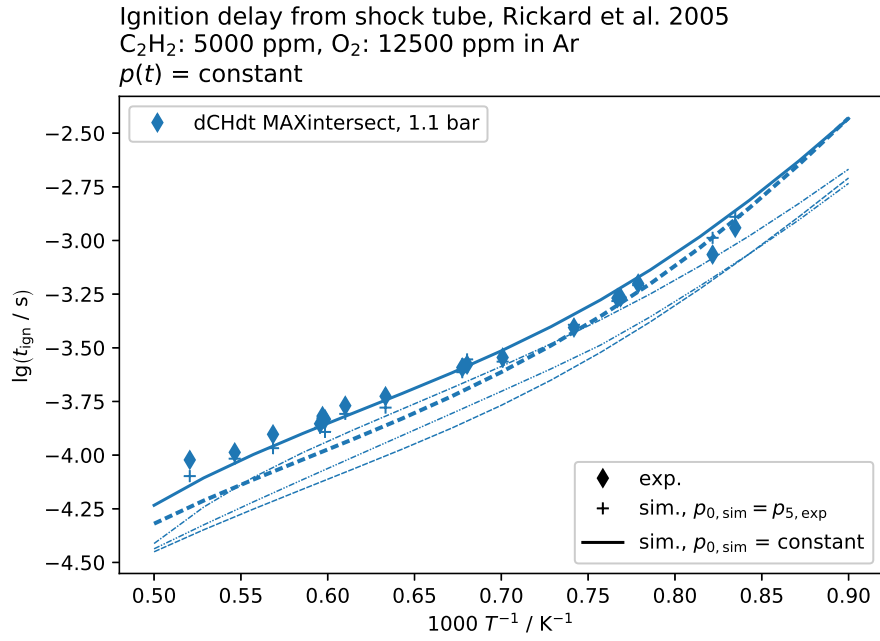


Figure 1.29: Ignition delay times from shock tube by Rickard, Hall, and Petersen [10] and corresponding simulation; fuel: C_2H_2 , $\varphi = 1.0$

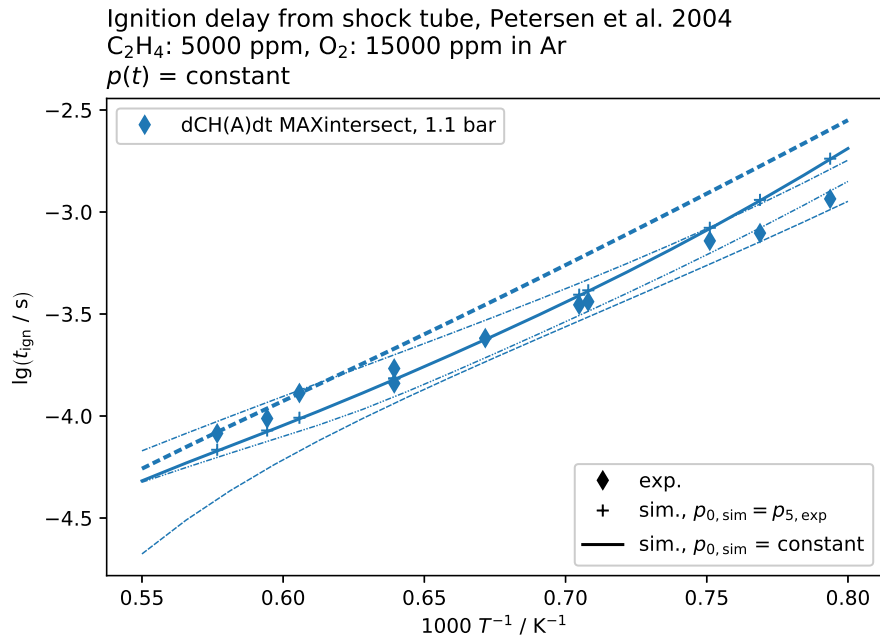


Figure 1.30: Ignition delay times from shock tube by Petersen et al. [11] and corresponding simulation; fuel: C_2H_4 , $\varphi = 1.0$

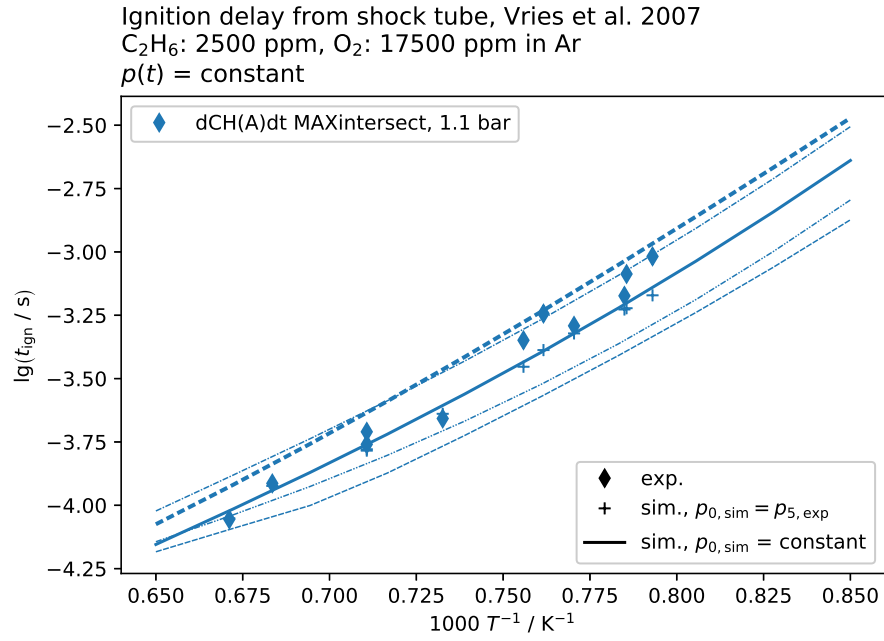


Figure 1.31: Ignition delay times from shock tube by Vries et al. [12] and corresponding simulation; fuel: C_2H_6 , $\varphi = 0.5$

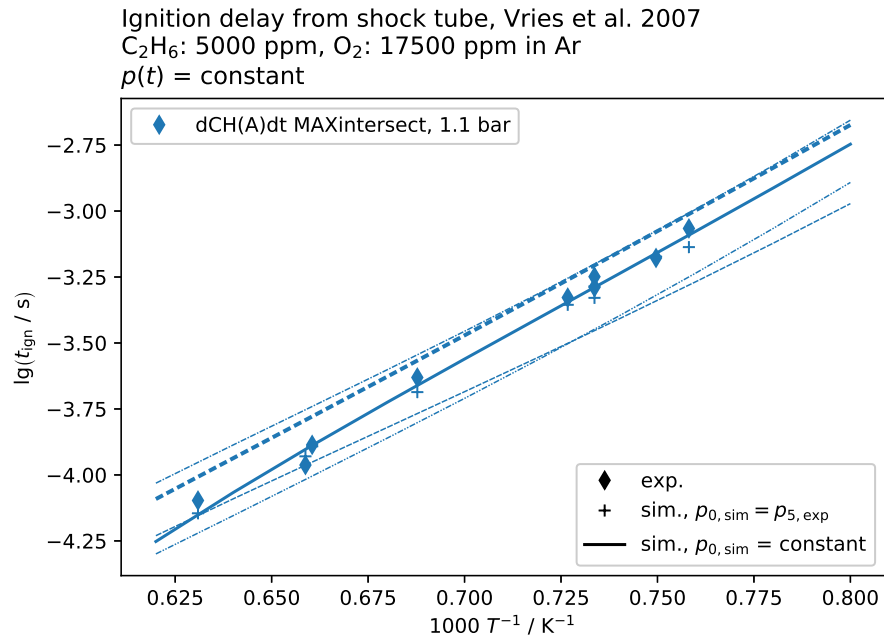


Figure 1.32: Ignition delay times from shock tube by Vries et al. [12] and corresponding simulation; fuel: C_2H_6 , $\varphi = 1.0$

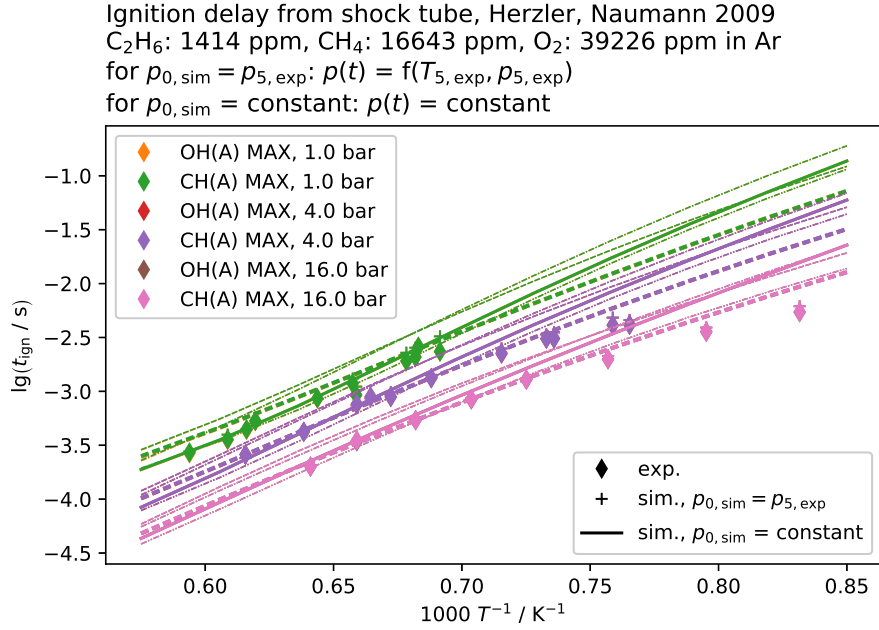


Figure 1.33: Ignition delay times from shock tube by Herzler and Naumann [13] and corresponding simulation; fuel: RG, $\varphi = 1.0$, $\text{RG} = \text{C}_2\text{H}_6/\text{CH}_4 = 8/92$

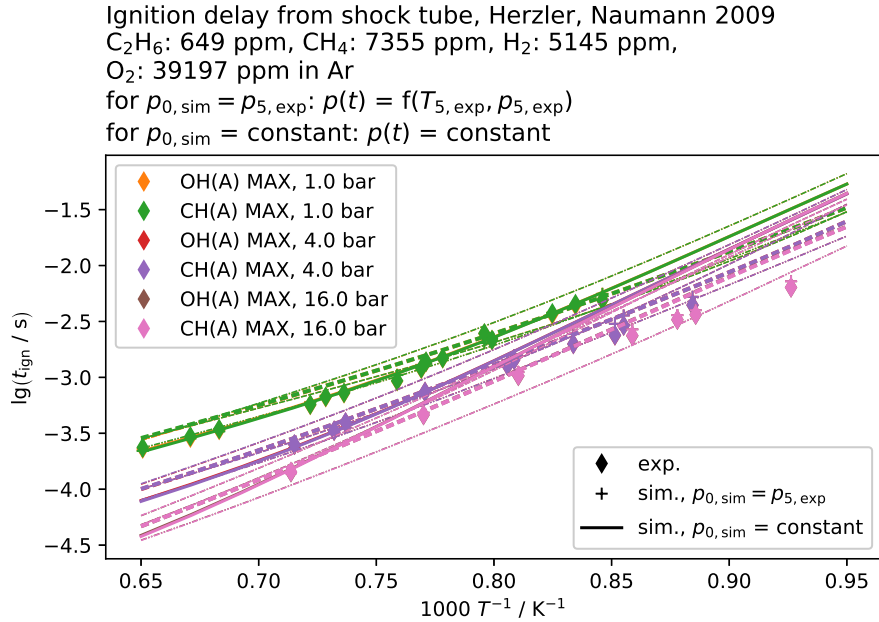


Figure 1.34: Ignition delay times from shock tube by Herzler and Naumann [13] and corresponding simulation; fuel: $\text{RG}/\text{H}_2 = 60/40$, $\varphi = 0.5$, $\text{RG} = \text{C}_2\text{H}_6/\text{CH}_4 = 8/92$

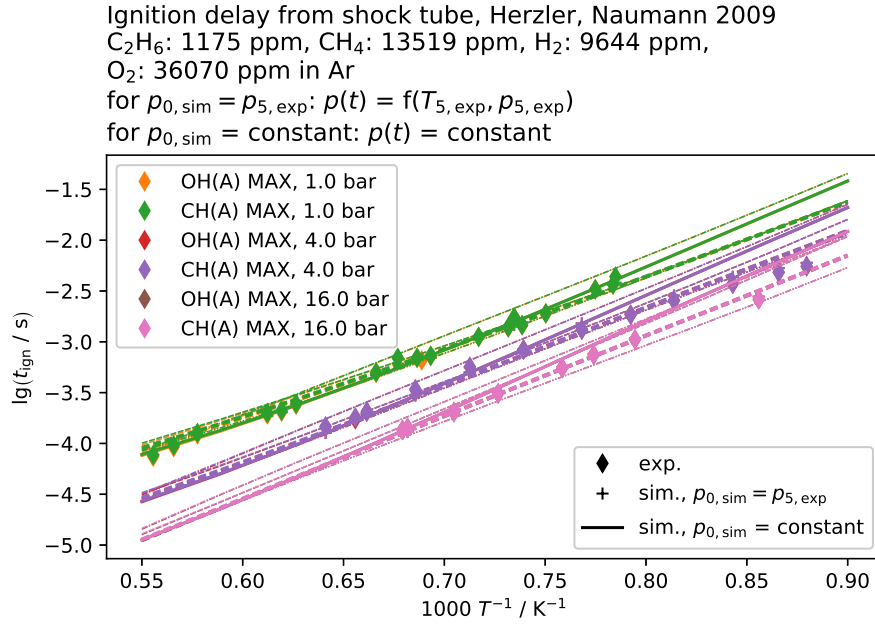


Figure 1.35: Ignition delay times from shock tube by Herzler and Naumann [13] and corresponding simulation; fuel: $\text{RG}/\text{H}_2 = 60/40$, $\varphi = 1.0$, $\text{RG} = \text{C}_2\text{H}_6/\text{CH}_4 = 8/92$

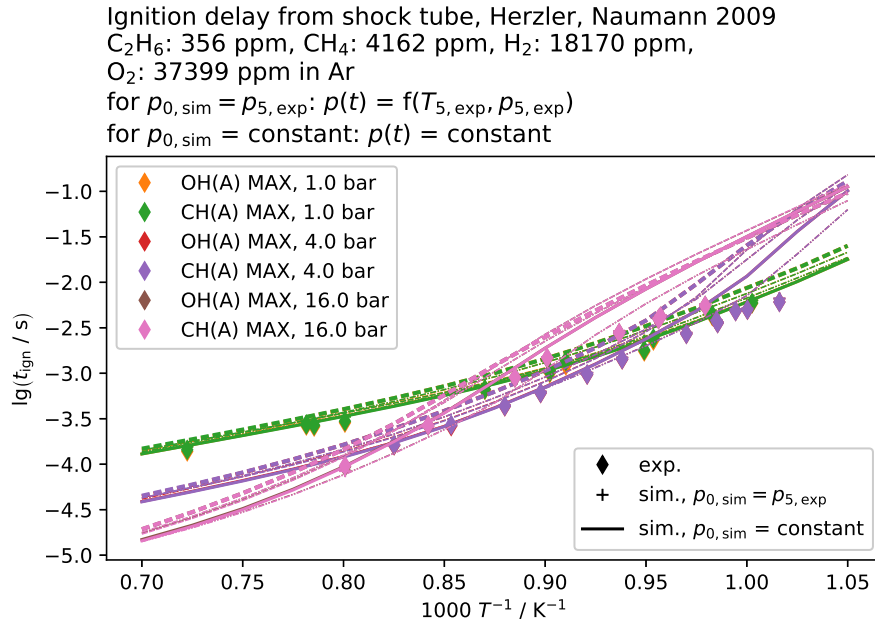


Figure 1.36: Ignition delay times from shock tube by Herzler and Naumann [13] and corresponding simulation; fuel: $\text{RG}/\text{H}_2 = 20/80$, $\varphi = 0.5$, $\text{RG} = \text{C}_2\text{H}_6/\text{CH}_4 = 8/92$

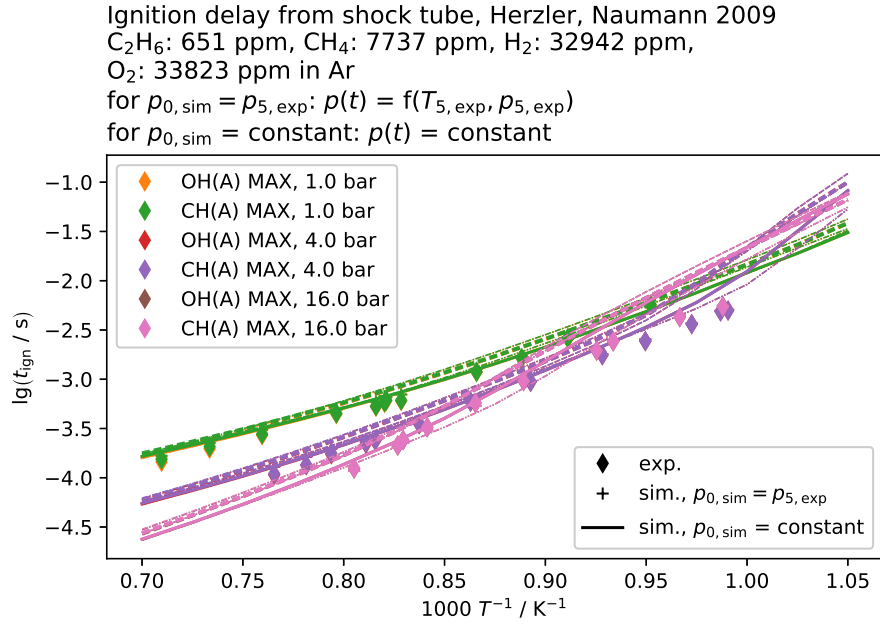


Figure 1.37: Ignition delay times from shock tube by Herzler and Naumann [13] and corresponding simulation; fuel: $\text{RG}/\text{H}_2 = 20/80$, $\varphi = 1.0$, $\text{RG} = \text{C}_2\text{H}_6/\text{CH}_4 = 8/92$

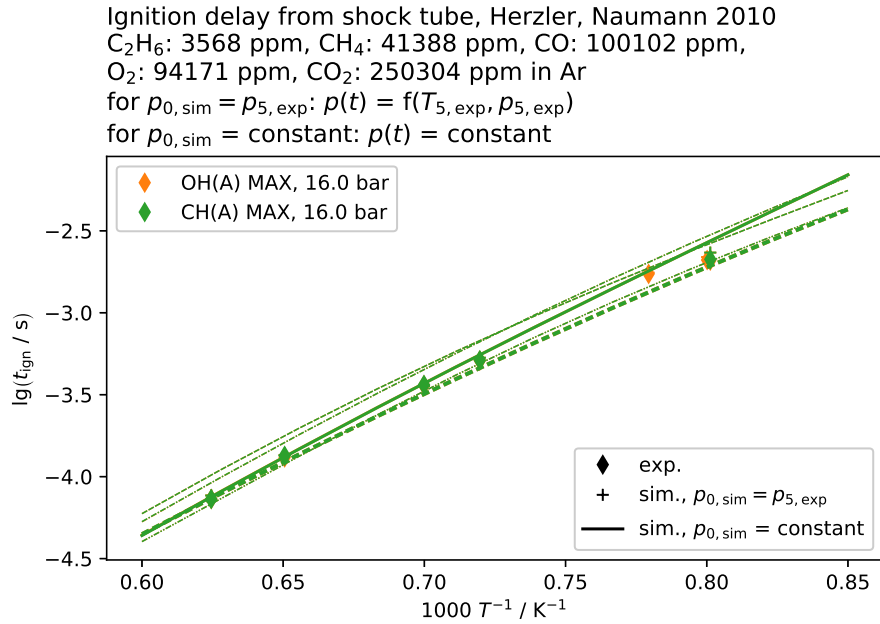


Figure 1.38: Ignition delay times from shock tube by Herzler and Naumann [14] and corresponding simulation; fuel: $\text{RG}/\text{CO} = 31/69$, $\varphi = 1.0$, $\text{RG} = \text{C}_2\text{H}_6/\text{CH}_4 = 8/92$

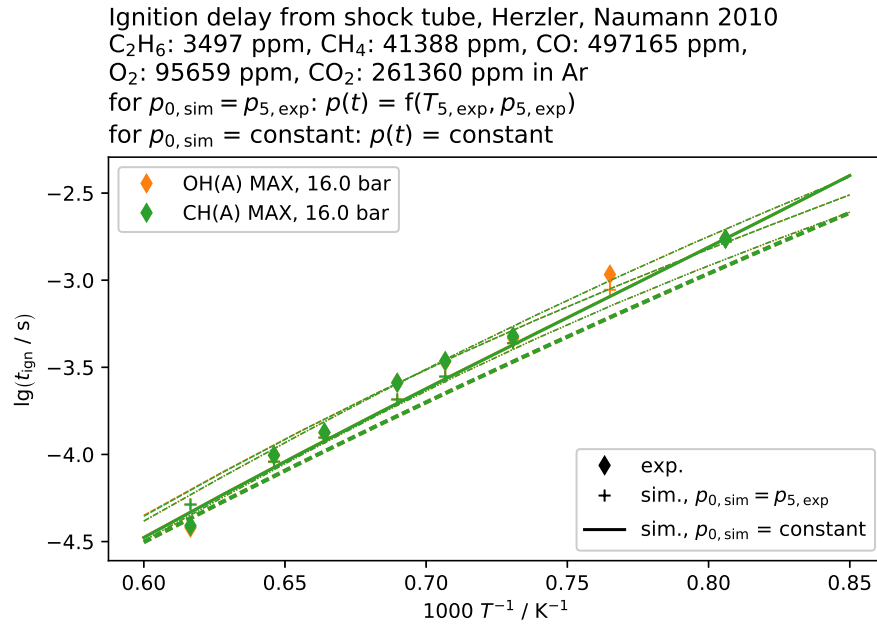
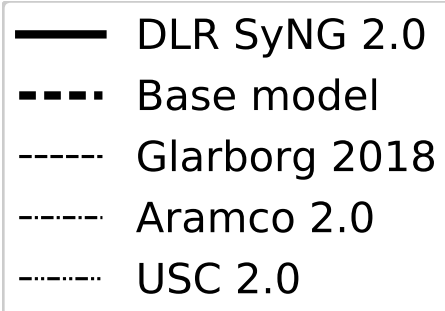


Figure 1.39: Ignition delay times from shock tube by Herzler and Naumann [14] and corresponding simulation; fuel: $\text{RG}/\text{CO} = 8/92$, $\varphi = 1.0$, $\text{RG} = \text{C}_2\text{H}_6/\text{CH}_4 = 8/92$

2 Species profiles in flow reactors



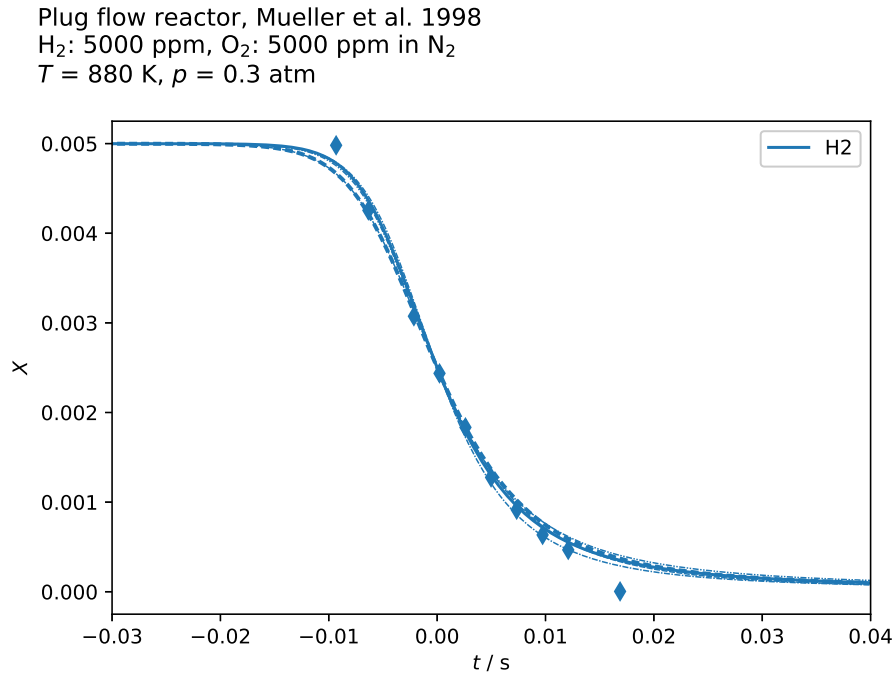


Figure 2.1: Flow reactor results by Mueller et al. [15] and its simulation; fuel: H_2 , $T = 880 \text{ K}$, $p = 0.3 \text{ atm}$, $\varphi = 0.5$,

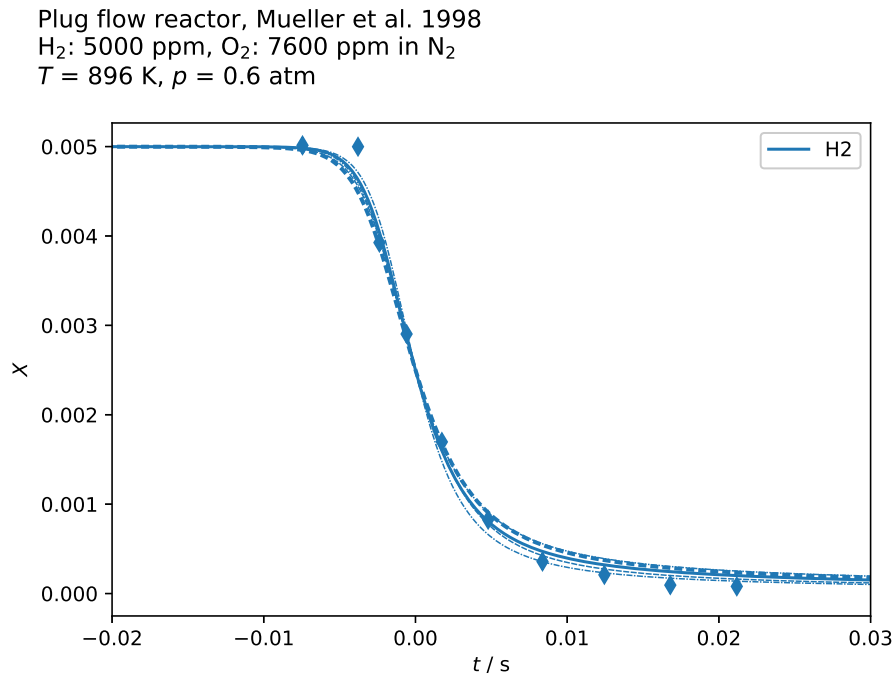


Figure 2.2: Flow reactor results by Mueller et al. [15] and its simulation; fuel: H_2 , $T = 896 \text{ K}$, $p = 0.6 \text{ atm}$, $\varphi = 0.3$,

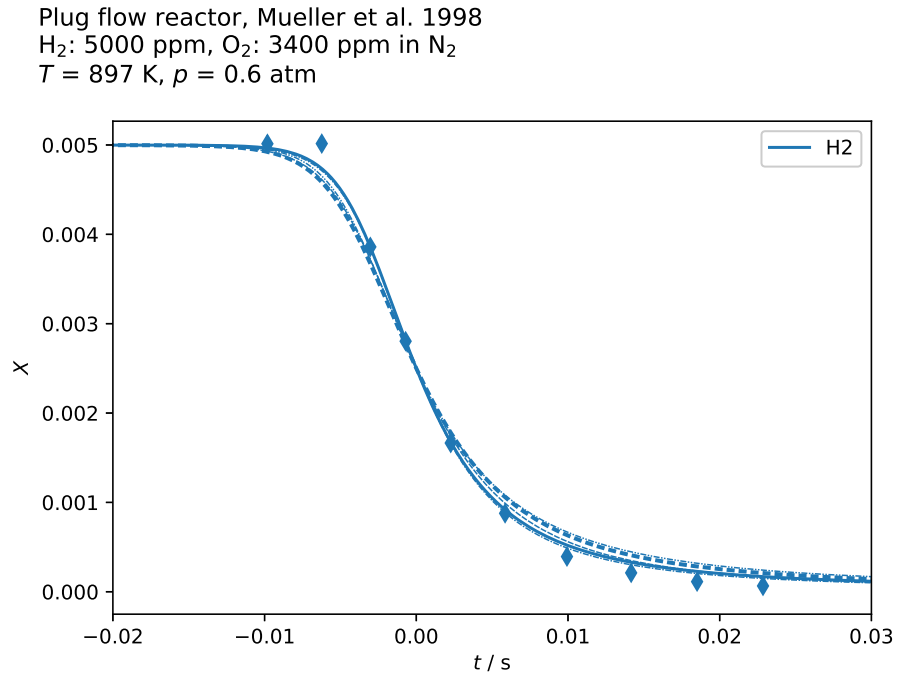


Figure 2.3: Flow reactor results by Mueller et al. [15] and its simulation; fuel: H_2 , $T = 897 \text{ K}$, $p = 0.6 \text{ atm}$, $\varphi = 0.8$,

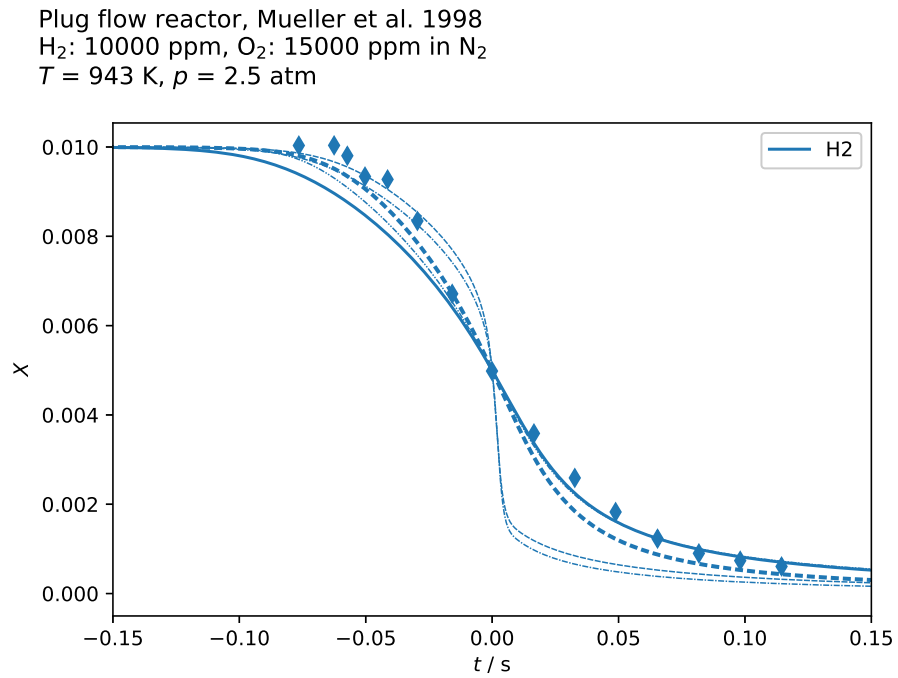


Figure 2.4: Flow reactor results by Mueller et al. [15] and its simulation; fuel: H_2 , $T = 943 \text{ K}$, $p = 2.5 \text{ atm}$, $\varphi = 0.3$,

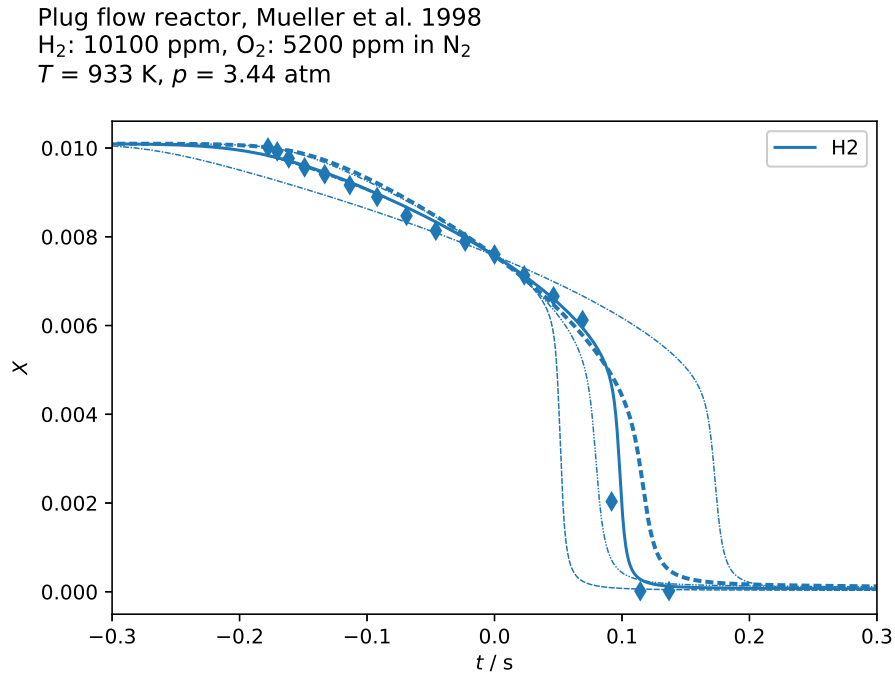


Figure 2.5: Flow reactor results by Mueller et al. [15] and its simulation; fuel: H_2 , $T = 933 \text{ K}$, $p = 3.44 \text{ atm}$, $\varphi = 1$,

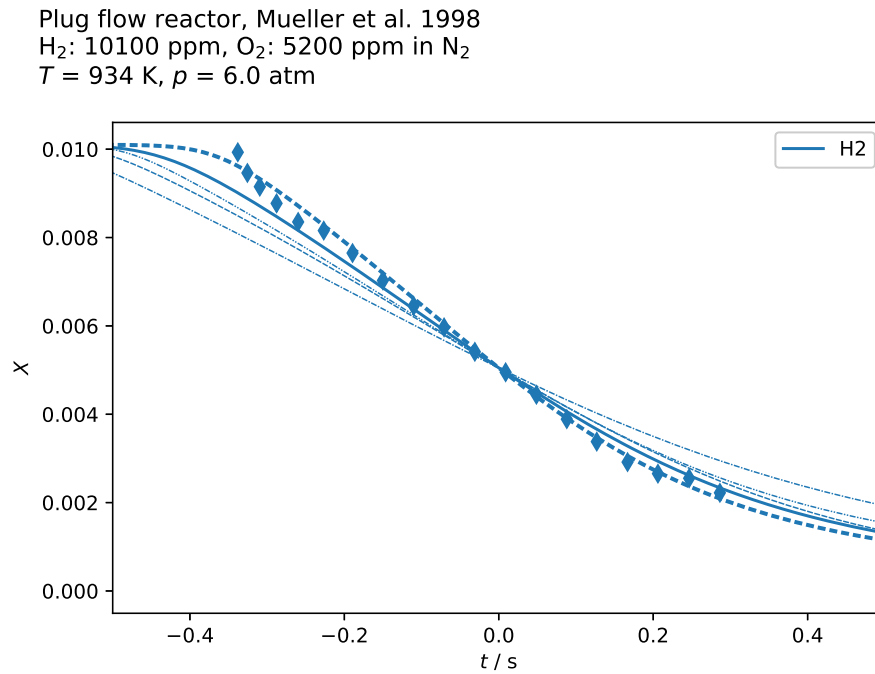


Figure 2.6: Flow reactor results by Mueller et al. [15] and its simulation; fuel: H_2 , $T = 934 \text{ K}$, $p = 6.0 \text{ atm}$, $\varphi = 1$,

Plug flow reactor, Mueller et al. 1998
 H_2 : 12900 ppm, O_2 : 21900 ppm in N_2
 $T = 884 \text{ K}$, $p = 6.5 \text{ atm}$

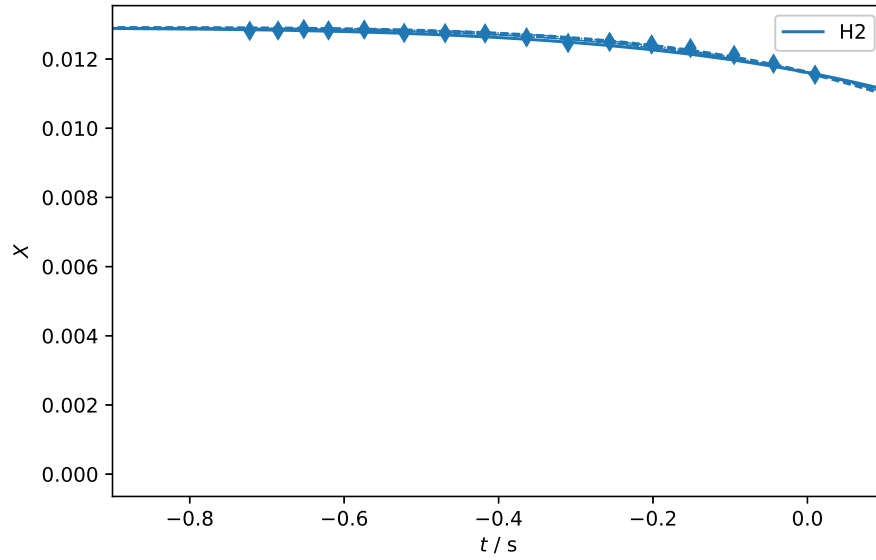


Figure 2.7: Flow reactor results by Mueller et al. [15] and its simulation; fuel: H_2 , $T = 884 \text{ K}$, $p = 6.5 \text{ atm}$, $\varphi = 0.3$,

Plug flow reactor, Mueller et al. 1998
 H_2 : 13000 ppm, O_2 : 22100 ppm in N_2
 $T = 889 \text{ K}$, $p = 6.5 \text{ atm}$

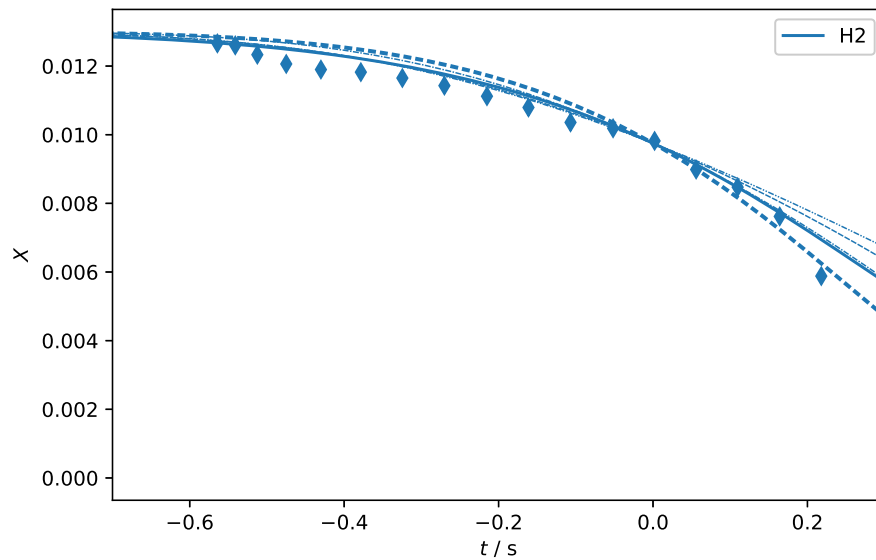


Figure 2.8: Flow reactor results by Mueller et al. [15] and its simulation; fuel: H_2 , $T = 889 \text{ K}$, $p = 6.5 \text{ atm}$, $\varphi = 0.3$,

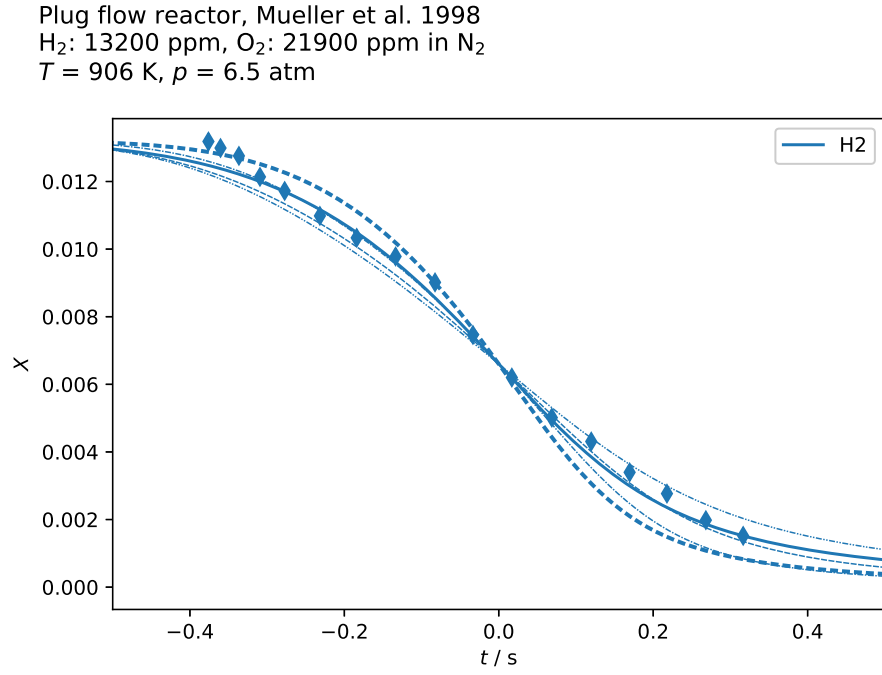


Figure 2.9: Flow reactor results by Mueller et al. [15] and its simulation; fuel: H_2 , $T = 906 \text{ K}$, $p = 6.5 \text{ atm}$, $\varphi = 0.3$,

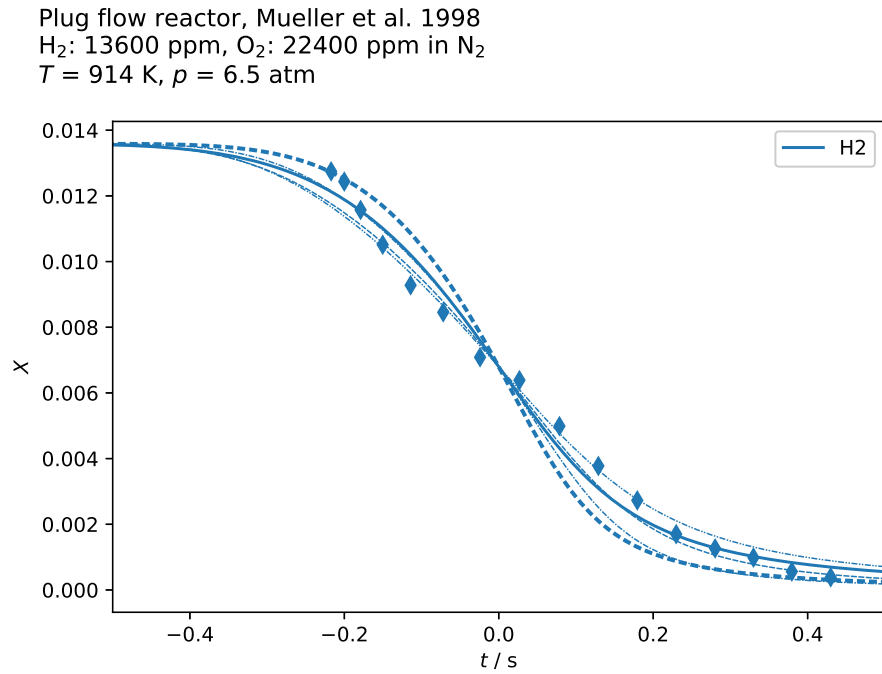


Figure 2.10: Flow reactor results by Mueller et al. [15] and its simulation; fuel: H_2 , $T = 914 \text{ K}$, $p = 6.5 \text{ atm}$, $\varphi = 0.3$,

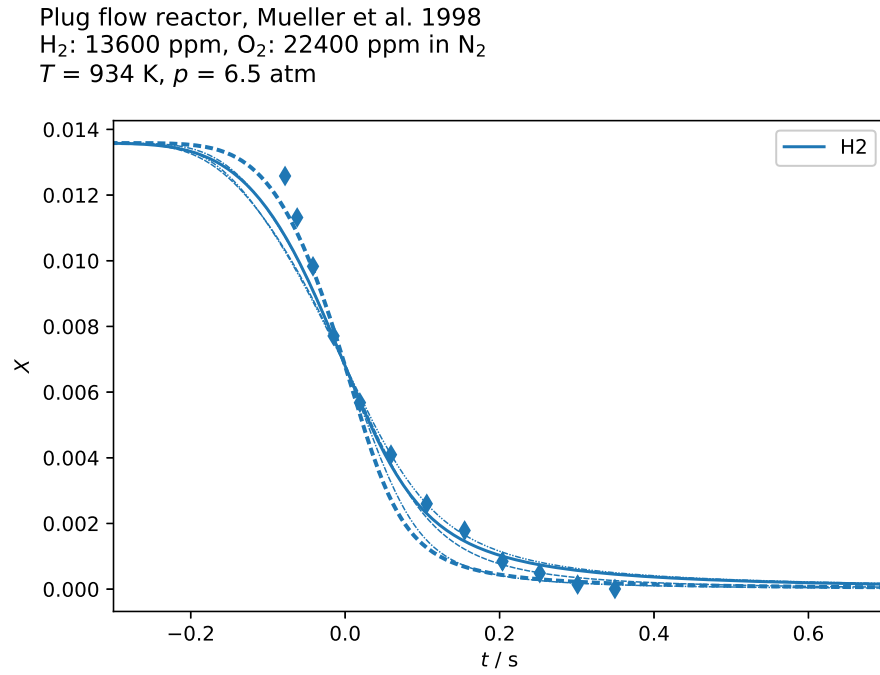


Figure 2.11: Flow reactor results by Mueller et al. [15] and its simulation; fuel: H_2 , $T = 934 \text{ K}$, $p = 6.5 \text{ atm}$, $\varphi = 0.3$,

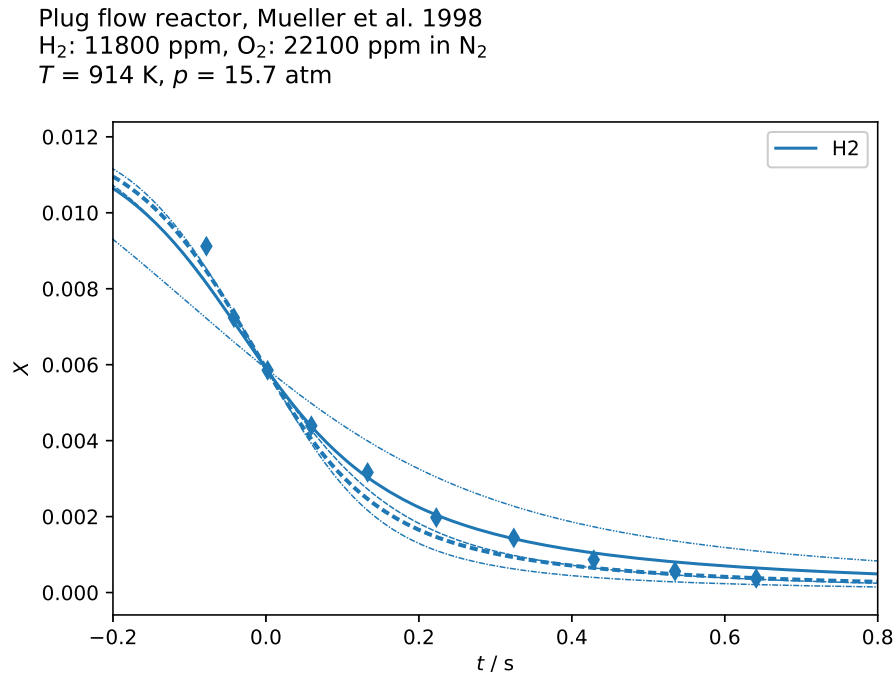


Figure 2.12: Flow reactor results by Mueller et al. [15] and its simulation; fuel: H_2 , $T = 914 \text{ K}$, $p = 15.7 \text{ atm}$, $\varphi = 0.3$,

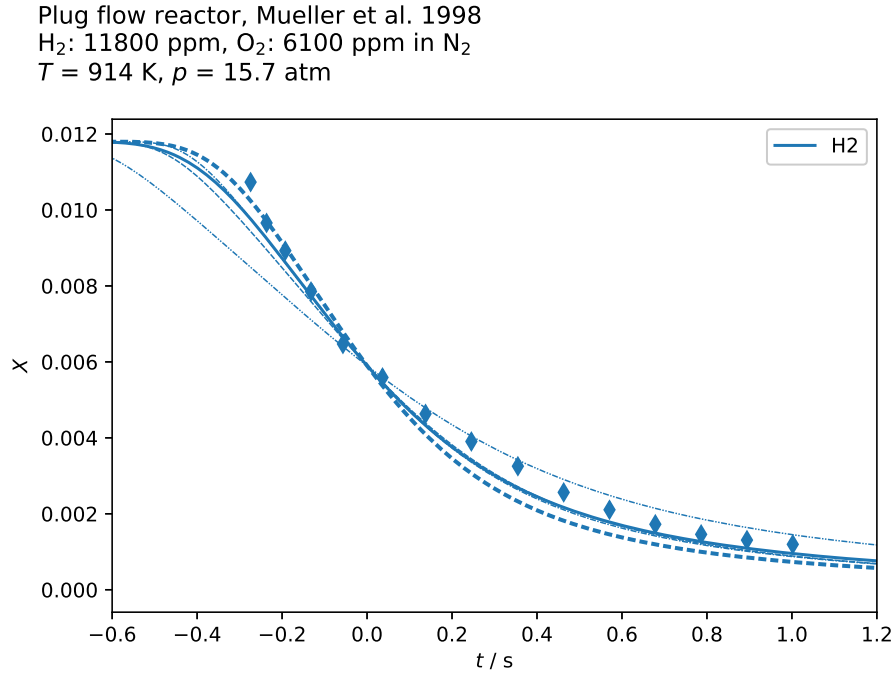


Figure 2.13: Flow reactor results by Mueller et al. [15] and its simulation; fuel: H_2 , $T = 914 \text{ K}$, $p = 15.7 \text{ atm}$, $\varphi = 1$,

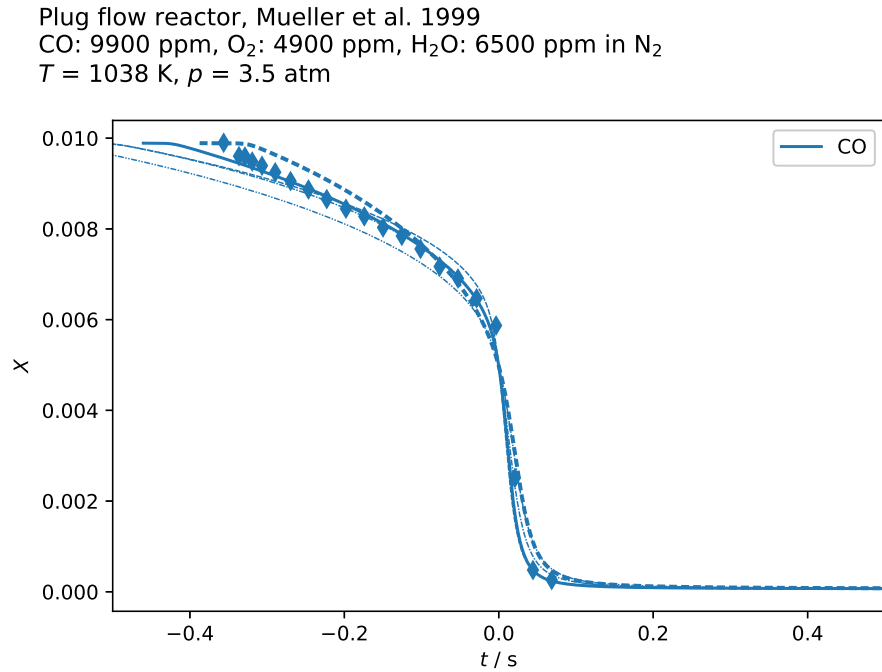


Figure 2.14: Flow reactor results by Mueller, Yetter, and Dryer [16] and its simulation; fuel: CO , $T = 1038 \text{ K}$, $p = 3.5 \text{ atm}$, $\varphi = 1$,

Plug flow reactor, Mueller et al. 1999
CO: 9900 ppm, O₂: 4900 ppm, H₂O: 6500 ppm in N₂
 $T = 1040$ K, $p = 9.6$ atm

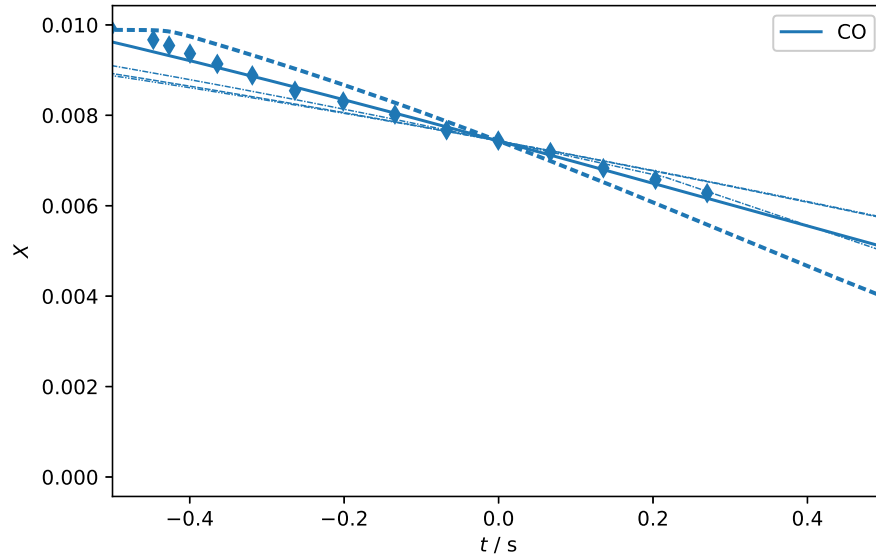


Figure 2.15: Flow reactor results by Mueller, Yetter, and Dryer [16] and its simulation; fuel: CO, $T = 1040$ K, $p = 9.6$ atm, $\varphi = 1$,

Plug flow reactor, Li et al. 2007
CH₂O: 100 ppm, O₂: 15000 ppm, H₂O: 3500 ppm in N₂
 $T = 852$ K, $p = 6.0$ atm

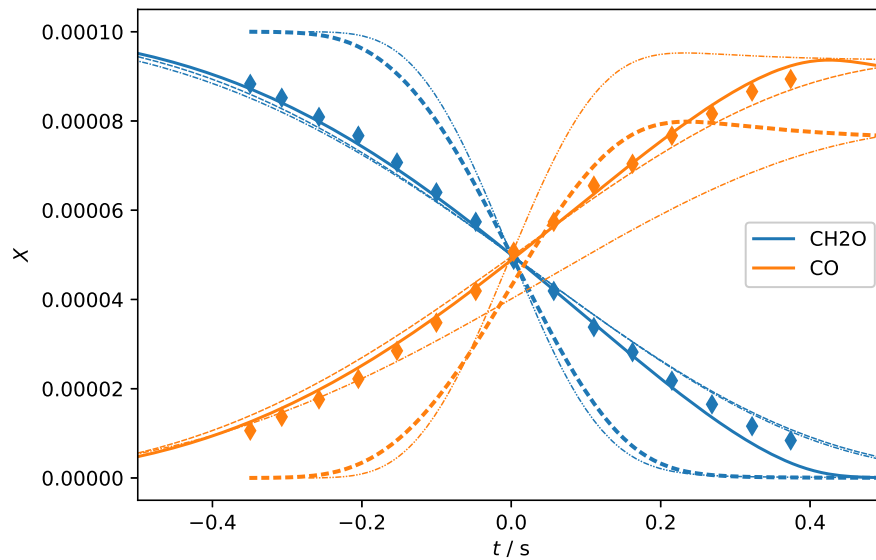


Figure 2.16: Flow reactor results by Li et al. [17] and its simulation; fuel: CH₂O, $T = 852$ K, $p = 6.0$ atm, $\lambda = 150$

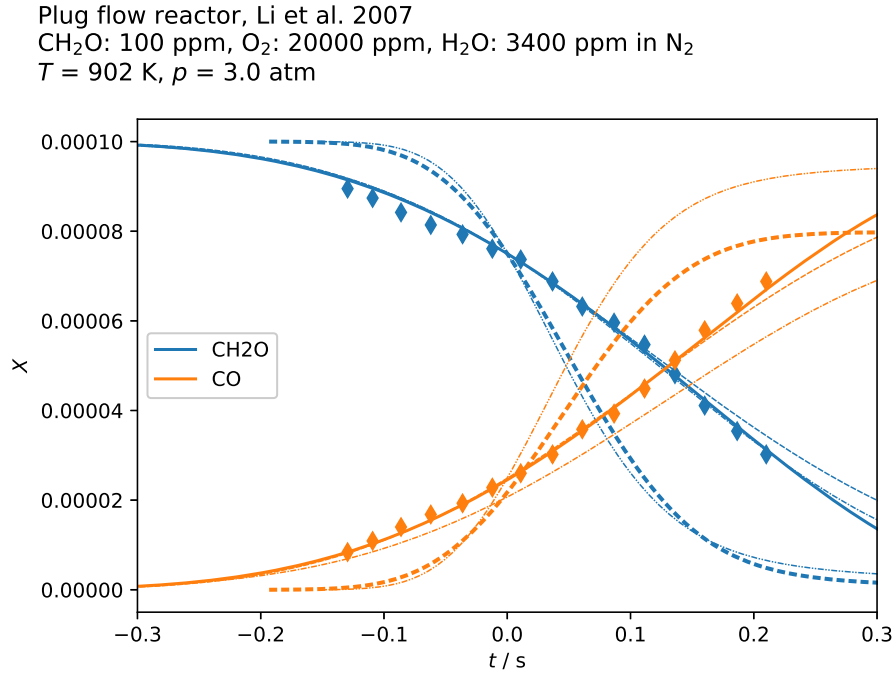


Figure 2.17: Flow reactor results by Li et al. [17] and its simulation; fuel: CH_2O , $T = 902 \text{ K}$, $p = 3.0 \text{ atm}$, $\lambda = 200$

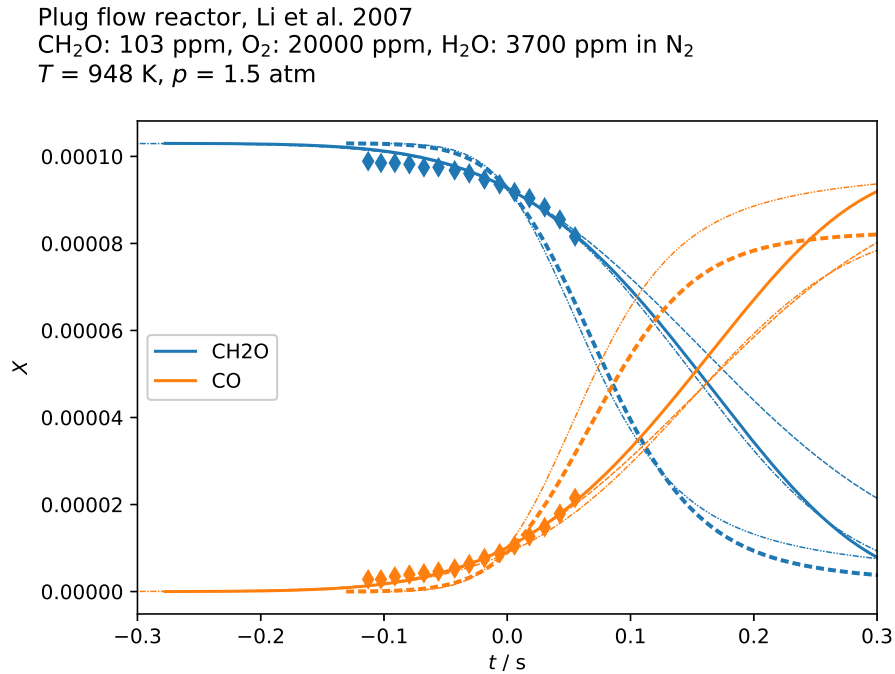


Figure 2.18: Flow reactor results by Li et al. [17] and its simulation; fuel: CH_2O , $T = 948 \text{ K}$, $p = 1.5 \text{ atm}$, $\lambda = 200$

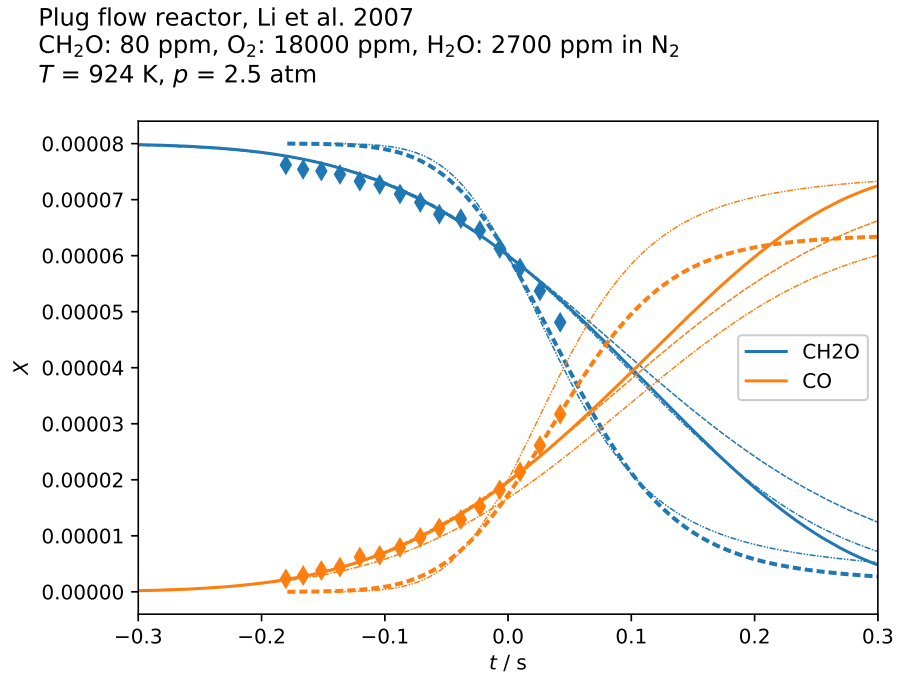


Figure 2.19: Flow reactor results by Li et al. [17] and its simulation; fuel: CH_2O , $T = 924 \text{ K}$, $p = 2.5 \text{ atm}$, $\lambda = 225$

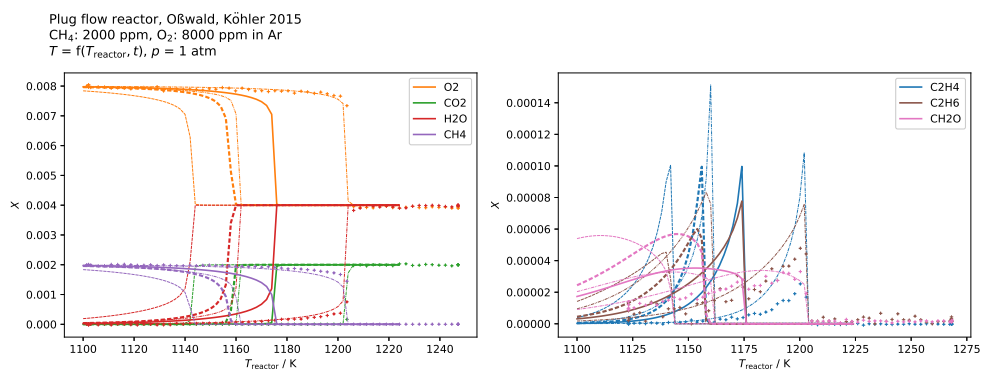


Figure 2.20: Flow reactor results by Oßwald and Köhler [18] and its simulation; fuel: CH_4 , $\varphi = 0.5$,

2 SPECIES PROFILES IN FLOW REACTORS

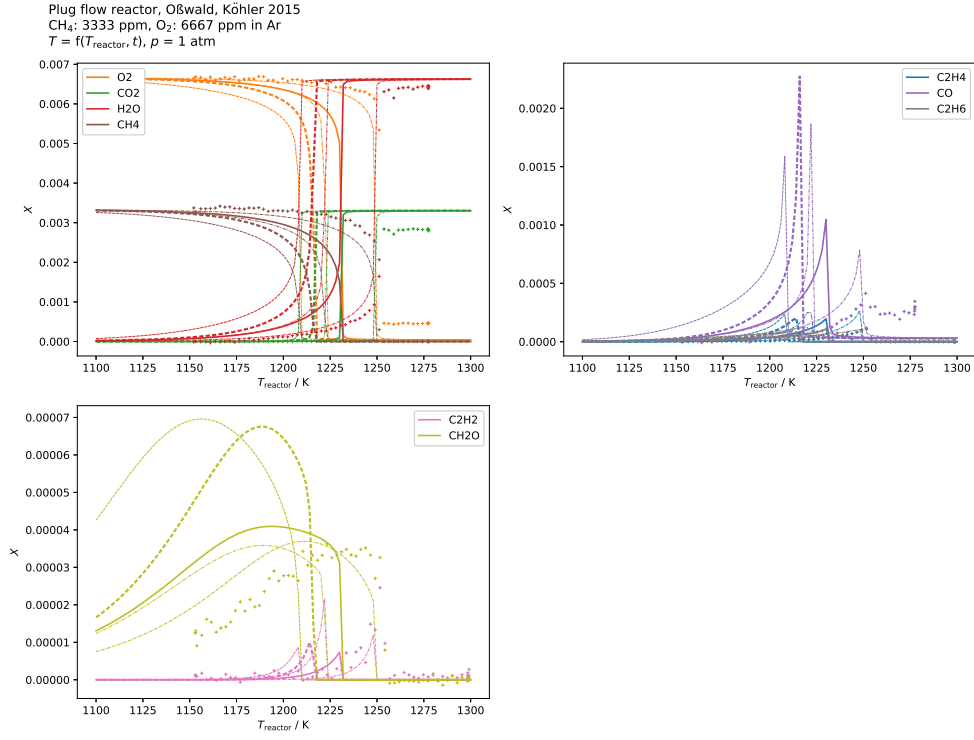


Figure 2.21: Flow reactor results by Oßwald and Köhler [18] and its simulation; fuel: CH₄, $\varphi = 1$,

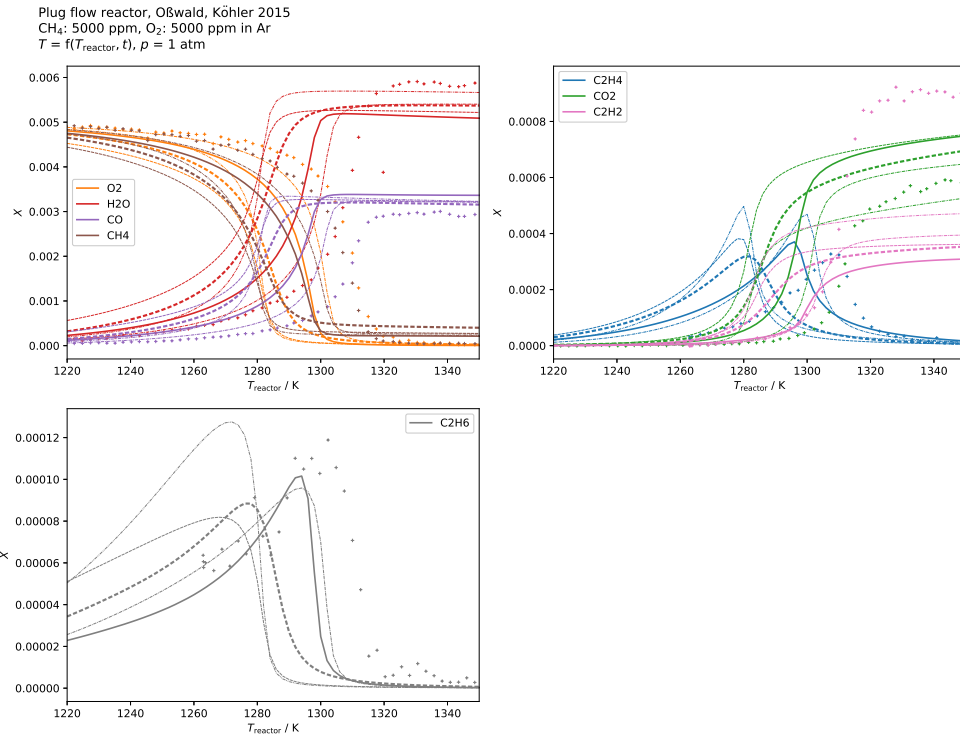


Figure 2.22: Flow reactor results by Oßwald and Köhler [18] and its simulation; fuel: CH_4 , $\varphi = 2$,

Plug flow reactor, Hashemi et al. 2016
 CH_4 : 1100 ppm, O_2 : 39600 ppm in N_2
 $t_{\text{res}} = 9586 \text{ K} / T \text{ s}$, $p = 100 \text{ bar}$

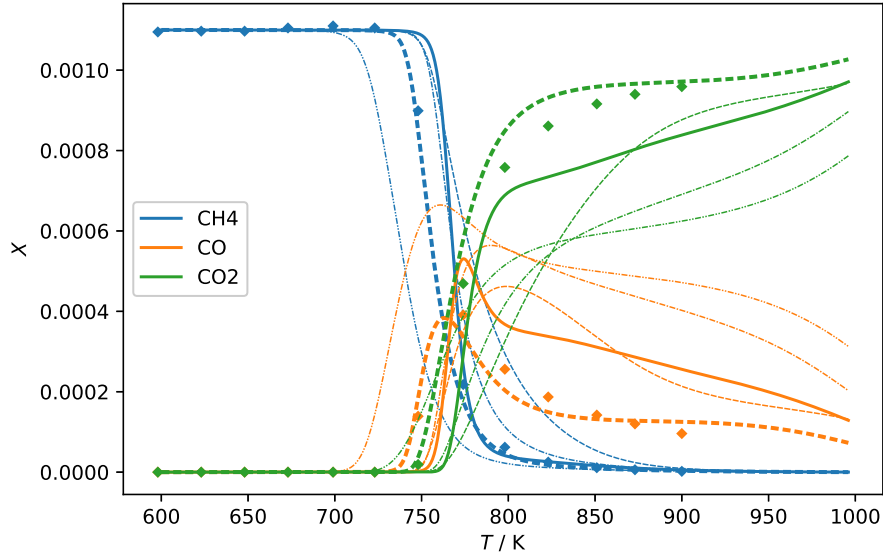


Figure 2.23: Flow reactor results by Hashemi et al. [19] and its simulation; fuel: CH_4 , $\varphi = 0.006$,

Plug flow reactor, Hashemi et al. 2016
 CH_4 : 1600 ppm, O_2 : 3100 ppm in N_2
 $t_{\text{res}} = 9586 \text{ K} / T \text{ s}$, $p = 100 \text{ bar}$

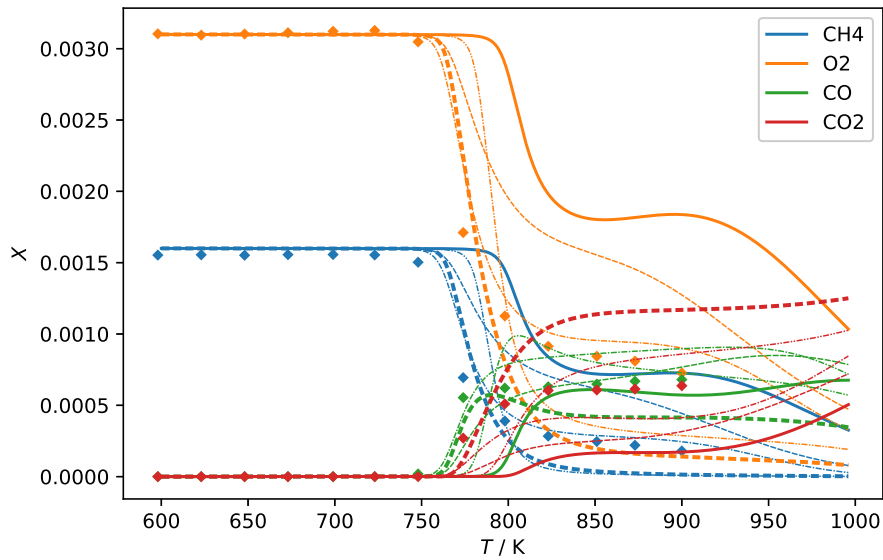


Figure 2.24: Flow reactor results by Hashemi et al. [19] and its simulation; fuel: CH_4 , $\varphi = 1$,

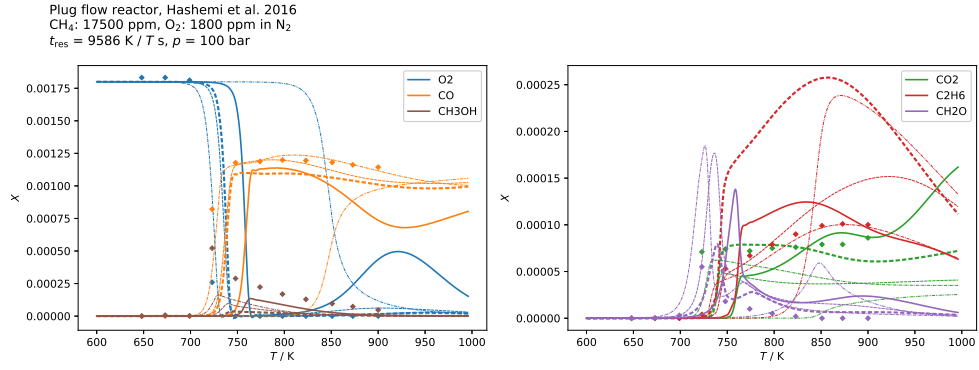


Figure 2.25: Flow reactor results by Hashemi et al. [19] and its simulation; fuel: CH_4 , $\varphi = 19.7$,

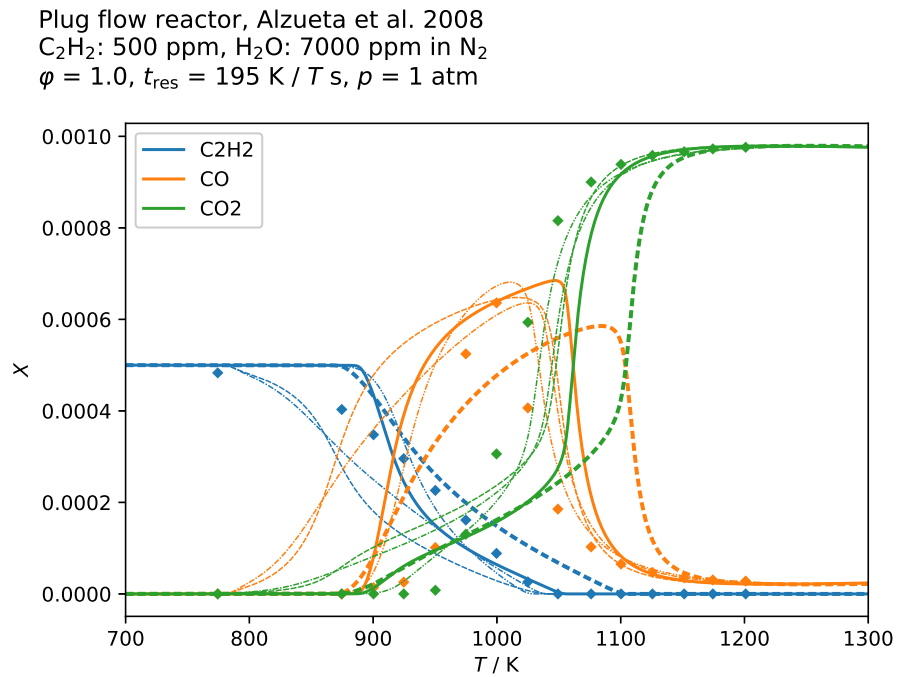


Figure 2.26: Flow reactor results by Alzueta et al. [20] and its simulation; fuel: C_2H_2 , $\varphi = 1$,

Plug flow reactor, Alzueta et al. 2008
 C_2H_2 : 500 ppm, H_2O : 7000 ppm in N_2
 $\phi = 1.4$, $t_{\text{res}} = 195 \text{ K} / T \text{ s}$, $p = 1 \text{ atm}$

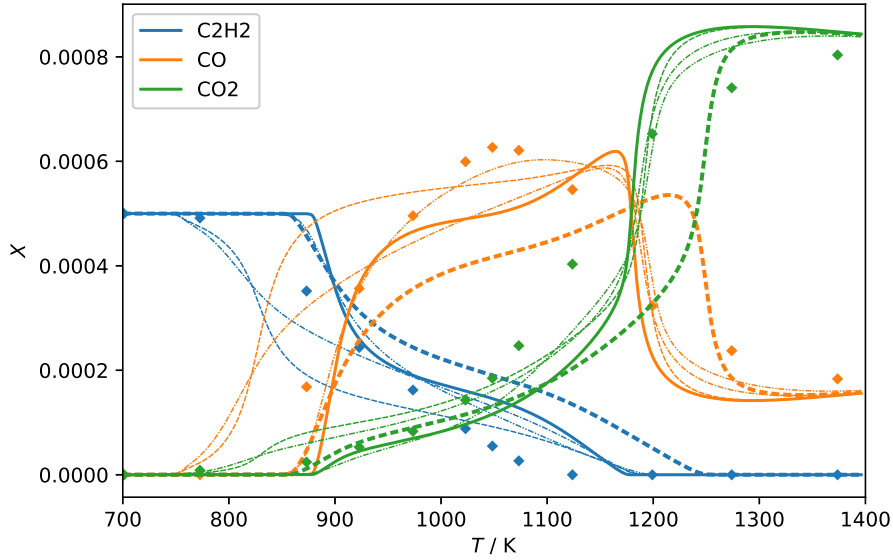


Figure 2.27: Flow reactor results by Alzueta et al. [20] and its simulation; fuel: C_2H_2 , $\phi = 1.4$,

Plug flow reactor, Oßwald, Köhler 2015
 C_2H_4 : 1430 ppm, O_2 : 8570 ppm in Ar
 $T = f(T_{\text{reactor}}, t)$, $p = 1 \text{ atm}$

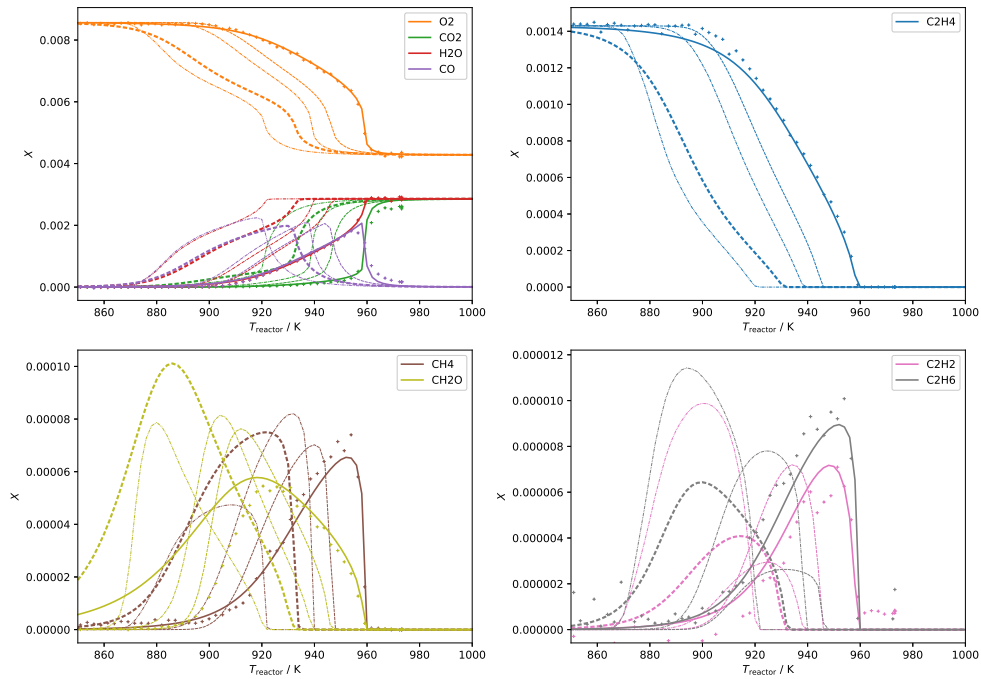


Figure 2.28: Flow reactor results by Oßwald and Köhler [18] and its simulation; fuel: C_2H_4 , $\phi = 0.5$,

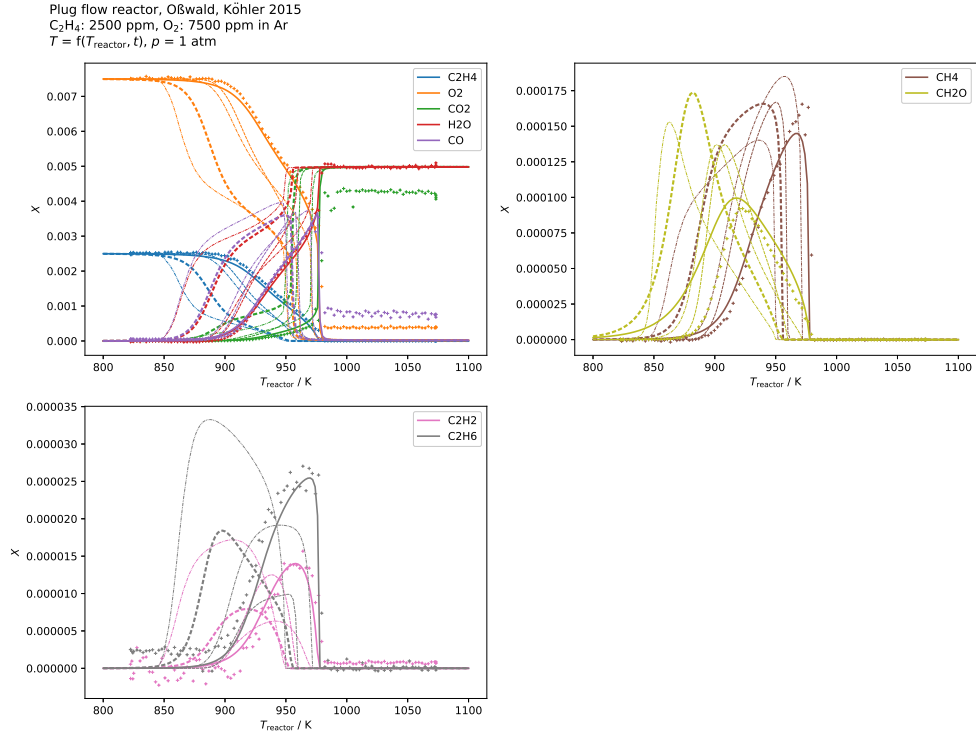


Figure 2.29: Flow reactor results by Oßwald and Köhler [18] and its simulation; fuel: C_2H_4 , $\varphi = 1$,

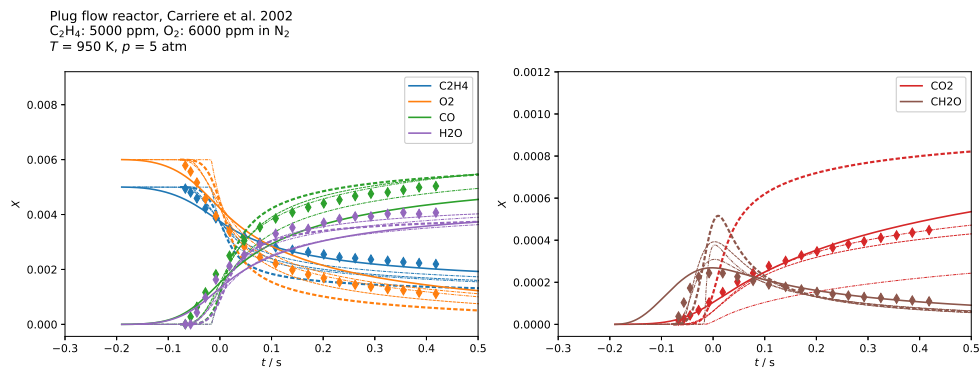


Figure 2.30: Flow reactor results by Carriere et al. [21] and its simulation; fuel: C_2H_4 , $T = 950 \text{ K}$, $p = 5.0 \text{ atm}$, $\varphi = 2.5$,

2 SPECIES PROFILES IN FLOW REACTORS

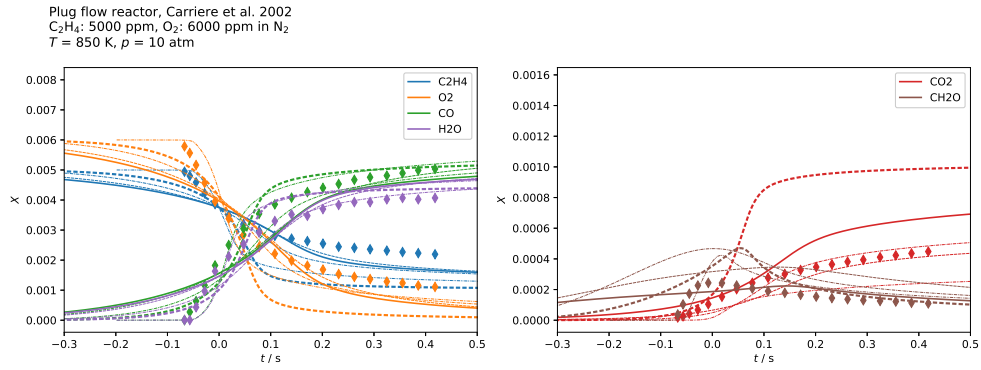
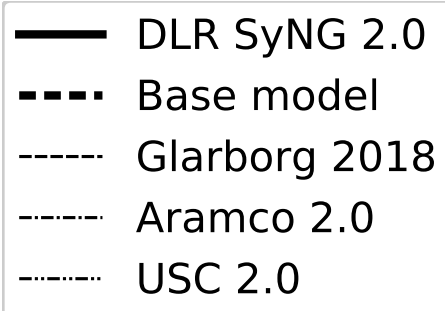


Figure 2.31: Flow reactor results by Carriere et al. [21] and its simulation; fuel: C_2H_4 ,
 $T = 850 \text{ K}$, $p = 10.0 \text{ atm}$, $\varphi = 2.5$,

3 Species profiles in jet stirred reactors



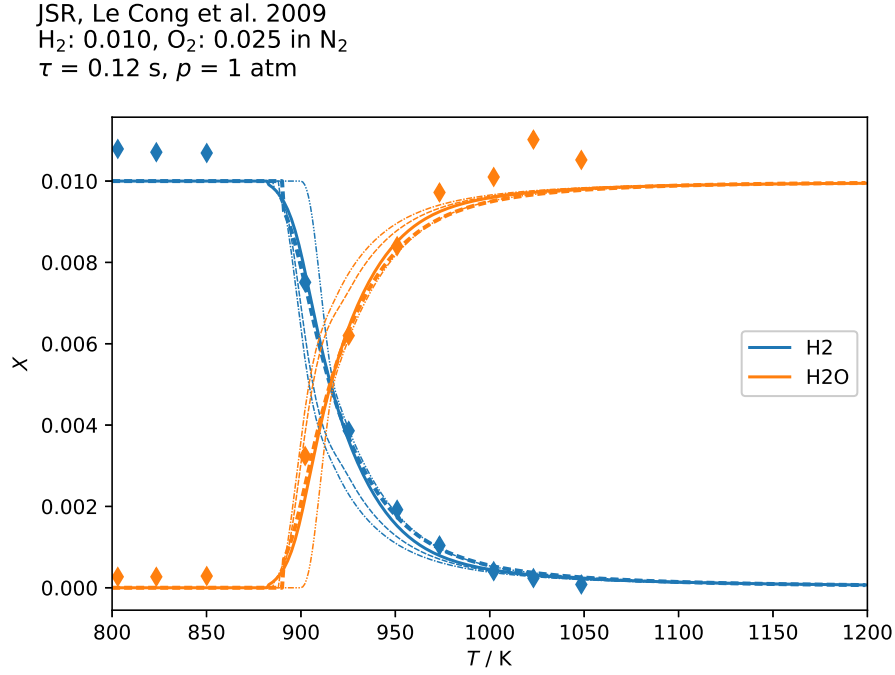


Figure 3.1: JSR results by Le Cong, Dagaut, and Dayma [22] and its simulation; fuel: H_2 , $p = 1.0 \text{ atm}$, $\varphi = 0.2$,

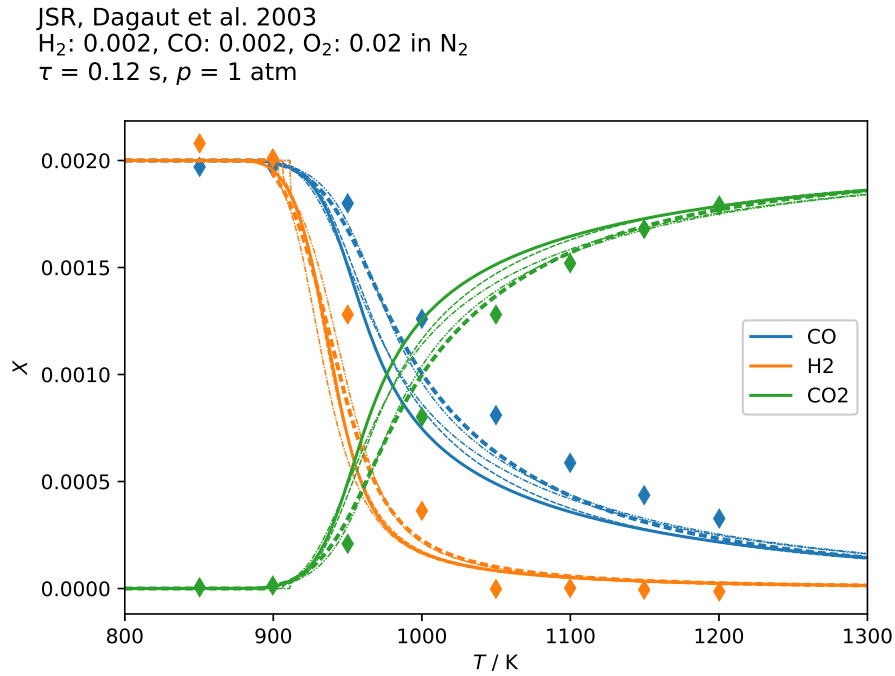


Figure 3.2: JSR results by Dagaut et al. [23] and its simulation; fuel: $\text{H}_2/\text{CO} = 50/50$, $p = 1.0 \text{ atm}$, $\varphi = 0.1$,

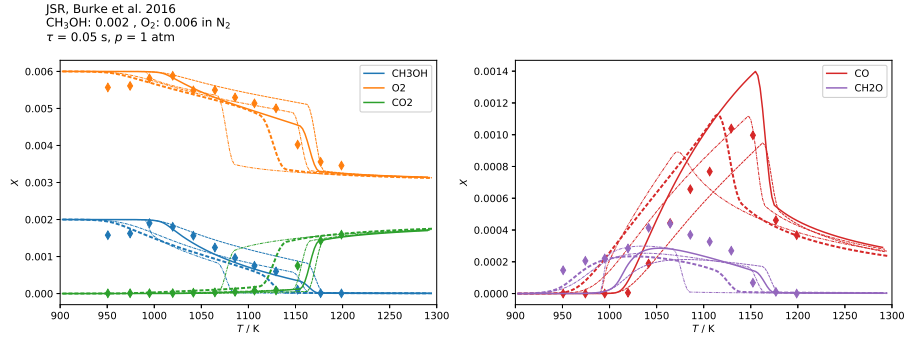


Figure 3.3: JSR results by Burke et al. [24] and its simulation; fuel: CH_3OH , $p = 1.0 \text{ atm}$, $\varphi = 0.5$,

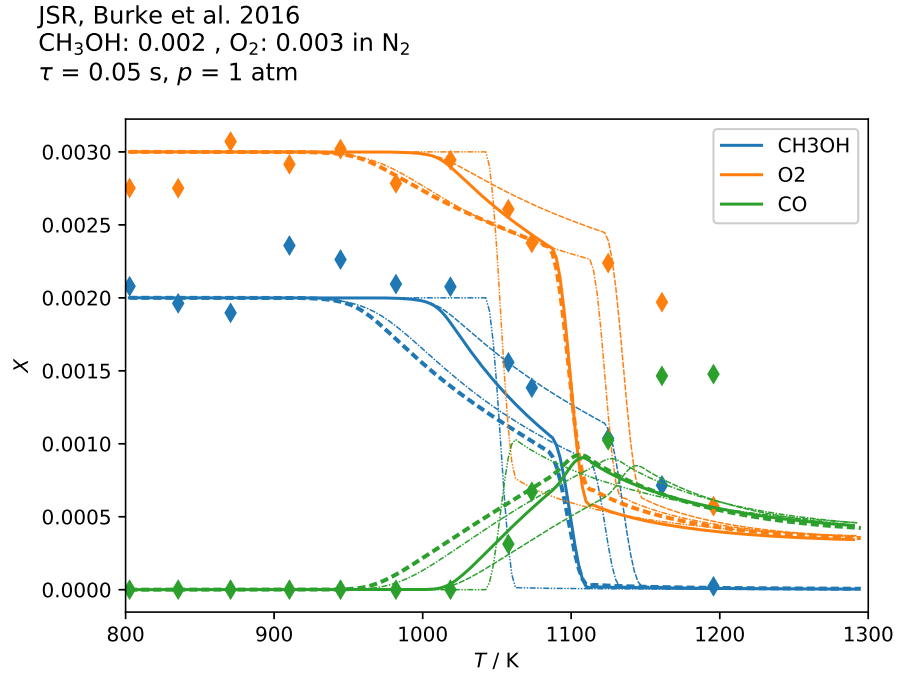


Figure 3.4: JSR results by Burke et al. [24] and its simulation; fuel: CH_3OH , $p = 1.0 \text{ atm}$, $\varphi = 1$,

3 SPECIES PROFILES IN JET STIRRED REACTORS

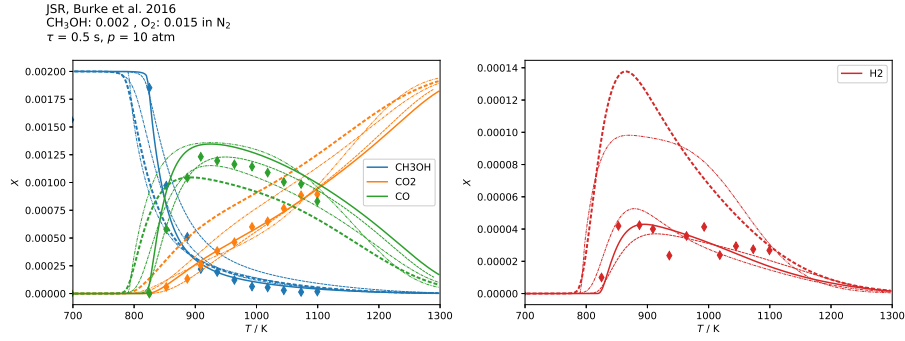


Figure 3.5: JSR results by Burke et al. [24] and its simulation; fuel: CH₃OH, $p = 10.0$ atm, $\varphi = 0.2$,

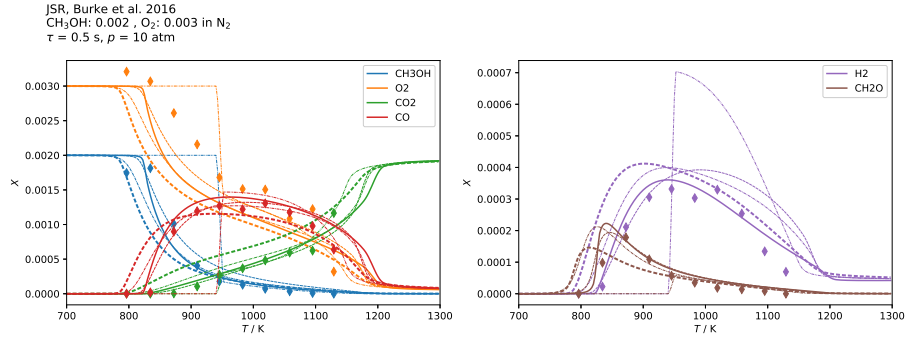


Figure 3.6: JSR results by Burke et al. [24] and its simulation; fuel: CH₃OH, $p = 10.0$ atm, $\varphi = 1$,

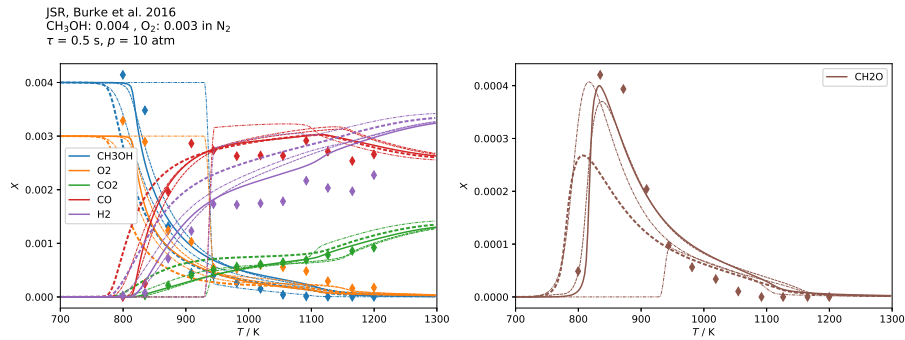


Figure 3.7: JSR results by Burke et al. [24] and its simulation; fuel: CH₃OH, $p = 10.0$ atm, $\varphi = 2$,

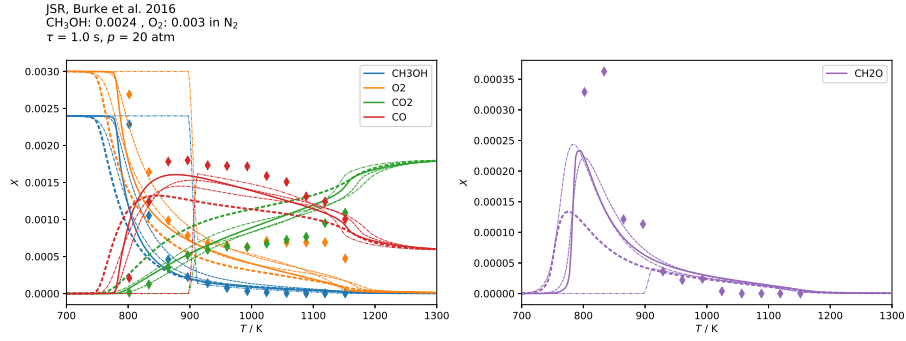


Figure 3.8: JSR results by Burke et al. [24] and its simulation; fuel: CH_3OH , $p = 20.0 \text{ atm}$, $\varphi = 1$,

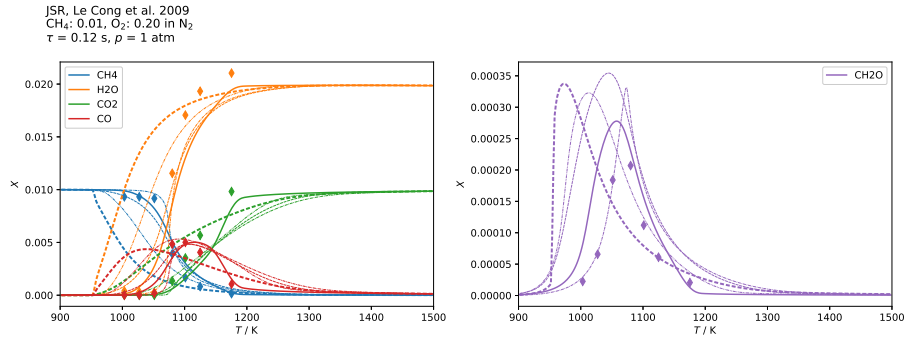


Figure 3.9: JSR results by Le Cong, Dagaut, and Dayma [22] and its simulation; fuel: CH_4 , $p = 1.0 \text{ atm}$, $\varphi = 0.1$, $X_{\text{N}_2} = 79$

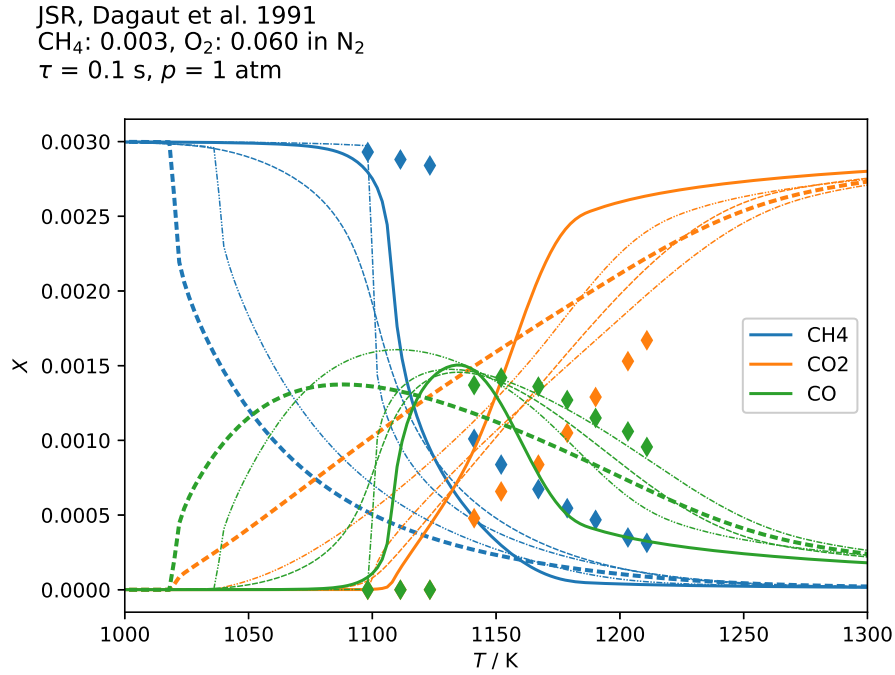


Figure 3.10: JSR results by Dagaut, Boettner, and Cathonnet [25] and its simulation; fuel: CH_4 , $p = 1.0 \text{ atm}$, $\varphi = 0.1$, $X_{\text{N}_2} = 94$

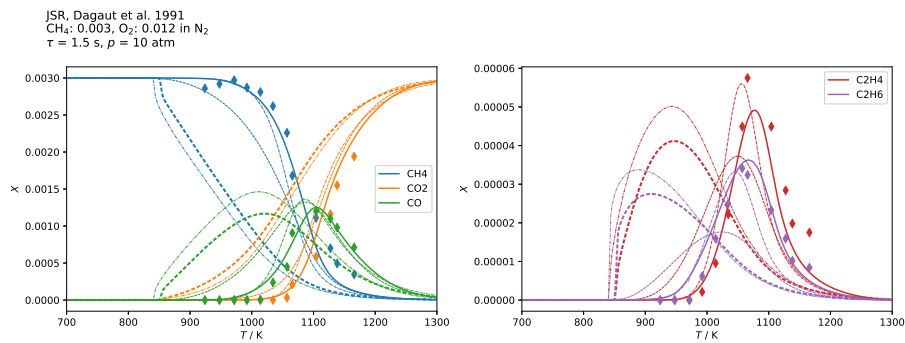


Figure 3.11: JSR results by Dagaut, Boettner, and Cathonnet [25] and its simulation; fuel: CH_4 , $p = 10.0 \text{ atm}$, $\varphi = 0.5$,

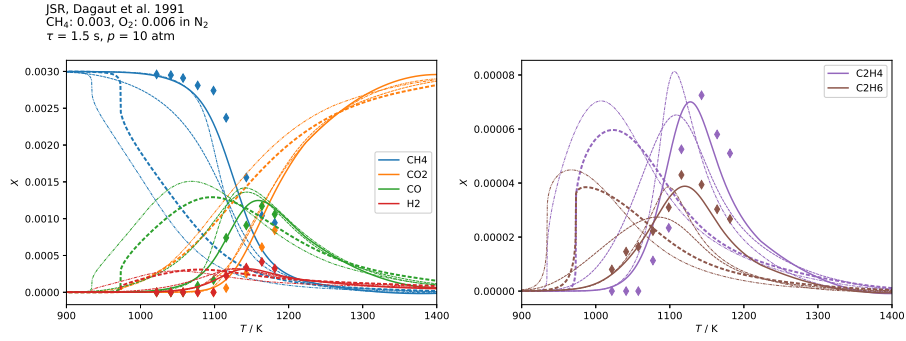


Figure 3.12: JSR results by Dagaut, Boettner, and Cathonnet [25] and its simulation; fuel: CH_4 , $p = 10.0 \text{ atm}$, $\varphi = 1$,

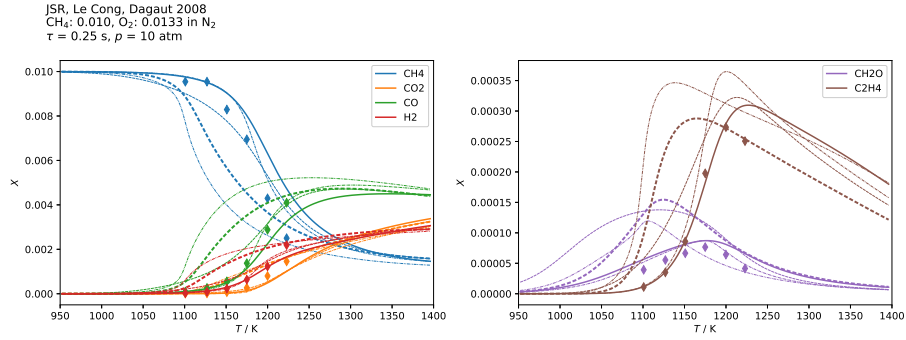


Figure 3.13: JSR results by Le Cong and Dagaut [26] and its simulation; fuel: CH_4 , $p = 10.0 \text{ atm}$, $\varphi = 1.5$,

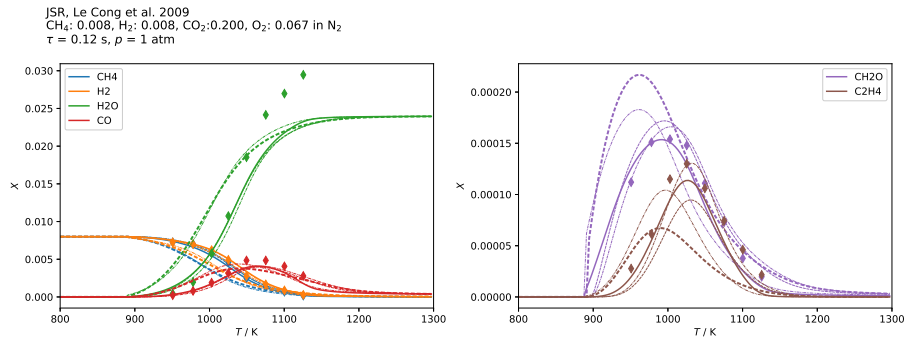


Figure 3.14: JSR results by Le Cong, Dagaut, and Dayma [22] and its simulation; fuel: $\text{CH}_4/\text{H}_2 = 50/50$, $p = 1.0 \text{ atm}$, $\varphi = 0.3$, $X_{\text{CO}_2} = 20$, $X_{\text{N}_2} = 72$

3 SPECIES PROFILES IN JET STIRRED REACTORS

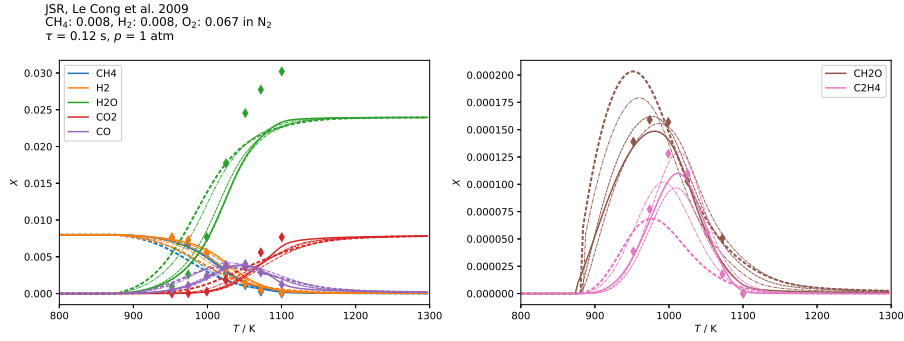


Figure 3.15: JSR results by Le Cong, Dagaut, and Dayma [22] and its simulation; fuel: $\text{CH}_4/\text{H}_2 = 50/50$, $p = 1.0$ atm, $\varphi = 0.3$, $X_{\text{N}_2} = 92$

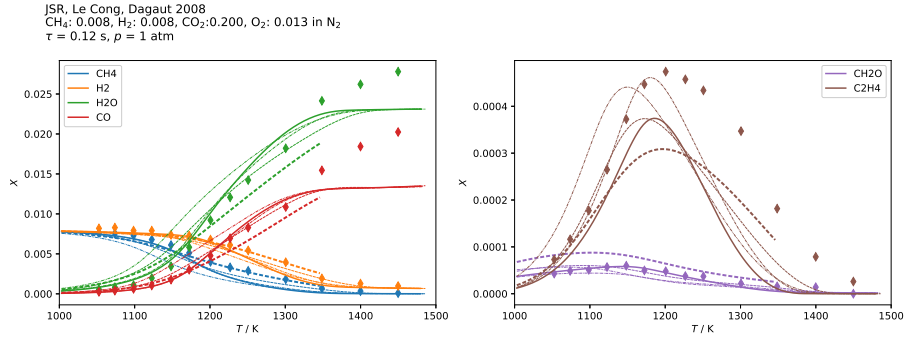


Figure 3.16: JSR results by Le Cong and Dagaut [26] and its simulation; fuel: $\text{CH}_4/\text{H}_2 = 50/50$, $p = 1.0$ atm, $\varphi = 1.5$, $X_{\text{CO}_2} = 20$, $X_{\text{N}_2} = 77$

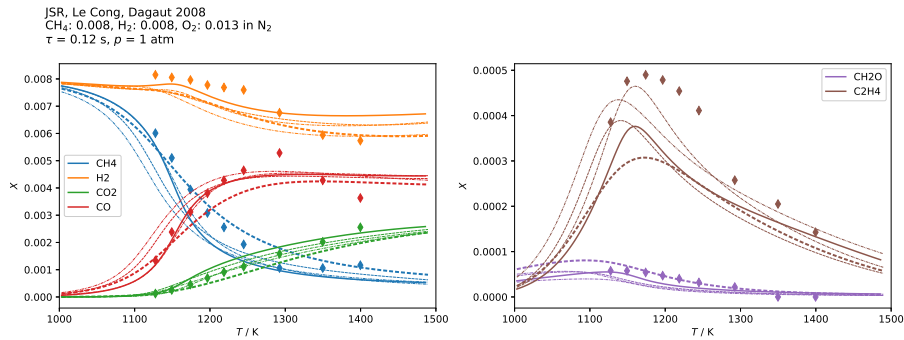


Figure 3.17: JSR results by Le Cong and Dagaut [26] and its simulation; fuel: $\text{CH}_4/\text{H}_2 = 50/50$, $p = 1.0$ atm, $\varphi = 1.5$, $X_{\text{N}_2} = 97$

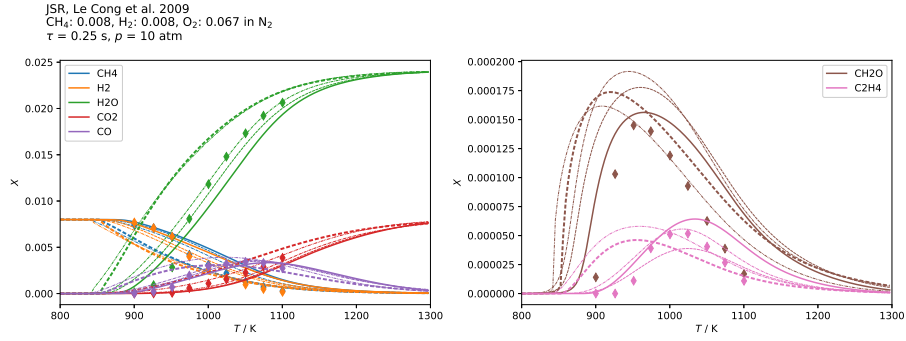


Figure 3.18: JSR results by Le Cong, Dagaut, and Dayma [22] and its simulation; fuel: $\text{CH}_4/\text{H}_2 = 50/50$, $p = 10.0 \text{ atm}$, $\varphi = 0.3$,

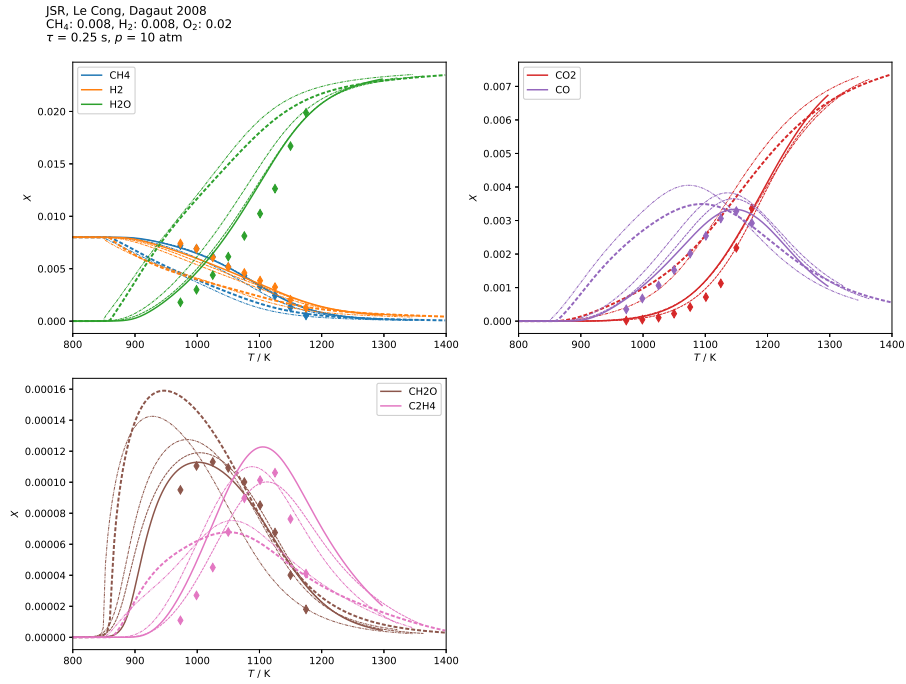


Figure 3.19: JSR results by Le Cong and Dagaut [26] and its simulation; fuel: $\text{CH}_4/\text{H}_2 = 50/50$, $p = 10.0 \text{ atm}$, $\varphi = 1$,

3 SPECIES PROFILES IN JET STIRRED REACTORS

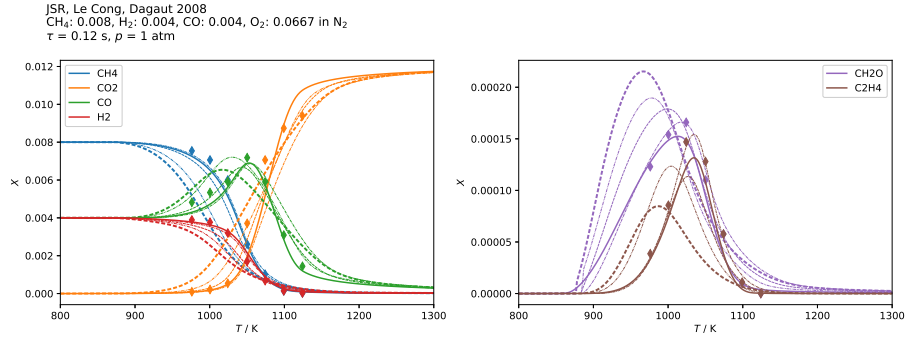


Figure 3.20: JSR results by Le Cong and Dagaut [26] and its simulation; fuel: $\text{CH}_4/\text{H}_2/\text{CO} = 50/25/25$, $p = 1.0$ atm, $\varphi = 0.3$,

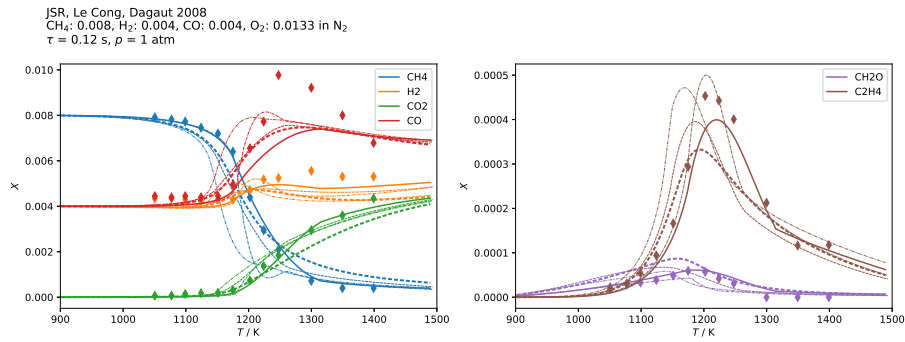


Figure 3.21: JSR results by Le Cong and Dagaut [26] and its simulation; fuel: $\text{CH}_4/\text{H}_2/\text{CO} = 50/25/25$, $p = 1.0$ atm, $\varphi = 1.5$,

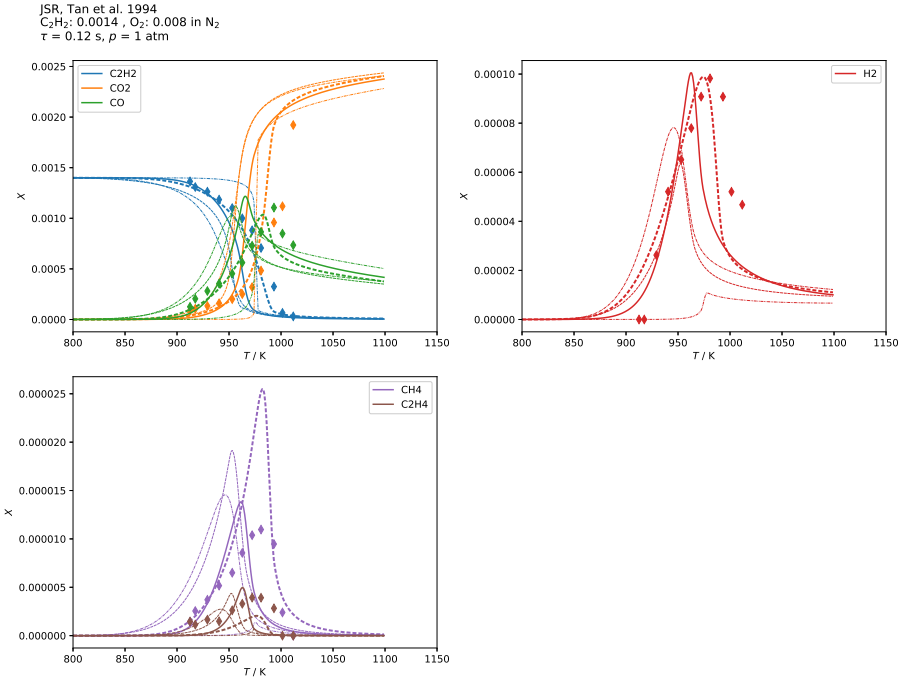


Figure 3.22: JSR results by Tan et al. [27] and its simulation; fuel: C_2H_2 , $p = 1.0$ atm, $\varphi = 0.4$,

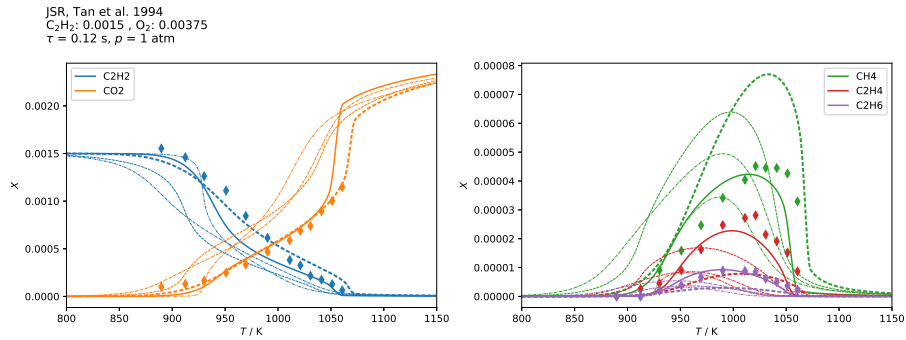
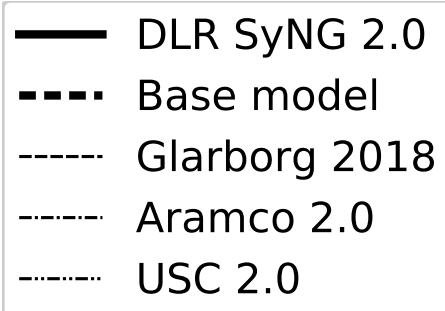


Figure 3.23: JSR results by Tan et al. [27] and its simulation; fuel: C_2H_2 , $p = 1.0$ atm, $\varphi = 1$,

4 Laminar burning velocities



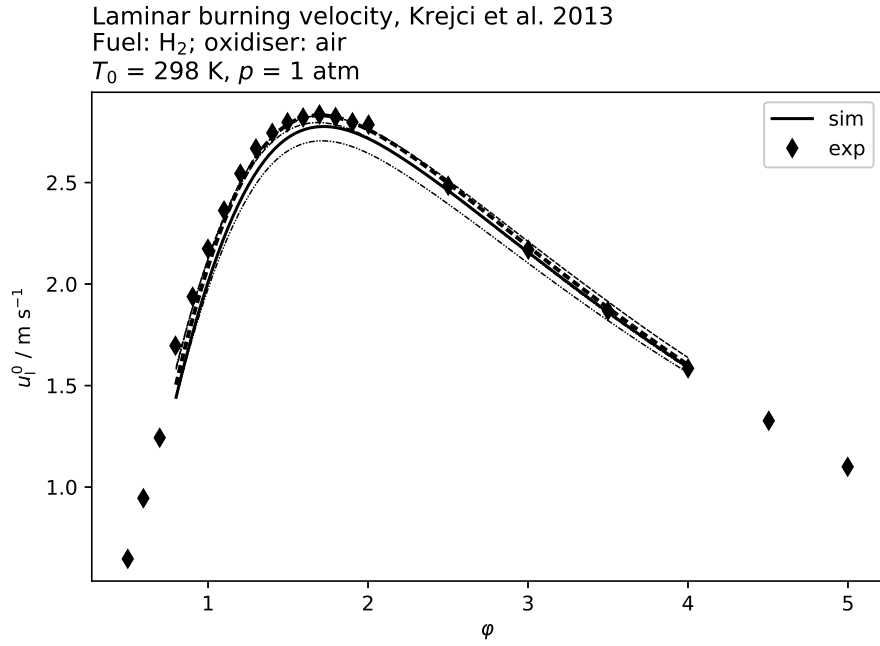


Figure 4.1: Burning velocities by Krejci et al. [28] and corresponding simulation; fuel: H_2 ,

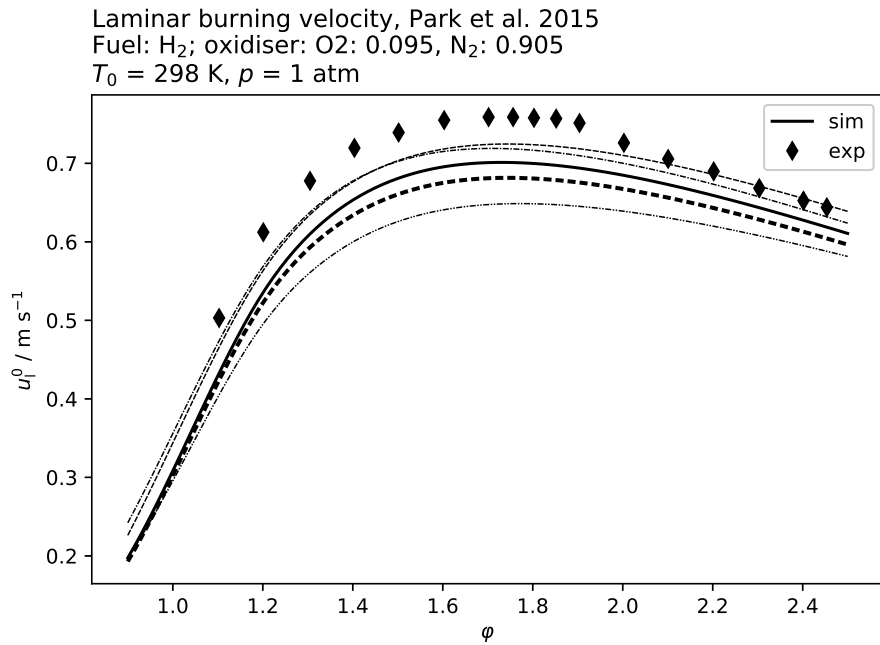


Figure 4.2: Burning velocities by Park et al. [29] and corresponding simulation; fuel: H_2 , oxidiser: $\text{O}_2/\text{N}_2 = 9.5/90.5$

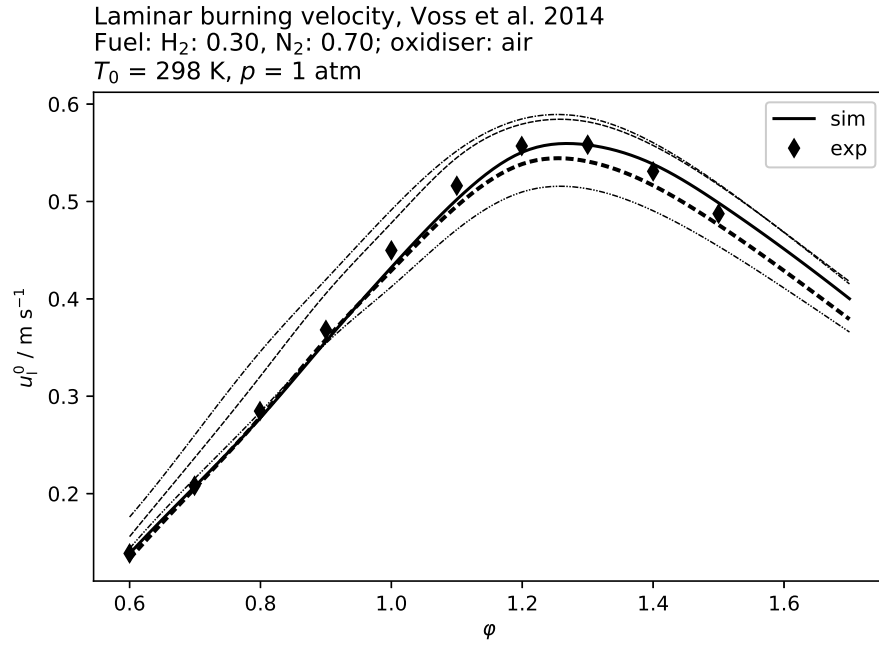


Figure 4.3: Burning velocities by Voss, Hartl, and Hasse [30] and corresponding simulation;
 fuel: $\text{H}_2/\text{N}_2 = 30/70$,

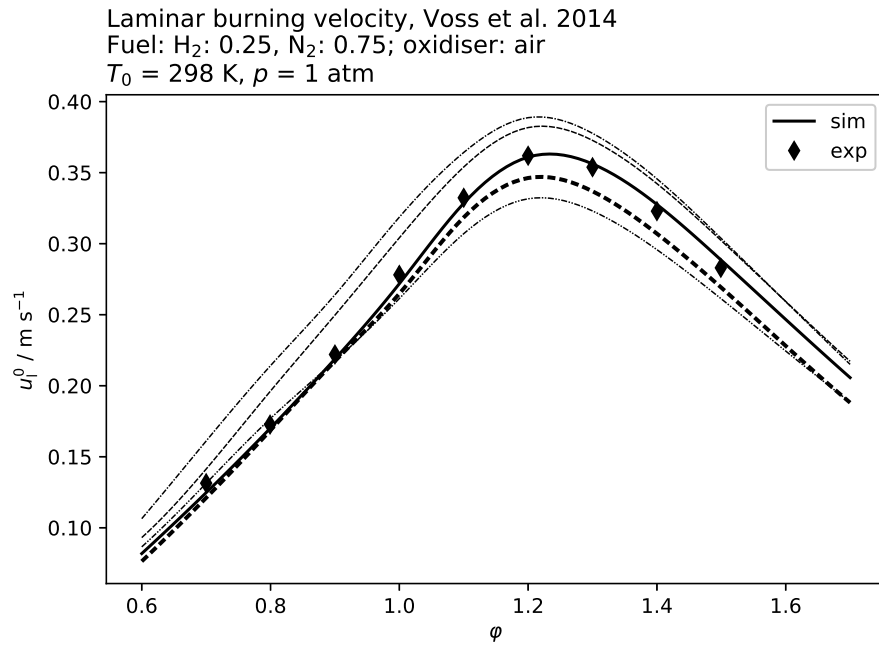


Figure 4.4: Burning velocities by Voss, Hartl, and Hasse [30] and corresponding simulation;
 fuel: $\text{H}_2/\text{N}_2 = 25/75$,

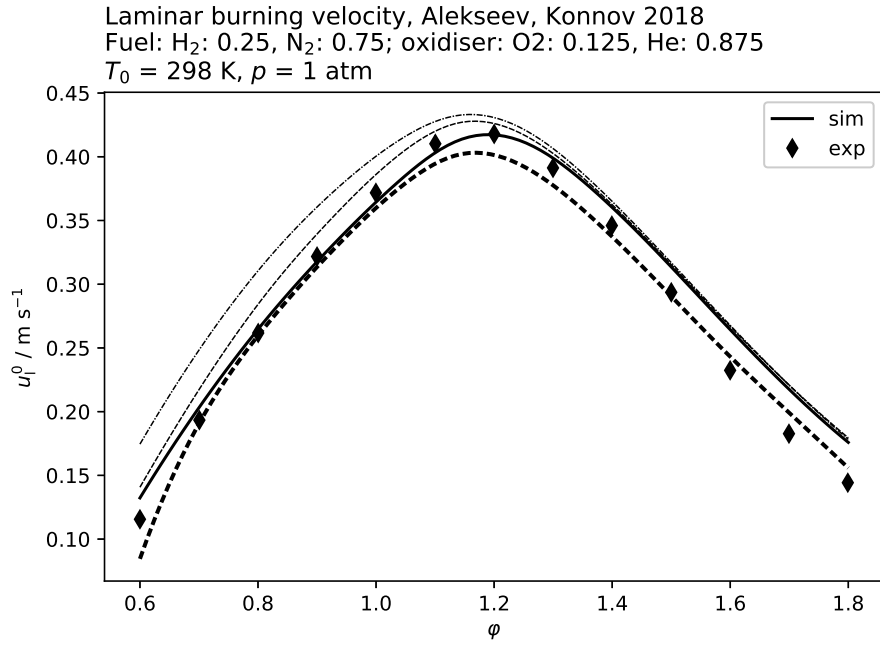


Figure 4.5: Burning velocities by Alekseev and Konnov [31] and corresponding simulation; fuel: $\text{H}_2/\text{N}_2 = 25/75$, oxidiser: $\text{O}_2/\text{He} = 12.5/87.5$

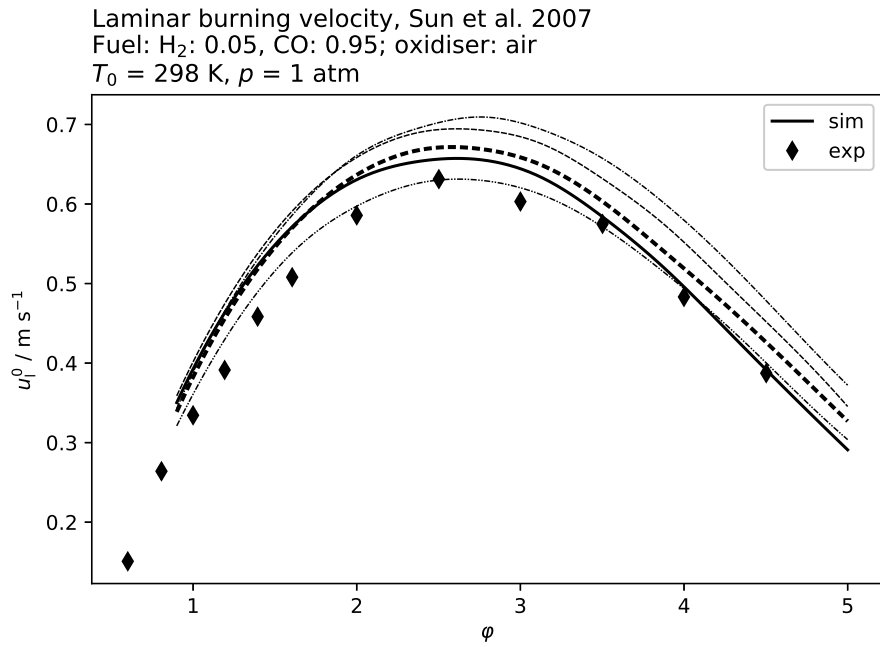


Figure 4.6: Burning velocities by Sun et al. [32] and corresponding simulation; fuel: $\text{H}_2/\text{CO} = 5/95$,

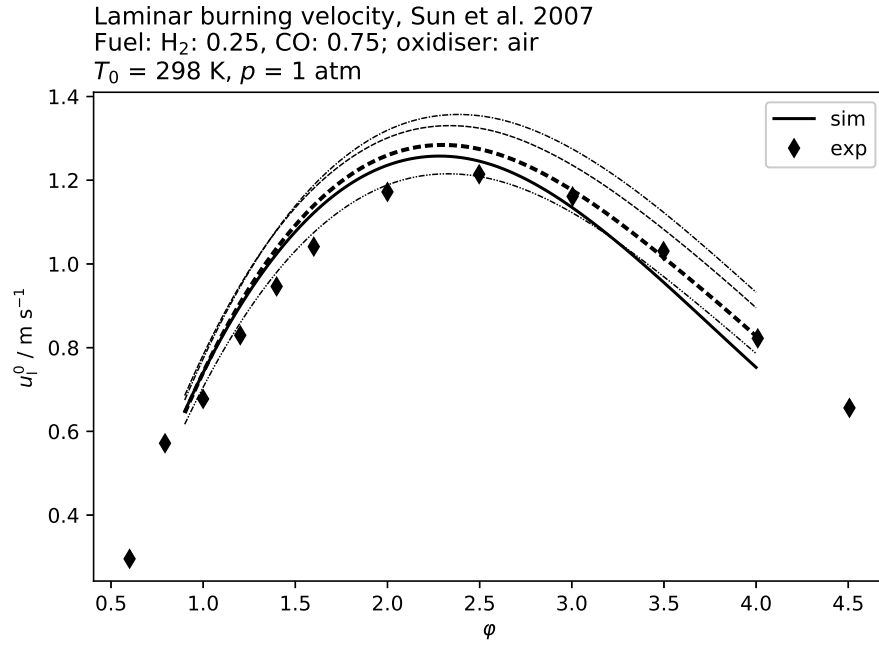


Figure 4.7: Burning velocities by Sun et al. [32] and corresponding simulation; fuel: $\text{H}_2/\text{CO} = 25/75$,

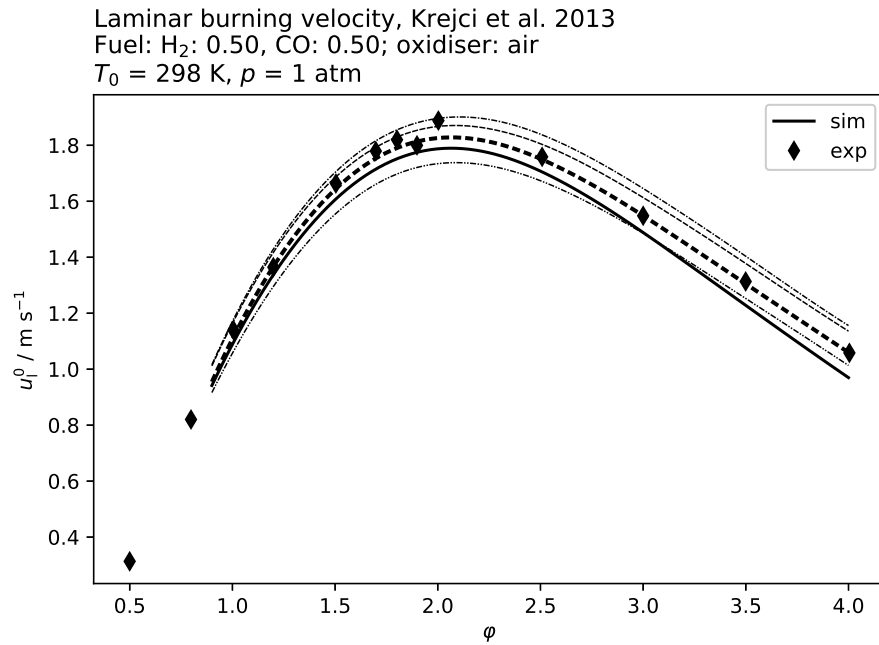


Figure 4.8: Burning velocities by Krejci et al. [28] and corresponding simulation; fuel: $\text{H}_2/\text{CO} = 50/50$, $p = 1 \text{ atm}$,

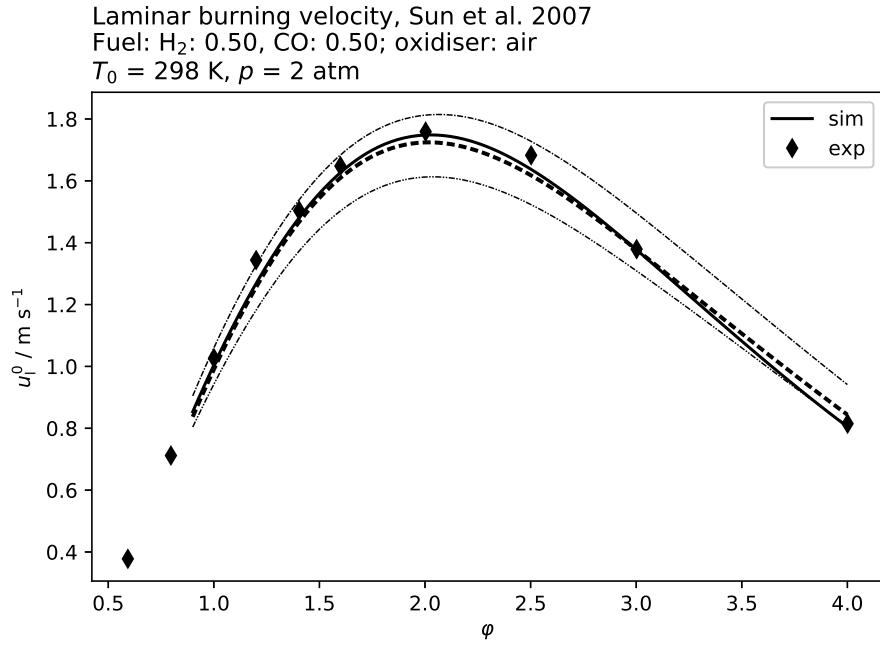


Figure 4.9: Burning velocities by Sun et al. [32] and corresponding simulation; fuel: $\text{H}_2/\text{CO} = 50/50$, $p = 2 \text{ atm}$,

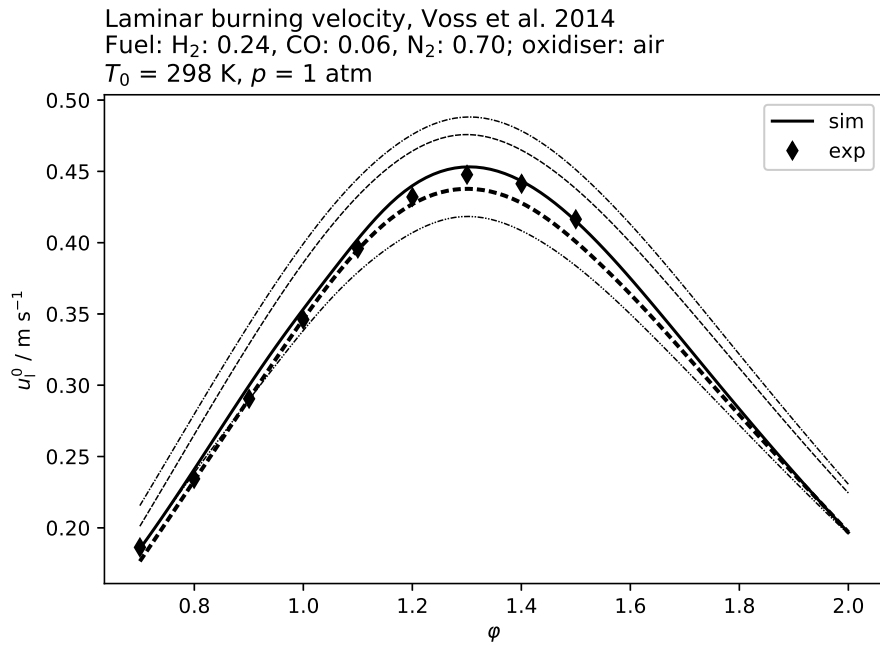


Figure 4.10: Burning velocities by Voss, Hartl, and Hasse [30] and corresponding simulation; fuel: $\text{H}_2/\text{CO}/\text{N}_2 = 24/6/70$,

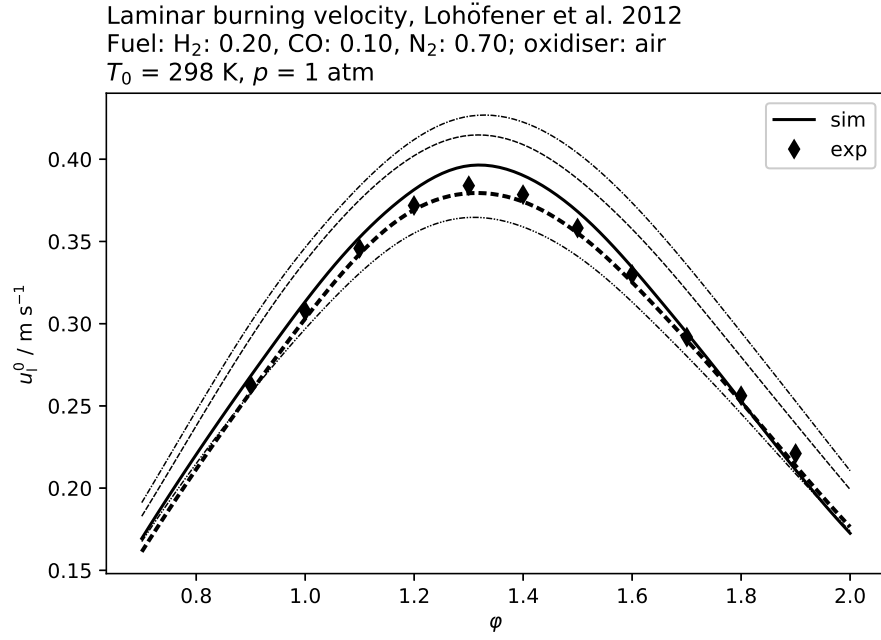


Figure 4.11: Burning velocities by Lohöfener et al. [33] and corresponding simulation; fuel: H₂/CO/N₂ = 20/10/70,

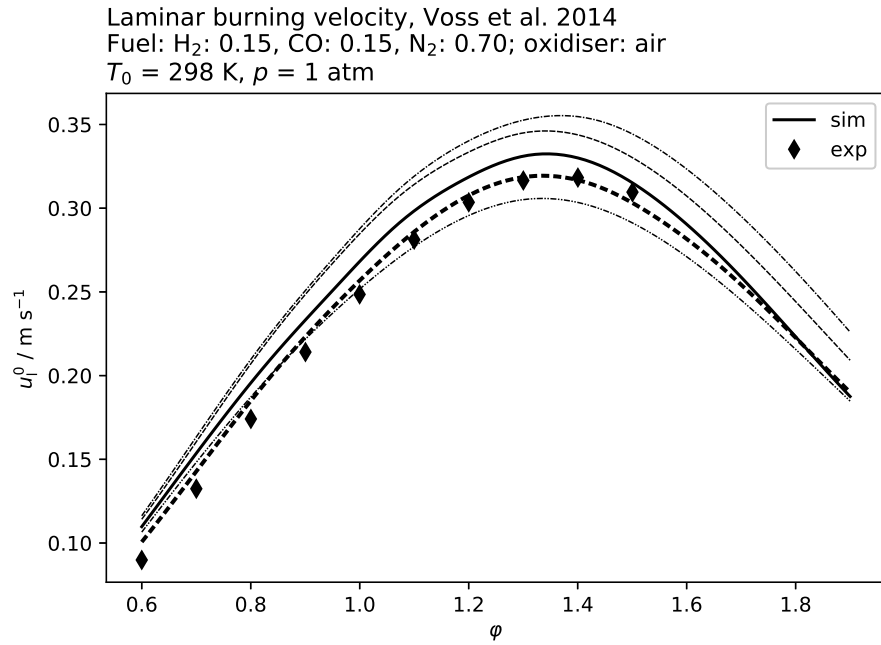


Figure 4.12: Burning velocities by Voss, Hartl, and Hasse [30] and corresponding simulation; fuel: H₂/CO/N₂ = 15/15/70,

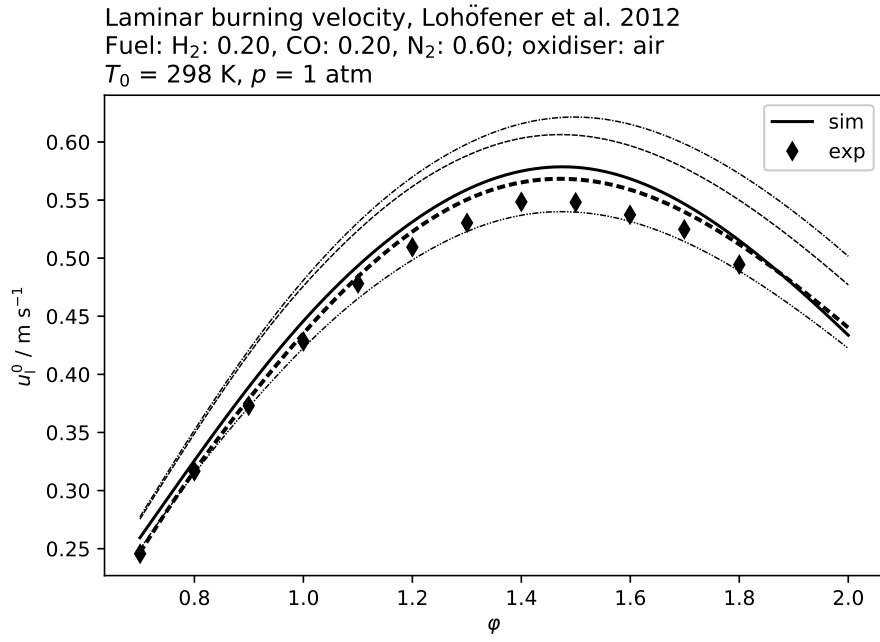


Figure 4.13: Burning velocities by Lohöfener et al. [33] and corresponding simulation; fuel: H₂/CO/N₂ = 20/20/60,

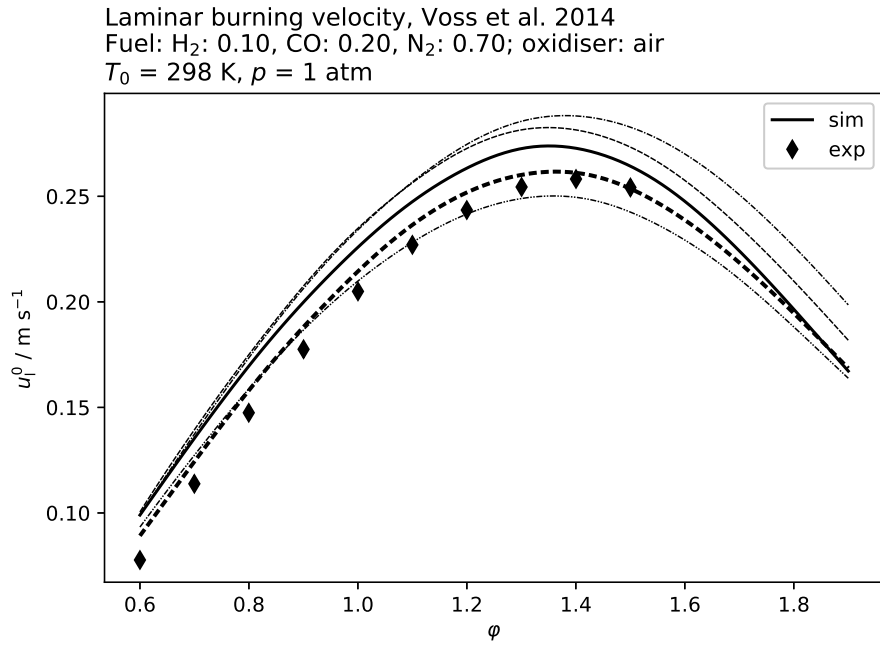


Figure 4.14: Burning velocities by Voss, Hartl, and Hasse [30] and corresponding simulation; fuel: H₂/CO/N₂ = 10/20/70,

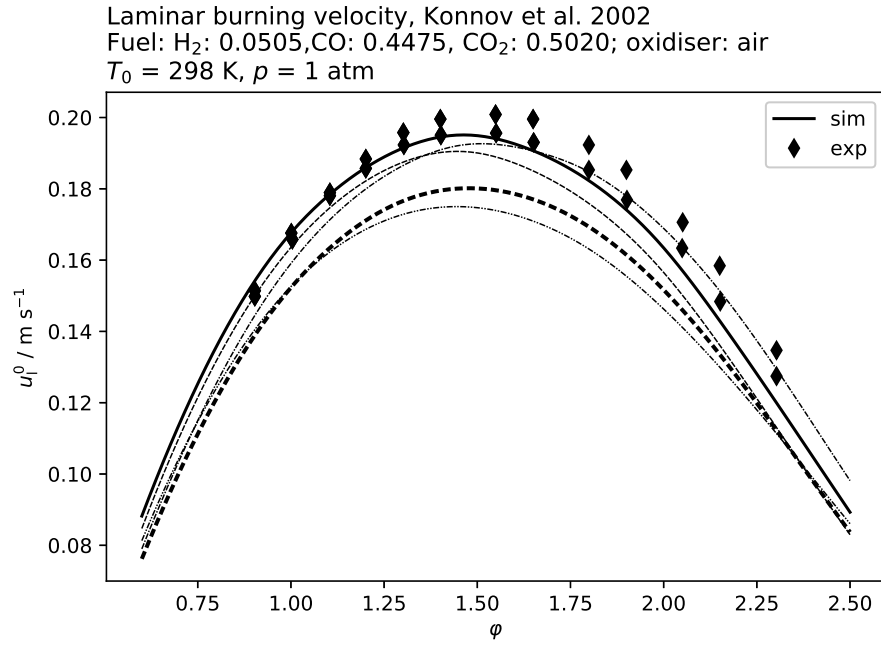


Figure 4.15: Burning velocities by Konnov, Dyakov, and Ruyck [34] and corresponding simulation; fuel: $\text{H}_2/\text{CO}/\text{CO}_2 = 5/45/50$,

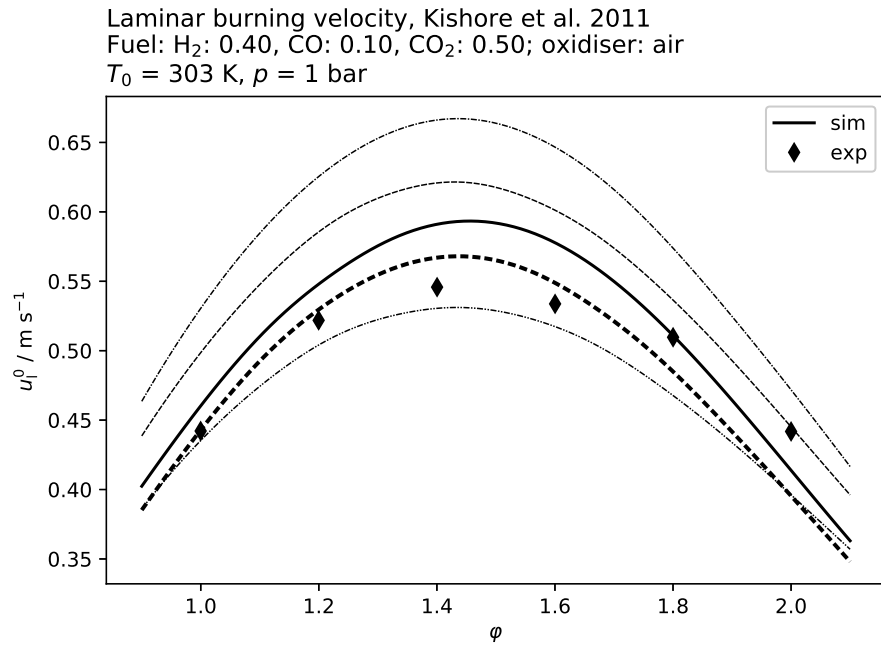


Figure 4.16: Burning velocities by Kishore, Ravi, and Ray [35] and corresponding simulation; fuel: $\text{H}_2/\text{CO}/\text{CO}_2 = 40/10/50$,

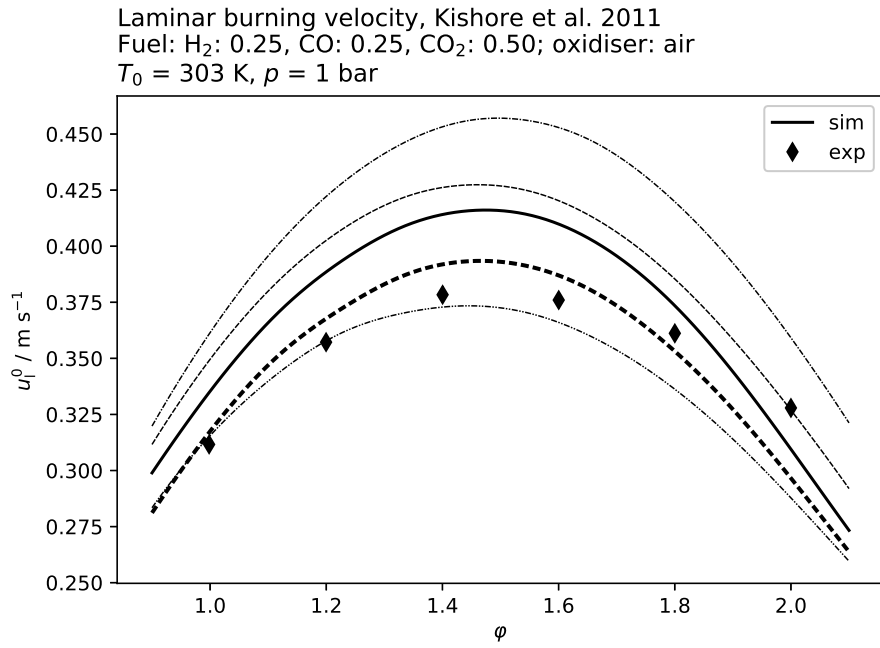


Figure 4.17: Burning velocities by Kishore, Ravi, and Ray [35] and corresponding simulation; fuel: $\text{H}_2/\text{CO}/\text{CO}_2 = 25/25/50$,

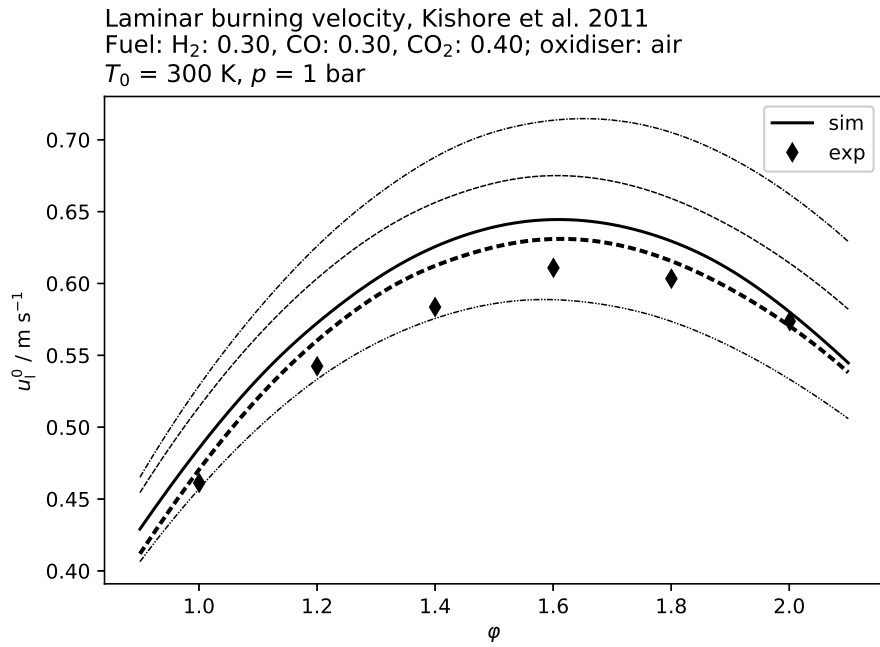


Figure 4.18: Burning velocities by Kishore, Ravi, and Ray [35] and corresponding simulation; fuel: $\text{H}_2/\text{CO}/\text{CO}_2 = 30/30/40$,

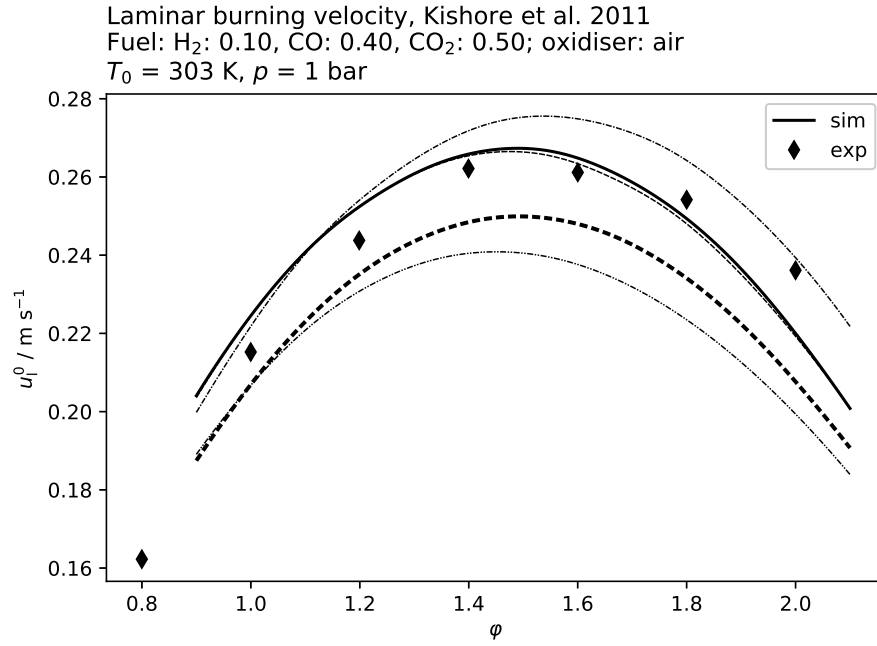


Figure 4.19: Burning velocities by Kishore, Ravi, and Ray [35] and corresponding simulation; fuel: $\text{H}_2/\text{CO}/\text{CO}_2 = 10/40/50$,

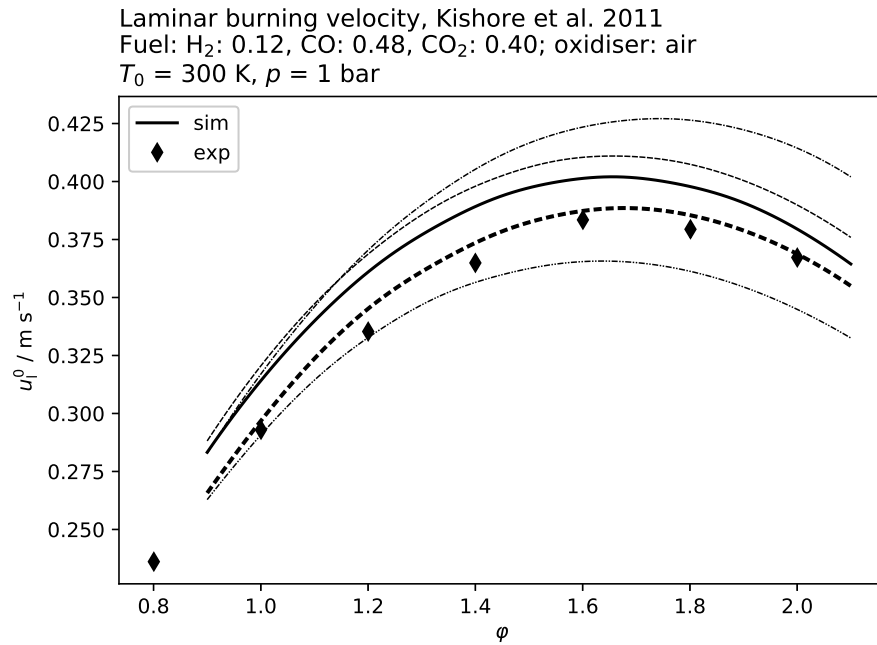


Figure 4.20: Burning velocities by Kishore, Ravi, and Ray [35] and corresponding simulation; fuel: $\text{H}_2/\text{CO}/\text{CO}_2 = 12/48/40$,

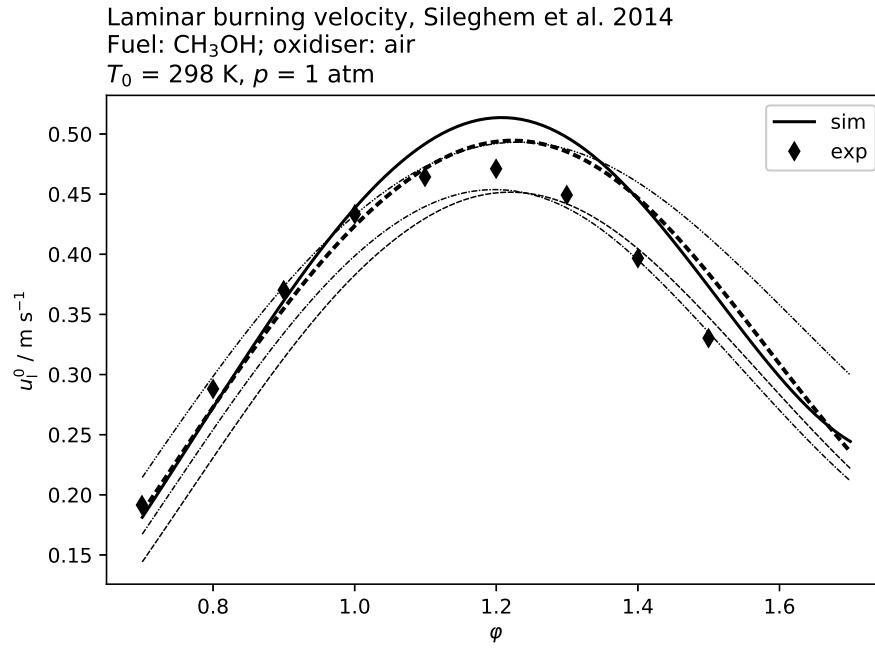


Figure 4.21: Burning velocities by Sileghem et al. [36] and corresponding simulation; fuel: CH₃OH, $T = 298 \text{ K}$,

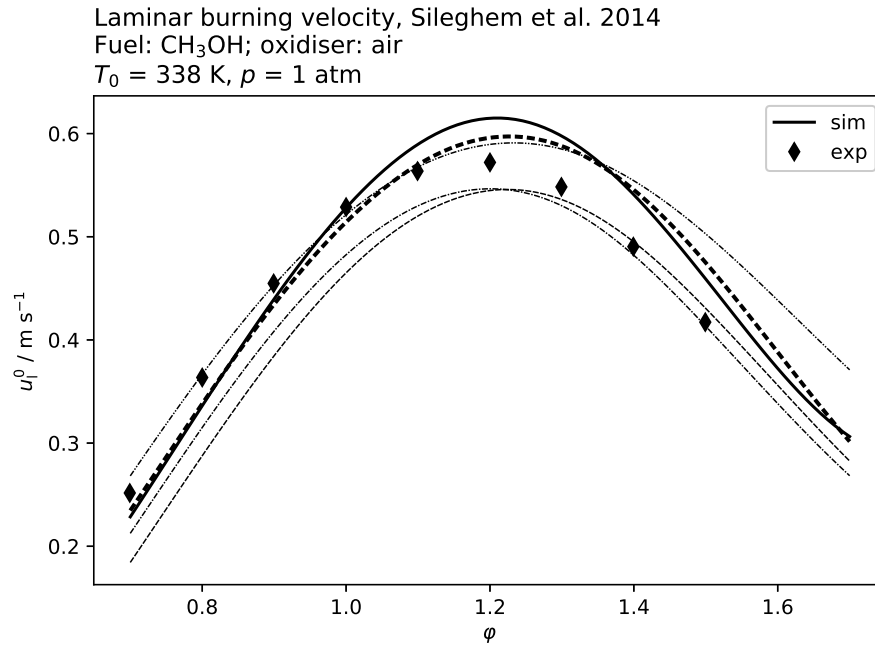


Figure 4.22: Burning velocities by Sileghem et al. [36] and corresponding simulation; fuel: CH₃OH, $T = 338 \text{ K}$,

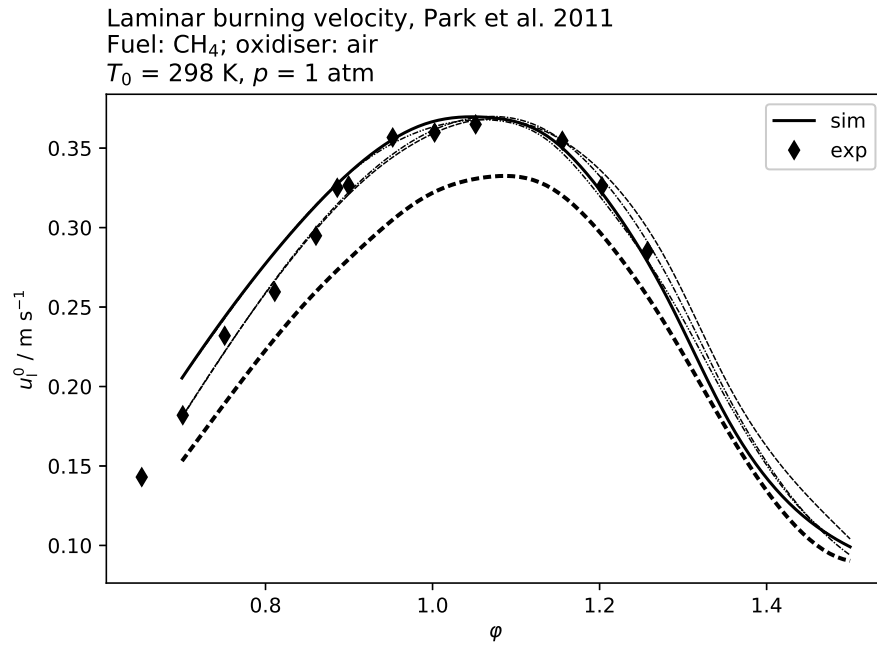


Figure 4.23: Burning velocities by Park et al. [37] and corresponding simulation; fuel: CH₄, $p = 1 \text{ atm}$,

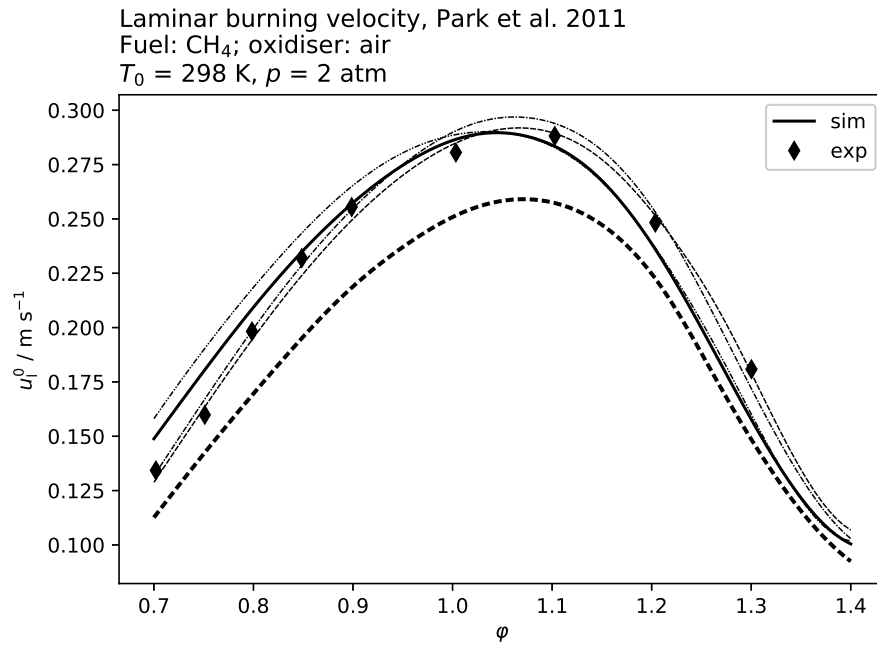


Figure 4.24: Burning velocities by Park et al. [37] and corresponding simulation; fuel: CH₄, $p = 2 \text{ atm}$,

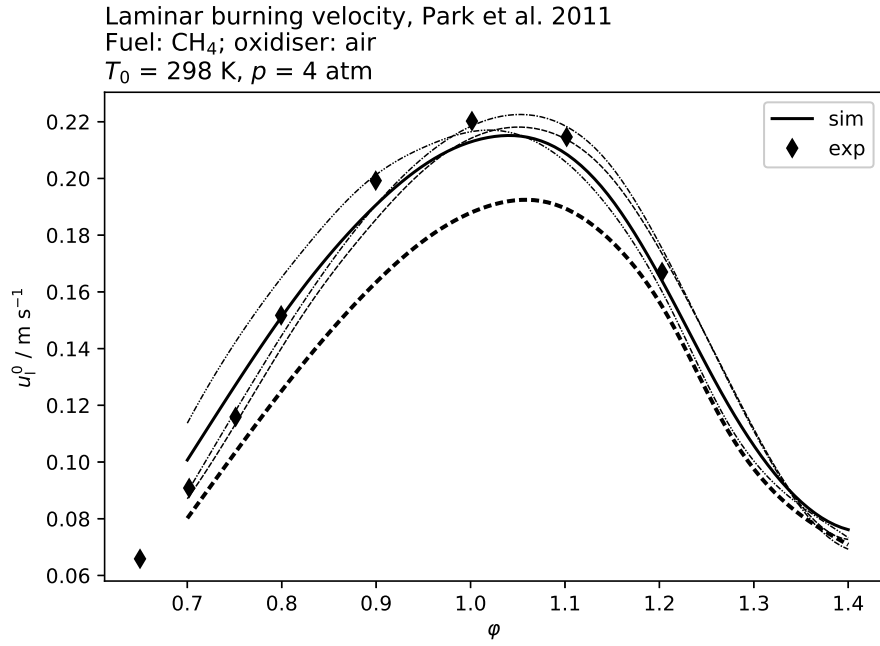


Figure 4.25: Burning velocities by Park et al. [37] and corresponding simulation; fuel: CH₄, $p = 4$ atm,

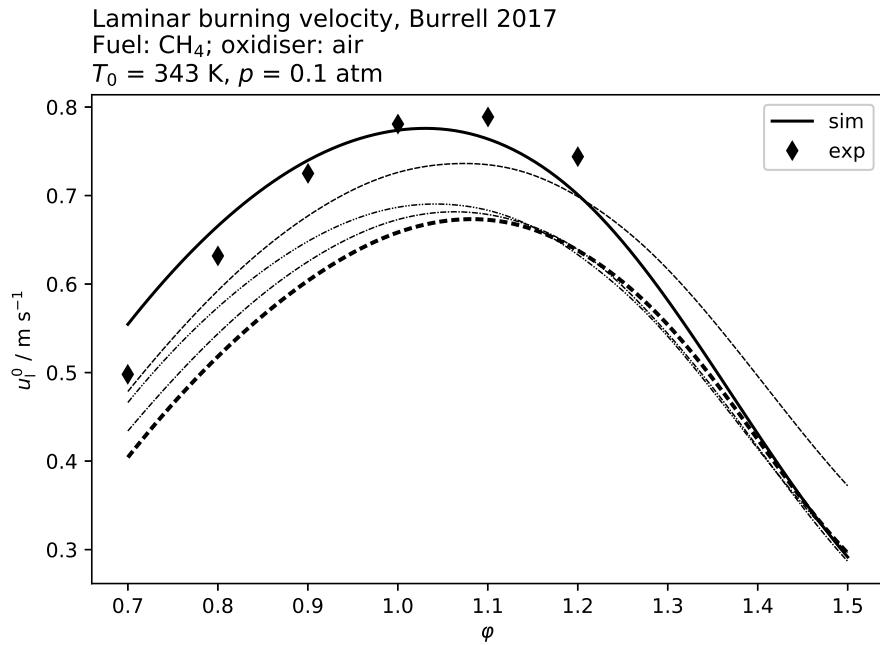


Figure 4.26: Burning velocities by Burrell [38] and corresponding simulation; fuel: CH₄, $p = 0.1$ atm,

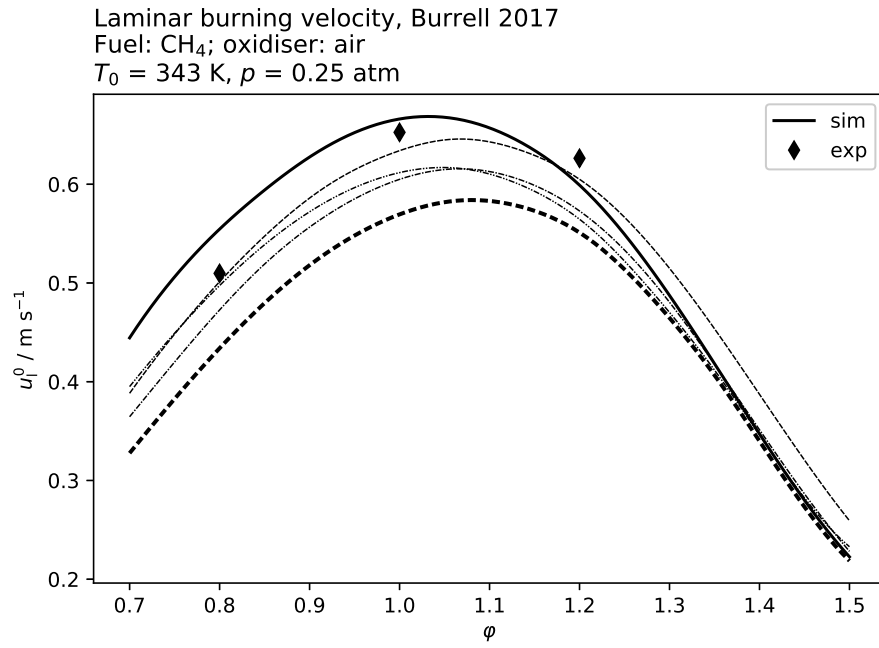


Figure 4.27: Burning velocities by Burrell [38] and corresponding simulation; fuel: CH₄, $p = 0.25 \text{ atm}$,

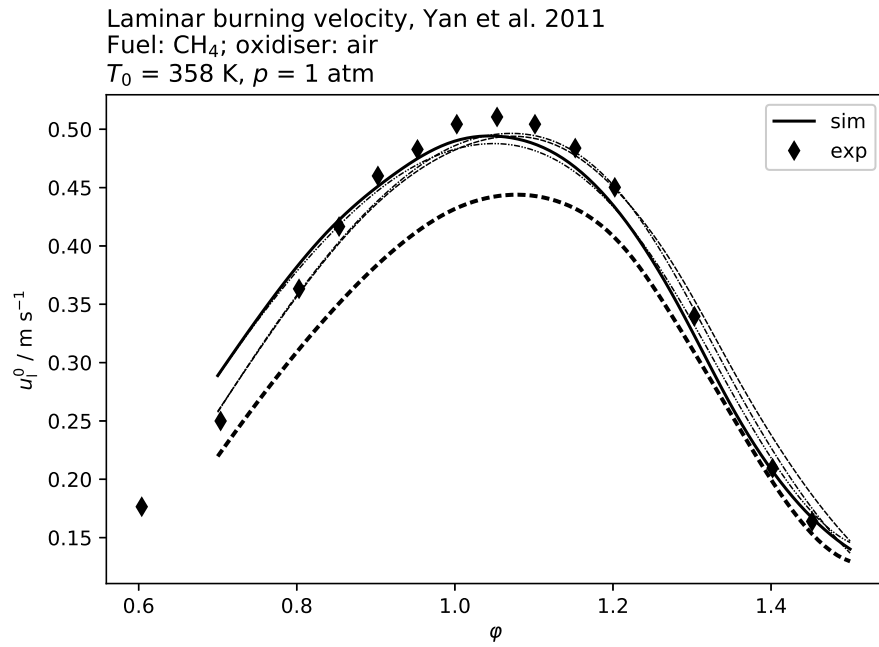


Figure 4.28: Burning velocities by Yan et al. [39] and corresponding simulation; fuel: CH₄, $T = 358 \text{ K}$,

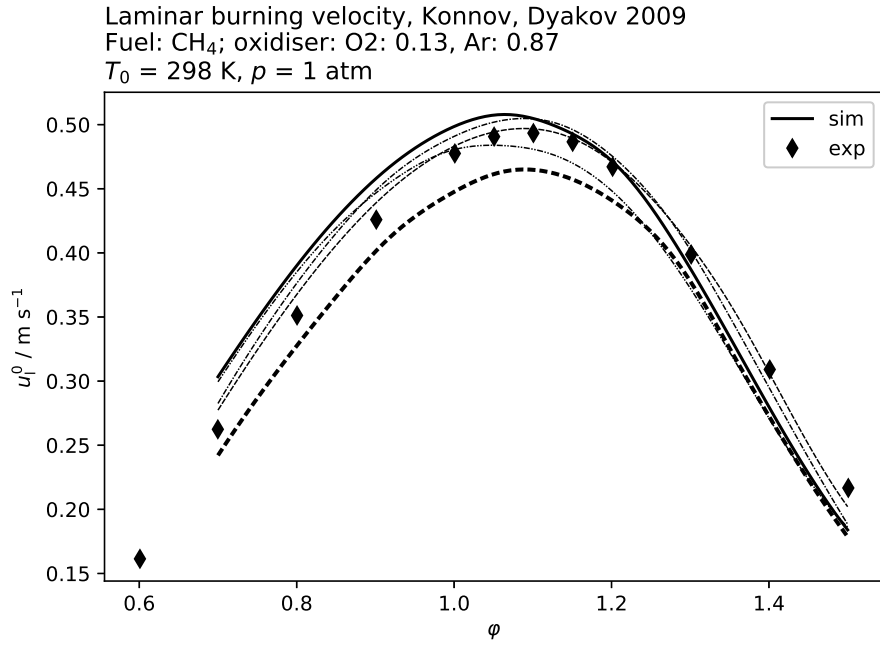


Figure 4.29: Burning velocities by Konnov and Dyakov [40] and corresponding simulation; fuel: CH₄, oxidiser: O₂/Ar = 17/83

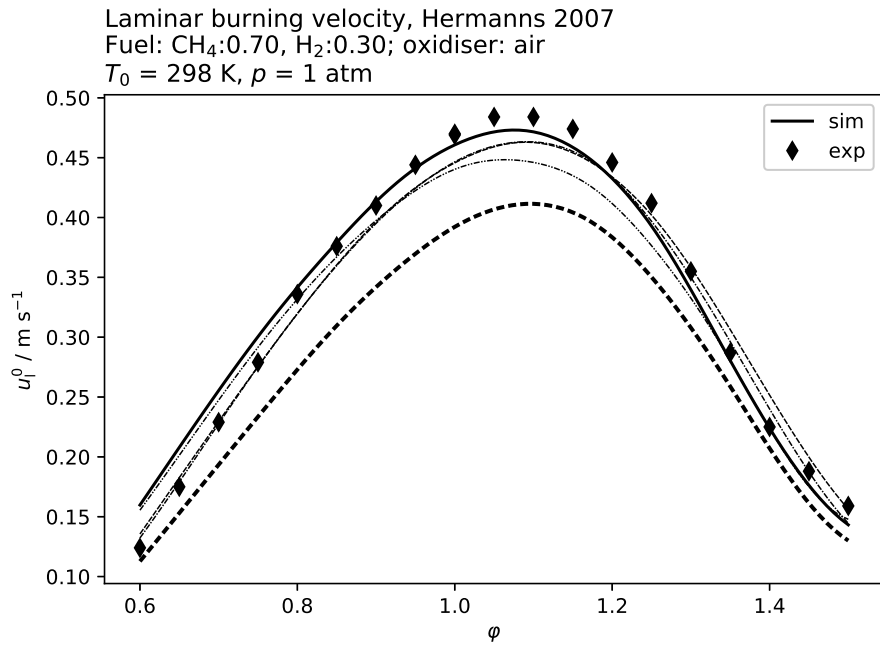


Figure 4.30: Burning velocities by Hermanns [41] and corresponding simulation; fuel: H₂/CH₄ = 30/70,

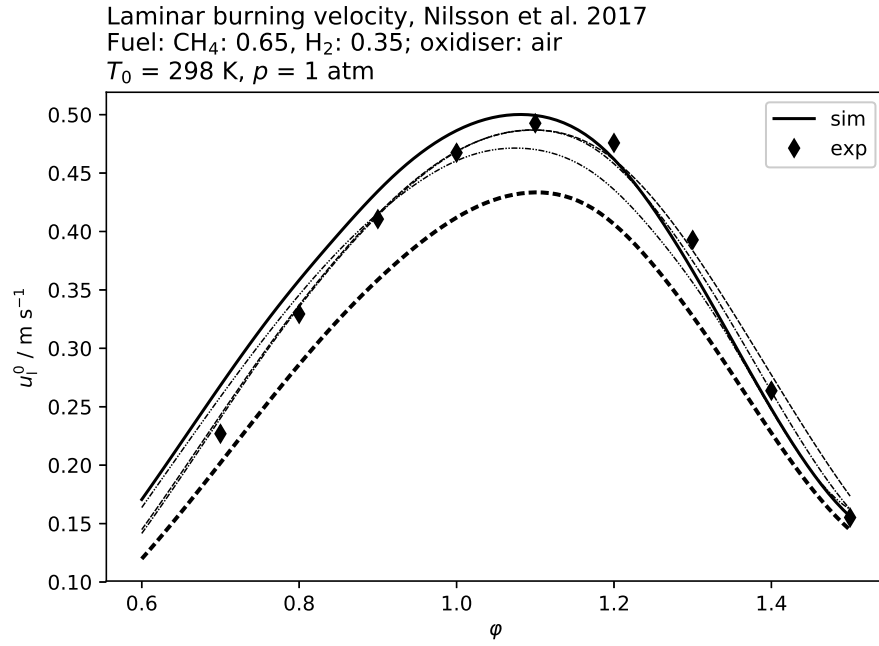


Figure 4.31: Burning velocities by Nilsson et al. [42] and corresponding simulation; fuel: $\text{H}_2/\text{CH}_4 = 35/65$,

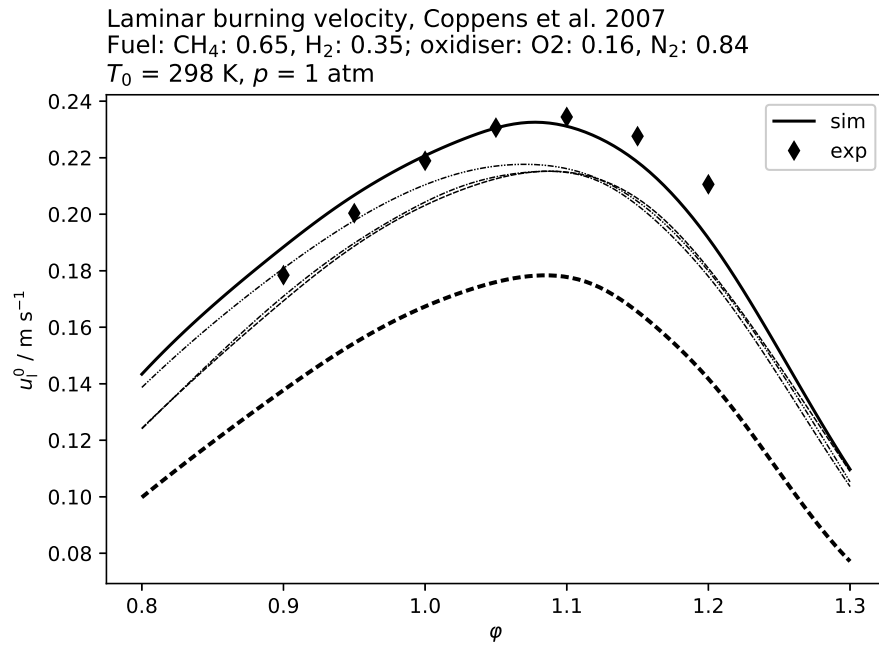


Figure 4.32: Burning velocities by Coppens, De Ruyck, and Konnov [43] and corresponding simulation; fuel: $\text{H}_2/\text{CH}_4 = 35/65$, oxidiser: $\text{O}_2/\text{N}_2 = 16/84$

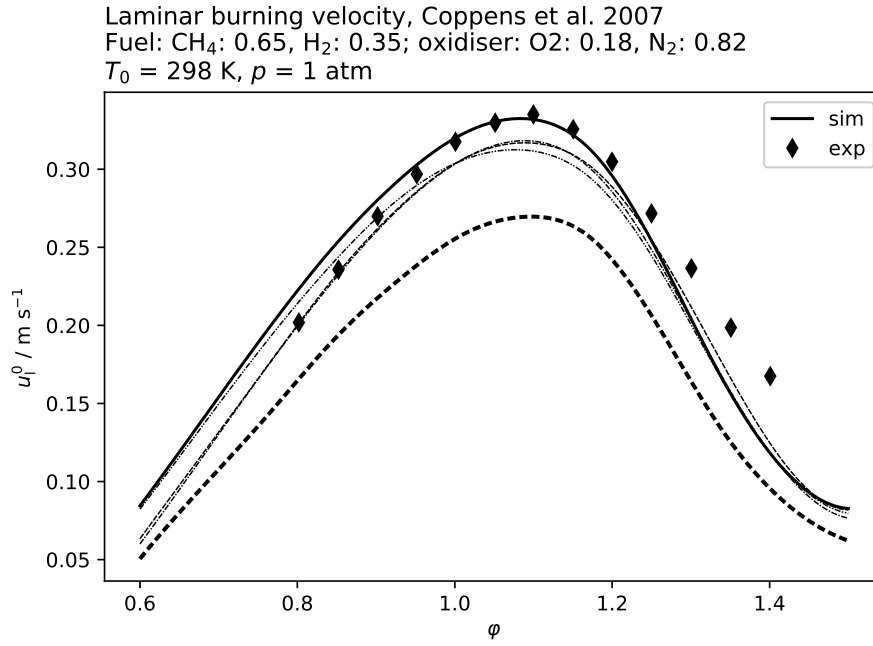


Figure 4.33: Burning velocities by Coppens, De Ruyck, and Konnov [43] and corresponding simulation; fuel: H₂/CH₄ = 35/65, oxidiser: O₂/N₂ = 18/82

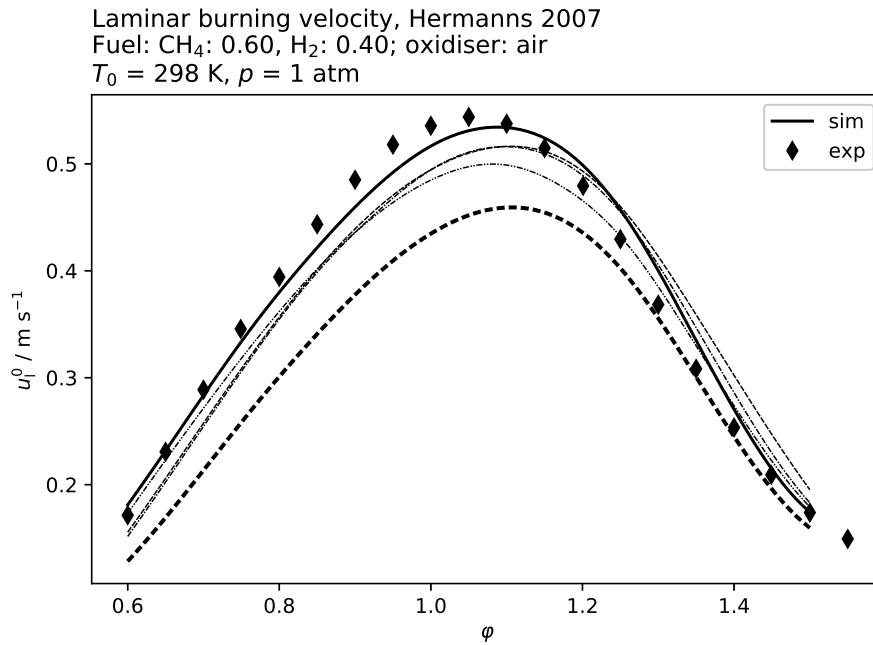


Figure 4.34: Burning velocities by Hermanns [41] and corresponding simulation; fuel: H₂/CH₄ = 40/60,

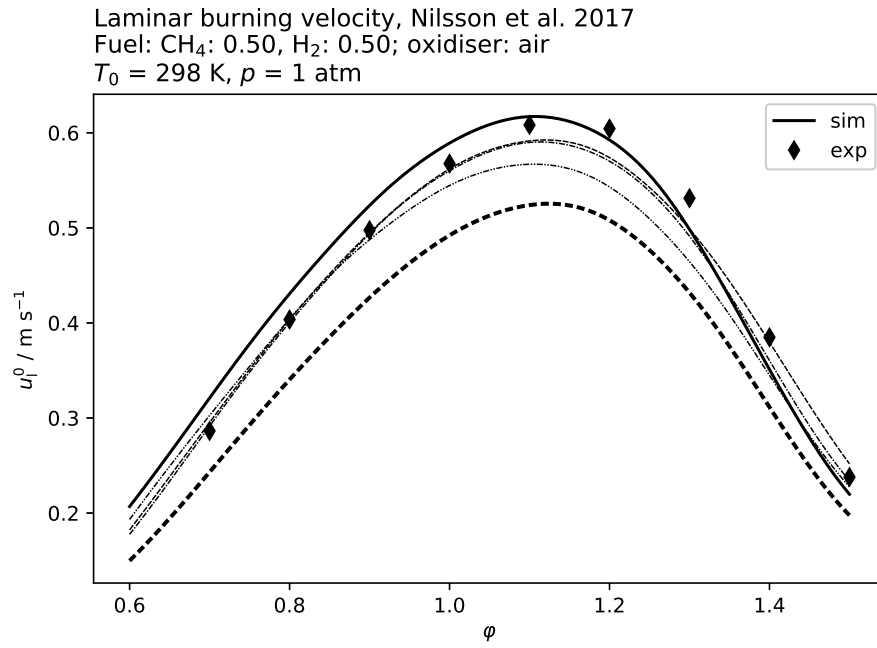


Figure 4.35: Burning velocities by Nilsson et al. [42] and corresponding simulation; fuel: $\text{H}_2/\text{CH}_4 = 50/50$,

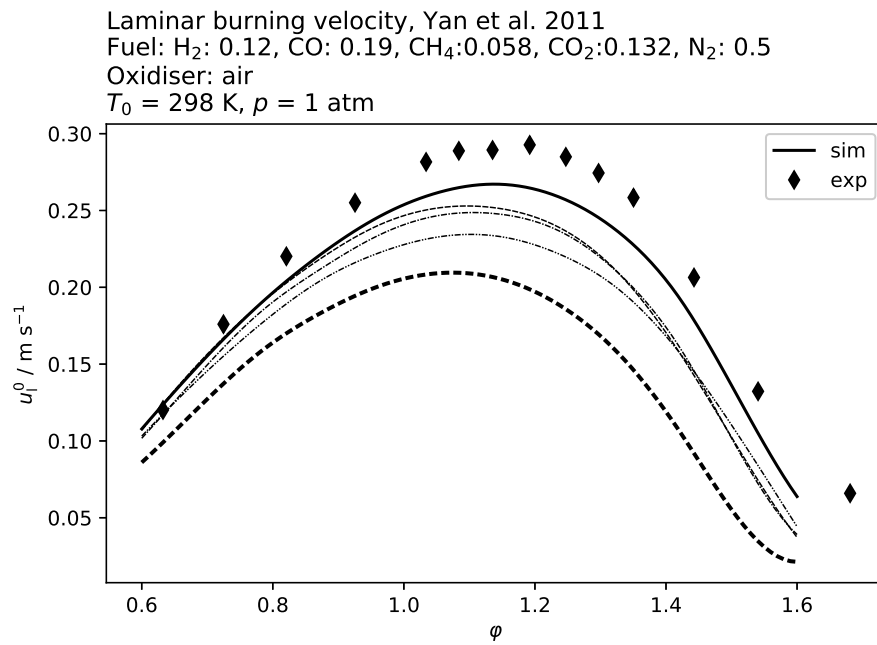


Figure 4.36: Burning velocities by Yan et al. [39] and corresponding simulation; fuel: Bio-genic mix 1,

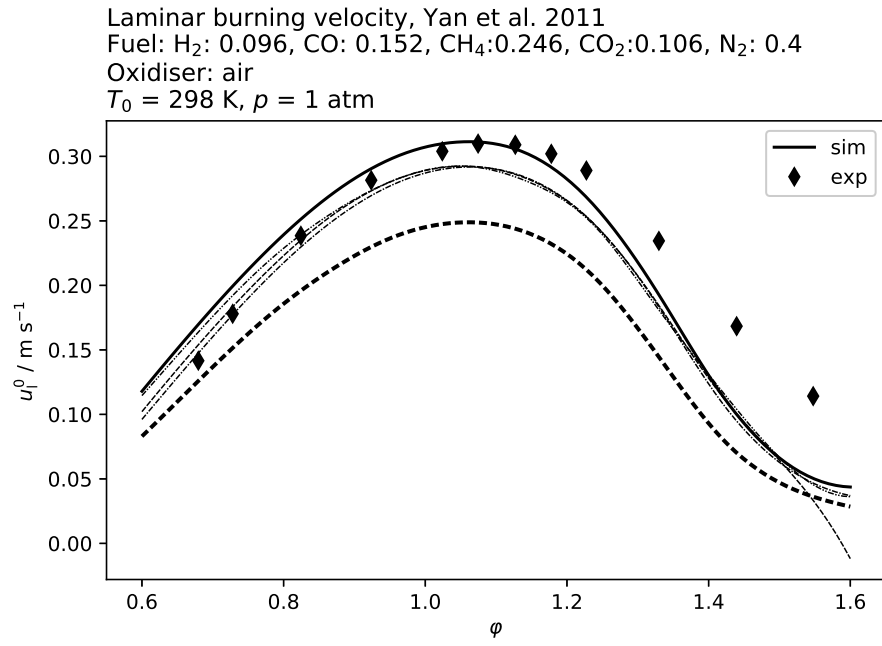


Figure 4.37: Burning velocities by Yan et al. [39] and corresponding simulation; fuel: Bio-genic mix 2,

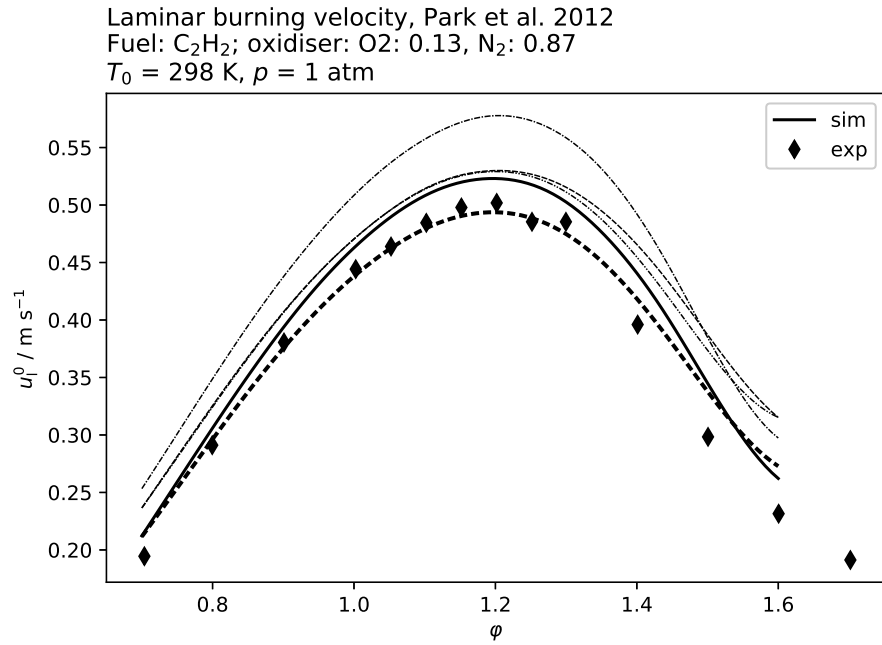


Figure 4.38: Burning velocities by Park, Veloo, and Egolfopoulos [44] and corresponding simulation; fuel: C_2H_2 ,

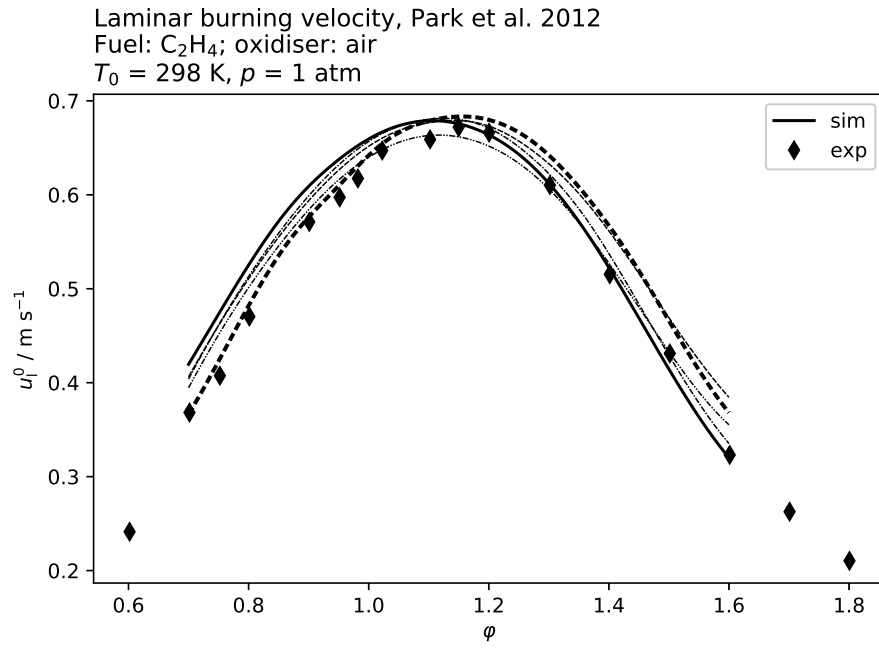


Figure 4.39: Burning velocities by Park, Veloo, and Egolfopoulos [44] and corresponding simulation; fuel: C_2H_4 ,

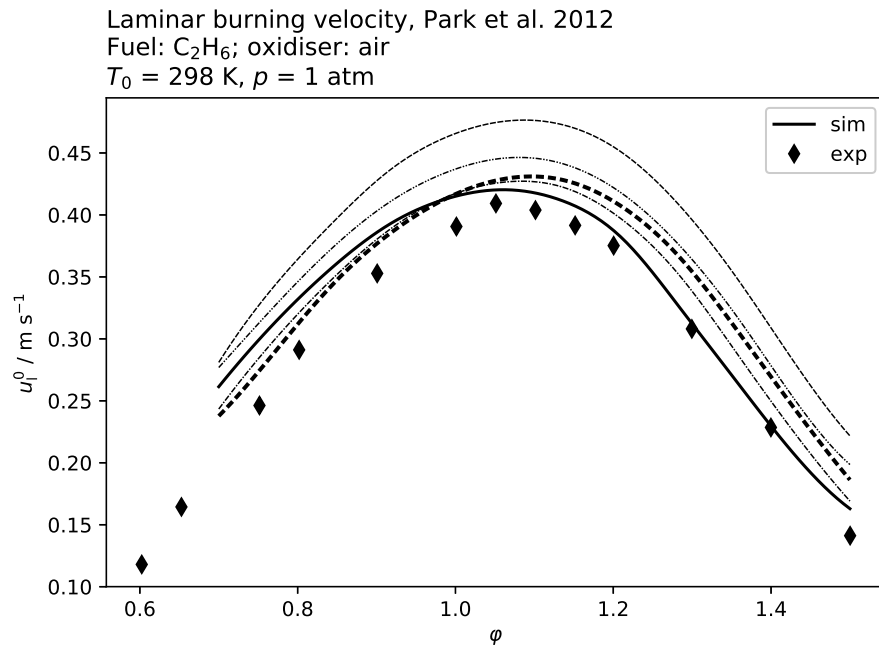


Figure 4.40: Burning velocities by Park, Veloo, and Egolfopoulos [44] and corresponding simulation; fuel: C_2H_6 ,

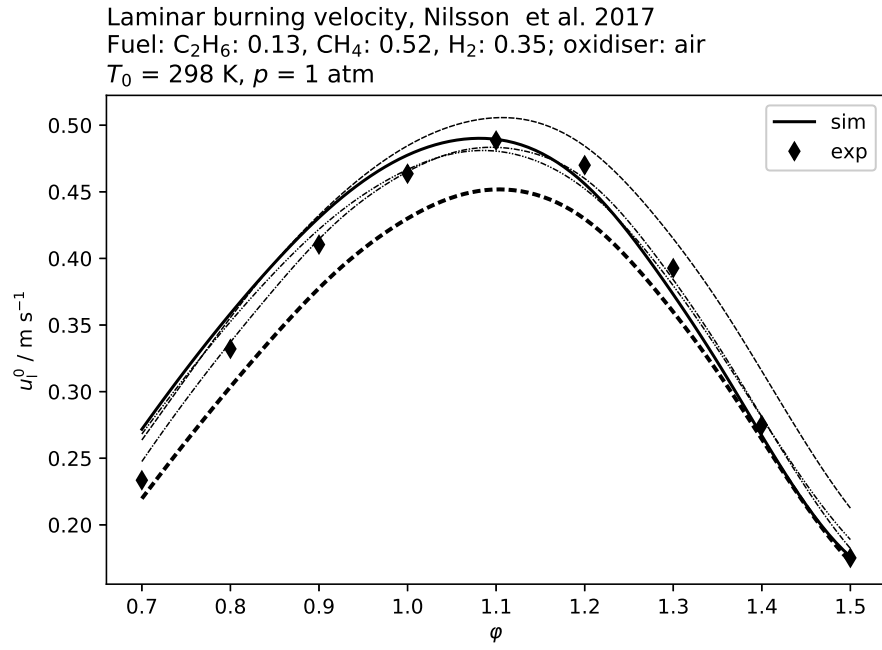
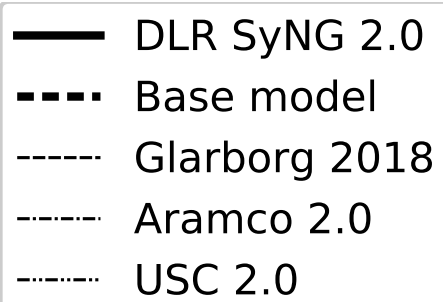


Figure 4.41: Burning velocities by Nilsson et al. [42] and corresponding simulation; fuel: $\text{H}_2/\text{CH}_4/\text{C}_2\text{H}_6 = 35/52/13$,

5 Species profiles in burner stabilised flames



5 SPECIES PROFILES IN BURNER STABILISED FLAMES

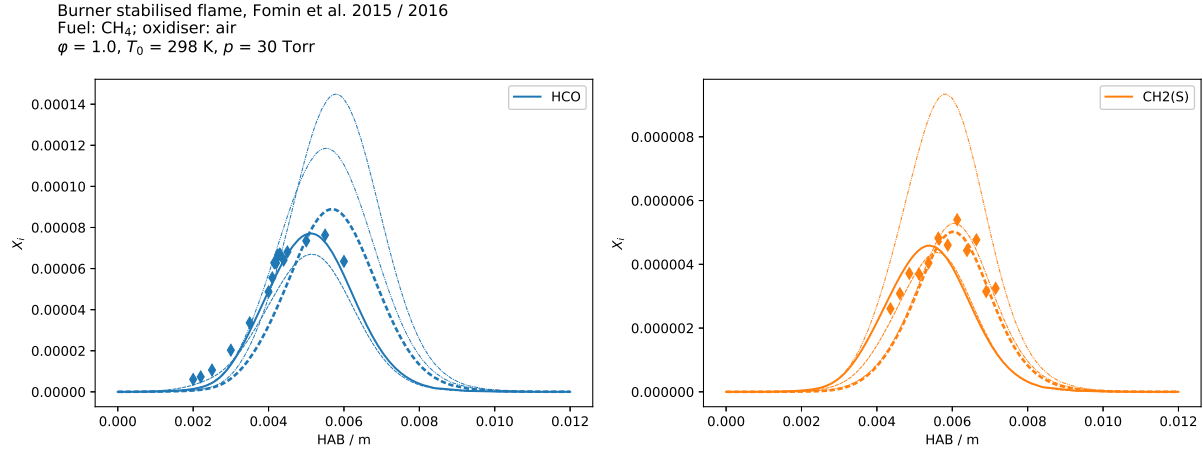


Figure 5.1: Burner flame species profiles by Fomin et al. [45, 46] and corresponding simulation; fuel CH₄, $\varphi = 1.0$

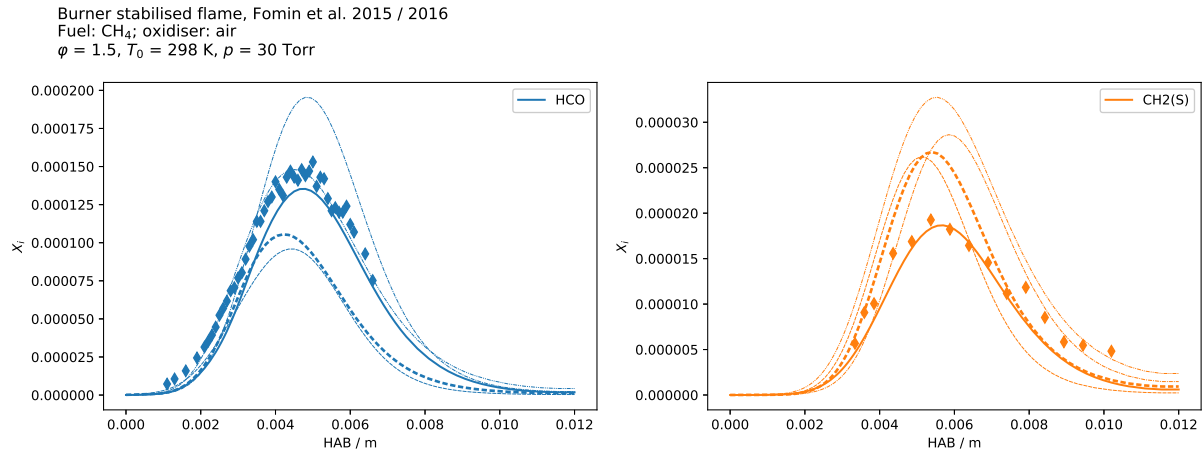


Figure 5.2: Burner flame species profiles by Fomin et al. [45, 46] and corresponding simulation; fuel CH₄, $\varphi = 1.5$

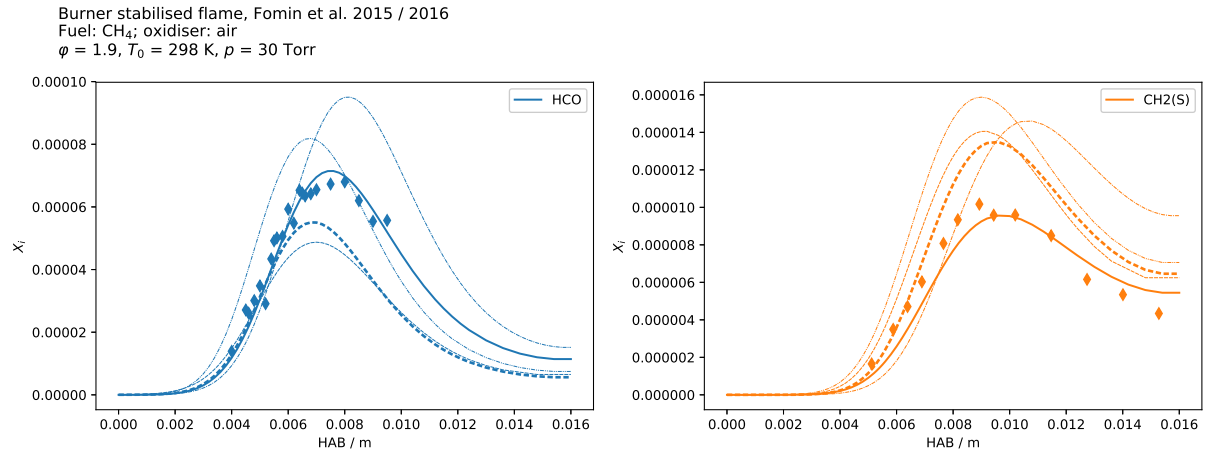


Figure 5.3: Burner flame species profiles by Fomin et al. [45, 46] and corresponding simulation; fuel CH₄, $\varphi = 1.9$

Bibliography

- [1] L. D. Thi, Y. Zhang, and Z. Huang. “Shock tube study on ignition delay of multi-component syngas mixtures—Effect of equivalence ratio”. In: *international journal of hydrogen energy* 39.11 (2014), pp. 6034–6043.
- [2] J. Herzler, C. Naumann, and P. Griebel. “Ignition Delay Time Measurements for the Validation of Reaction Mechanisms for Fuels from Gasification Processes”. In: *Proceedings of the European Combustion Meeting - 2011*. 336. European Combustion Meeting. Cardiff, UK, 2011.
- [3] D. M. Kalitan, J. D. Mertens, M. W. Crofton, and E. L. Petersen. “Ignition and oxidation of lean CO/H₂ fuel blends in air”. In: *Journal of propulsion and power* 23.6 (2007), pp. 1291–1303.
- [4] J. Herzler and C. Naumann. “Ignition Delay Time Measurements for the Validation of Reaction Mechanisms for Different Alcohols”. In: *Proceedings of the European Combustion Meeting - 2013*. P3-8. European Combustion Meeting. Lund, Sweden, 2013.
- [5] E. L. Petersen, J. M. Hall, S. D. Smith, J. de Vries, A. R. Amadio, and M. W. Crofton. “Ignition of lean methane-based fuel blends at gas turbine pressures”. In: *Journal of Engineering for Gas Turbines and Power* 129.4 (2007), pp. 937–944.
- [6] J. Herzler, J. Herbst, T. Kick, C. Naumann, M. Braun-Unkhoff, and U. Riedel. “Alternative fuels based on biomass: An investigation of combustion properties of product gases”. In: *Journal of Engineering for Gas Turbines and Power* 135.3 (2013), p. 031401.
- [7] W. Zeng, H. Ma, Y. Liang, and E. Hu. “Experimental and modeling study on effects of N₂ and CO₂ on ignition characteristics of methane/air mixture”. In: *Journal of advanced research* 6.2 (2015), pp. 189–201.
- [8] B. Koroglu, O. M. Pryor, J. Lopez, L. Nash, and S. S. Vasu. “Shock tube ignition delay times and methane time-histories measurements during excess CO₂ diluted oxy-methane combustion”. In: *Combustion and flame* 164 (2016), pp. 152–163.

- [9] N. Lokachari, U. Burke, A. Ramalingam, M. Turner, R. Hesse, K. P. Somers, J. Beeckmann, K. A. Heufer, E. L. Petersen, and H. J. Curran. “New experimental insights into acetylene oxidation through novel ignition delay times, laminar burning velocities and chemical kinetic modelling”. In: *Proceedings of the Combustion Institute* 37.1 (2019), pp. 583–591.
- [10] M. Rickard, J. Hall, and E. Petersen. “Effect of silane addition on acetylene ignition behind reflected shock waves”. In: *Proceedings of the Combustion Institute* 30.2 (2005), pp. 1915–1923.
- [11] E. L. Petersen, J. M. Hall, D. M. Kalitan, and M. J. Rickard. “Ignition Delay Time Measurements of C_2H_x Fuels and Comparison to Several Detailed Kinetics Mechanisms”. In: *ASME Paper No. GT2004-GT53926* (2004).
- [12] J. de Vries, J. M. Hall, S. L. Simmons, M. J. Rickard, D. M. Kalitan, and E. L. Petersen. “Ethane ignition and oxidation behind reflected shock waves”. In: *Combustion and flame* 150.1 (2007), pp. 137–150.
- [13] J. Herzler and C. Naumann. “Shock-tube study of the ignition of methane/ethane/hydrogen mixtures with hydrogen contents from 0% to 100% at different pressures”. In: *Proceedings of the combustion institute* 32.1 (2009), pp. 213–220.
- [14] J. Herzler and C. Naumann. *Oxy-fuel ignition delay time Measurements for validation of reaction mechanisms*. Tech. rep. D1.4.1003. German Aerospace Center, 2010.
- [15] M. Mueller, T. Kim, R. Yetter, and F. Dryer. “Flow reactor studies and kinetic modeling of the H_2/O_2 reaction”. In: *International Journal of Chemical Kinetics* 31.2 (1999), pp. 113–125.
- [16] M. A. Mueller, R. Yetter, and F. Dryer. “Flow reactor studies and kinetic modeling of the $H_2/O_2/NO_x$ and $CO/H_2O/O_2/NO_x$ reactions”. In: *International Journal of Chemical Kinetics* 31.10 (1999), pp. 705–724.
- [17] J. Li, Z. Zhao, A. Kazakov, M. Chaos, F. L. Dryer, and J. J. Scire Jr. “A comprehensive kinetic mechanism for CO, CH_2O , and CH_3OH combustion”. In: *International Journal of Chemical Kinetics* 39.3 (2007), pp. 109–136.
- [18] P. Oßwald and M. Köhler. “An atmospheric pressure high-temperature laminar flow reactor for investigation of combustion and related gas phase reaction systems”. In: *Review of Scientific Instruments* 86.10, 105109 (2015).

-
- [19] H. Hashemi, J. M. Christensen, S. Gersen, H. Levinsky, S. J. Klippenstein, and P. Glarborg. “High-pressure oxidation of methane”. In: *Combustion and Flame* 172 (2016), pp. 349–364.
- [20] M. Alzueta, M. Borruely, A. Callejas, A. Millera, and R. Bilbao. “An experimental and modeling study of the oxidation of acetylene in a flow reactor”. In: *Combustion and flame* 152.3 (2008), pp. 377–386.
- [21] T. Carriere, P. Westmoreland, A. Kazakov, Y. Stein, and F. Dryer. “Modeling ethylene combustion from low to high pressure”. In: *Proceedings of the Combustion Institute* 29.1 (2002), pp. 1257–1266.
- [22] T. Le Cong, P. Dagaut, and G. Dayma. “Oxidation of natural gas, natural gas/syngas mixtures, and effect of burnt gas recirculation: Experimental and detailed kinetic modeling”. In: *Journal of Engineering for Gas Turbines and Power* 130.4 (2008), p. 041502.
- [23] P. Dagaut, F. Lecomte, J. Mieritz, and P. Glarborg. “Experimental and kinetic modeling study of the effect of NO and SO₂ on the oxidation of CO-H₂ mixtures”. In: *International journal of chemical kinetics* 35.11 (2003), pp. 564–575.
- [24] U. Burke, W. K. Metcalfe, S. M. Burke, K. A. Heufer, P. Dagaut, and H. J. Curran. “A detailed chemical kinetic modeling, ignition delay time and jet-stirred reactor study of methanol oxidation”. In: *Combustion and Flame* 165 (2016), pp. 125–136.
- [25] P. Dagaut, J.-C. Boettner, and M. Cathonnet. “Methane oxidation: experimental and kinetic modeling study”. In: *Combustion science and technology* 77.1-3 (1991), pp. 127–148.
- [26] T. L. Le Cong and P. Dagaut. “Experimental and detailed kinetic modeling of the oxidation of methane and methane/syngas mixtures and effect of carbon dioxide addition”. In: *Combustion Science and Technology* 180.10-11 (2008), pp. 2046–2091.
- [27] Y. Tan, P. Dagaut, M. Cathonnet, and J.-C. Boettner. “Acetylene oxidation in a JSR from 1 to 10 atm and comprehensive kinetic modeling”. In: *Combustion science and technology* 102.1-6 (1994), pp. 21–55.
- [28] M. C. Krejci, O. Mathieu, A. J. Vissotski, S. Ravi, T. G. Sikes, E. L. Petersen, K. Alan, W. Metcalfe, H. J. Curran, et al. “Laminar flame speed and ignition delay time data for the kinetic modeling of hydrogen and syngas fuel blends”. In: *Journal of Engineering for Gas Turbines and Power* 135.2 (2013), p. 021503.

- [29] O. Park, P. S. Veloo, H. Burbano, and F. N. Egolfopoulos. “Studies of premixed and non-premixed hydrogen flames”. In: *Combustion and Flame* 162.4 (2015), pp. 1078–1094.
- [30] S. Voss, S. Hartl, and C. Hasse. “Determination of laminar burning velocities for lean low calorific H_2/N_2 and $\text{H}_2/\text{CO}/\text{N}_2$ gas mixtures”. In: *International Journal of Hydrogen Energy* 39.34 (2014), pp. 19810–19817.
- [31] V. A. Alekseev and A. A. Konnov. “Data consistency of the burning velocity measurements using the heat flux method: Hydrogen flames”. In: *Combustion and Flame* 194 (2018), pp. 28–36.
- [32] H. Sun, S. Yang, G. Jomaas, and C. Law. “High-pressure laminar flame speeds and kinetic modeling of carbon monoxide/hydrogen combustion”. In: *Proceedings of the Combustion Institute* 31.1 (2007), pp. 439–446.
- [33] B. Lohöfener, E. Roungos, S. Voss, and D. Trimis. “Burning velocities of low calorific value hydrogen and carbon monoxide gas mixtures”. In: *2nd Heat Flux Burner Workshop*. Warsaw University of Technology, Poland. 2012.
- [34] A. A. Konnov, I. V. Dyakov, and J. de Ruyck. “Nitric oxide formation in premixed flames of $\text{H}_2 + \text{CO} + \text{CO}_2$ and air”. In: *Proceedings of the Combustion Institute* 29.2 (2002), pp. 2171–2177.
- [35] V. R. Kishore, M. Ravi, and A. Ray. “Adiabatic burning velocity and cellular flame characteristics of $\text{H}_2\text{--CO--CO}_2$ –air mixtures”. In: *Combustion and flame* 158.11 (2011), pp. 2149–2164.
- [36] L. Sileghem, V. Alekseev, J. Vancoillie, E. Nilsson, S. Verhelst, and A. Konnov. “Laminar burning velocities of primary reference fuels and simple alcohols”. In: *Fuel* 115 (2014), pp. 32–40.
- [37] O. Park, P. S. Veloo, N. Liu, and F. N. Egolfopoulos. “Combustion characteristics of alternative gaseous fuels”. In: *Proceedings of the Combustion Institute* 33.1 (2011), pp. 887–894.
- [38] R. R. Burrell. “Studies of methane counterflow flames at low pressures”. PhD thesis. University of Southern California, 2017.

-
- [39] B. Yan, Y. Wu, C. Liu, J. Yu, B. Li, Z. Li, G. Chen, X. Bai, M. Aldén, and A. Konnov. “Experimental and modeling study of laminar burning velocity of biomass derived gases/air mixtures”. In: *international journal of hydrogen energy* 36.5 (2011), pp. 3769–3777.
- [40] A. A. Konnov and I. Dyakov. “Nitrous oxide conversion in laminar premixed flames of $\text{CH}_4 + \text{O}_2 + \text{Ar}$ ”. In: *Proceedings of the Combustion Institute* 32.1 (2009), pp. 319–326.
- [41] R. T. E. Hermanns. “Laminar burning velocities of methane-hydrogen-air mixtures”. PhD thesis. Technische Universiteit Eindhoven, 2007. DOI: 10.6100/IR630126.
- [42] E. J. Nilsson, A. van Sprang, J. Larfeldt, and A. A. Konnov. “The comparative and combined effects of hydrogen addition on the laminar burning velocities of methane and its blends with ethane and propane”. In: *Fuel* 189 (2017), pp. 369–376.
- [43] F. Coppens, J. De Ruyck, and A. A. Konnov. “The effects of composition on burning velocity and nitric oxide formation in laminar premixed flames of $\text{CH}_4 + \text{H}_2 + \text{O}_2 + \text{N}_2$ ”. In: *Combustion and Flame* 149.4 (2007), pp. 409–417.
- [44] O. Park, P. S. Veloo, and F. N. Egolfopoulos. “Flame studies of C_2 hydrocarbons”. In: *Proceedings of the Combustion Institute* 34.1 (2013), pp. 711–718.
- [45] A. Fomin, T. Zavlev, V. A. Alekseev, A. A. Konnov, I. Rahinov, and S. Cheskis. “Intracavity laser absorption spectroscopy study of HCO radicals during methane to hydrogen conversion in very rich flames”. In: *Energy & Fuels* 29.9 (2015), pp. 6146–6154.
- [46] A. Fomin, T. Zavlev, V. A. Alekseev, I. Rahinov, S. Cheskis, and A. A. Konnov. “Experimental and modelling study of $^1\text{CH}_2$ in premixed very rich methane flames”. In: *Combustion and Flame* 171 (2016), pp. 198–210.